# WATER MOVEMENT AND CONNECTIVITY IN A FORESTED GLACIAL DRIFT WATERSHED

A Dissertation

Presented to the Faculty of the Graduate School

of Cornell University

In Partial Fulfillment of the Requirements for the Degree of

Doctor of Philosophy

by

Kathryn Levine Hofmeister

August 2018

WATER MOVEMENT AND CONNECTIVITY IN A FORESTED GLACIAL DRIFT WATERSHED

Kathryn Levine Hofmeister, Ph. D.
Cornell University 2018

Water movement through the landscape to streams provides a fundamental linkage between terrestrial and aquatic environments in headwater systems. Headwater streams, which are the smallest and most abundant streams, are critical components of drainage systems, connecting important terrestrial and aquatic biogeochemical cycles and influencing the nutrient dynamics of downstream ecosystems. Given the importance of water presence and movement as a driver of biogeochemical transformations and the transport of material from terrestrial to aquatic ecosystems, the primary goal of this research was to quantify the distribution across and movement of water and other elements through a forested watershed to a headwater stream and ultimately to an inland lake in the glacial drift landscape of northern Michigan, U.S.A. To investigate the temporal dynamics and spatial patterns of water across the watershed and in Honeysuckle Creek, stream discharge, shallow groundwater levels, soil moisture, and water chemistry were measured from 2015–2017. Along the stream, surface flow was seasonal in the main stem and perennial flow was spatially discontinuous for all but the lowest reaches. Spring snowmelt was the dominant hydrological event in the year with peak flows an order of magnitude larger than annual mean discharge. Topography and soil characteristics strongly influence water and dissolved matter movement through the landscape. Water presence across the watershed was highly variable with perennial soil saturation and shallow groundwater within 10 cm of the surface at the lowest landscape positions, low soil moisture and nonexistent groundwater in upland outwash

ecosystems, and a mixture of these conditions in the heterogeneous till parent material ecosystems of middle landscape positions. Shallow groundwater was the primary source of water to the headwater stream throughout the year; originating from snowmelt in the spring and shifting to recent precipitation in summer and autumn seasons. The riparian areas and the outwash-lake plain wetland likely have a much stronger influence on stream chemistry and discharge than the upland landscape units, due to the perennial connections between shallow groundwater from these wetland areas and surface water.

# BIOGRAPHICAL SKETCH

Kathryn Hofmeister grew up in Minnesota and Wisconsin, where she was raised with respect for the environment and interest in preserving water resources, fueled by annual family vacations on the shore of Lake Superior. Born into a family of scientists and educators, she became passionate about engaging with and communicating about nature and science to the public, as well as doing research related to environmental issues. She graduated from Hampshire College in 2013 with a strong interest in research related to the effects of climate change on the natural environment, particularly water resources, and a clear understanding of the pressing need to translate research findings effectively to non-scientific audiences. While at Hampshire, Kathryn designed her own academic program including numerous research projects that provided a solid foundation for quantitative ecological and hydrological research and science education and community outreach programs. In 2013 Kathryn joined the Soil and Water Lab at Cornell University to study with Dr. M. Todd Walter. At Cornell, Kathryn has used field research and geospatial analysis to explore how water moves through and interacts with ecosystems as well as working to increase awareness about water resource issues and stimulating interest in the environment in the broader community.

# ACKNOWLEDGMENTS

I would like to thank the members of my committee – Dr. M. Todd Walter, Dr. Susan Riha, Dr. Rebecca Schneider, and Dr. Paul Drevnick – for their invaluable guidance and support of my research. I am grateful for your insights and feedback on my research. I would especially like to thank Todd for his lighthearted spirit, enjoyment of public radio, and being understanding about the important things in life. This research would not have been possible without the vital assistance of Phoebe Aron, Margaret Conly, Ariadna Covarrubias Ornelas, Kate Heckman, Kate Hogan, Gabby Kitch, Jim Le Moine, Lizy Michaelson, Adam Schubel, Jason Tallant, Carl Thompson, Nick Van Dyke, Tim Veverica, and Paula Zermeño and in the field and lab. I would like to give a special thank you to Renee Knudstrup for her wonderful company and willingness to tromp around the woods with me. I would also like to thank Art Gold for his enthusiasm, encouragement, and love of UMBS. I am very grateful for the generous support Knute Nadelhoffer and Karie Slavik have provided for this project and for my time at UMBS. Many thanks to all of my friends at Cornell and at UMBS for your friendship and encouragement. I am especially grateful to the UMBS staff for your company during the long winters and for all those coffee break chats.

To my family, thank you for continual love, support, and supply of chocolate. Thank you to my mother for being the world's best editor, my father for always making me laugh, and my grandparents for being the most inspiring people I know. And finally, I want to thank Luke, my partner in life and in science, for going on this adventure with me.

My research at Cornell University and UMBS would not have been possible without the funding provided by the National Science Foundation Graduate Research Fellowship Program, the USDA-NIFA McIntire-Stennis Cooperative Forestry Research Program, the University of Michigan Biological Station Graduate Research Fellowship Fund, the University of Michigan

Graham Sustainability Institute, and the International Soil Carbon Network Radiocarbon Collaborative.

TABLE OF CONTENTS

BIOGRAPHICAL SKETCH ... iii
ACKNOWLEDGEMENTS ... iv
TABLE OF CONTENTS ... vi
LIST OF FIGURES ... vii
LIST OF TABLES ... ix

**CHAPTER 1:** SEASONAL DYNAMICS AND EXPORTS OF ELEMENTS FROM A FIRST-ORDER STREAM TO A LARGE INLAND LAKE IN MICHIGAN ... 1
- Abstract ... 1
- Introduction ... 2
- Methods ... 7
- Results ... 13
- Discussion ... 26
- Conclusions ... 32
- References ... 34

**CHAPTER 2:** SOILS AND TOPOGRAPHY CONTROL SEASONAL AND SPATIAL PATTERNS OF FOREST SOIL MOISTURE AND WATER TABLE POSITION ... 41
- Abstract ... 41
- Introduction ... 42
- Methods ... 45
- Results ... 56
- Discussion ... 68
- Conclusions ... 73
- References ... 74

**CHAPTER 3:** LANDSCAPE HYDROLOGIC UNITS, WATER CONNECTIVITY, AND CHEMISTRY IN A GREAT LAKES GLACIAL DRIFT WATERSHED ... 82
- Abstract ... 82
- Introduction ... 83
- Methods ... 87
- Results ... 98
- Discussion ... 118
- Conclusions ... 127
- References ... 128

LIST OF FIGURES

**CHAPTER 1**

Figure 1.1 ..................................................................................................9
Honeysuckle Creek watershed location in northern Lower Michigan with stream and three flumes marked.

Figure 1.2 ..................................................................................................15
Honeysuckle Creek discharge at all three flumes and stream temperature at the mouth shown in panel A during 2015-2016 hydrologic year. Precipitation and snow depth shown in panel B.

Figure 1.3 ..................................................................................................16
Distribution of daily precipitation measured during the study year (October 2015–September 2016).

Figure 1.4 ..................................................................................................21
*C*-*Q* relationships for TSS, C, and biologically cycled anions ($NO_3^-$, $PO_4^{3-}$, $SO_4^{2-}$) at all three flumes (mouth, mid, upper), with season indicated by point shape and color.

Figure 1.5 ..................................................................................................22
*C*-*Q* relationships for cations ($Na^+$, $K^+$, $Mg^{2+}$, $Ca^{2+}$) at all three flumes (mouth, mid, upper), with season indicated by point shape and color. Probability of saturation excess runoff being generated at each STI value for the five study sites.

Figure 1.6 ..................................................................................................23
*C*-*Q* relationships for anions ($Cl^-$, $F^-$) associated with parent material weathering at all three flumes (mouth, mid, upper), with season indicated by point shape and color.

Figure 1.7 ..................................................................................................25
Stream DOC and DOC $\delta^{13}C$ at the mouth, mid, and upper flumes.

Figure 1.8 ..................................................................................................26
Measurements of soil carbon $\Delta^{14}C$ and $\delta^{13}C$ from upland and wetland soil horizons.

**CHAPTER 2**

Figure 2.1 ..................................................................................................46
Digital Elevation Model of the UMBS landscape, with the Honeysuckle Creek watershed outlined in black.

Figure 2.2 ..................................................................................................52
Landscape Ecosystem map units of the Honeysuckle Creek watershed.

Figure 2.3 ..................................................................................................54
STI values across the Honeysuckle Creek watershed.

Figure 2.4 ..................................................................................................58
*C*-*Q* relationships for TSS, C, and biologically cycled anions ($NO_3^-$, $PO_4^{3-}$, $SO_4^{2-}$) at all three flumes (mouth, mid, upper), with season indicated by point shape and color.

Figure 2.5 ..................................................................................................60
Mean soil VWC within Landscape Ecosystem type groups during the period of observation (July–November 2015, April–November 2016).

Figure 2.6 ..................................................................................................63

Mean daily water table position within Landscape Ecosystem types and precipitation for June 2016–June 2017.

Figure 2.7 ... 65
Relationships between STI and soil VWC, by season, for sample points grouped by parent material (outwash v. till).

Figure 2.8 ... 67
Relationships between STI and water table position, by season, for individual wells.

**CHAPTER 3**

Figure 3.1 ... 89
Shallow groundwater wells and stream flumes across the Honeysuckle Creek watershed.

Figure 3.2 ... 93
Paired soil VWC and water table position measurements for 18 of the shallow groundwater wells sampled for chemistry. Three hydrologic groups (disconnected, periodically connected, consistently connected) were developed to describe three fundamental relationships between soil water in the top 20 cm of the profile and shallow groundwater.

Figure 3.3 ... 94
Precipitation and water table position for each hydrologic group during April–November 2017.

Figure 3.4 ... 100
Total streamflow at the mouth and mid flumes along Honeysuckle Creek, the estimated baseflow contribution to the stream, and precipitation for the April–November 2017 sampling period.

Figure 3.5 ... 101
Seasonal BFI values for the mouth and mid flumes during 2017.

Figure 3.6 ... 102
Precipitation, shallow groundwater, and surface water isotopes ($\delta^{18}O$, $\delta D$) for the spring, summer, and autumn seasons combined.

Figure 3.7 ... 103
Precipitation, shallow groundwater, and surface water isotopes ($\delta^{18}O$, $\delta D$) for the spring, summer, and autumn seasons.

Figure 3.8 ... 108
Mean DIC, $Ca^{2+}$, $Mg^{2+}$ concentrations, conductivity, and DOC $\delta^{13}C$ signatures by hydrologic group (D=disconnected, P=periodically connected, C=continuously connected).

Figure 3.9 ... 110
Mean DIC, $Ca^{2+}$, $Mg^{2+}$ concentrations, and conductivity by soil texture class (whole profile).

Figure 3.10 ... 111
Mean DOC concentration, DOC $\delta^{13}C$, and pH by well depth.

Figure 3.11 ... 113
Relationship between STI and DIC, $Ca^{2+}$, and conductivity.

Figure 3.12 ... 116
Mixing diagrams of shallow groundwater sources and surface waters based on DIC and DOC concentrations (panels A, C, E, G) and DIC $\delta^{13}C$ and $\delta D$ isotopic signatures (panels B, D, F, H).

Figure 3.13 ... 120
Distribution of soils across the upper, mid, and mouth watersheds.

LIST OF TABLES

**CHAPTER 1**

Table 1.1 .......... 16
Weekly mean precipitation chemistry by season from October 2015–September 2016.

Table 1.2 .......... 17
Mean stream water analyte concentrations ± SD during October 2015–August 2016 sample period.

Table 1.3 .......... 19
Two-Way ANOVA results for the comparison of stream analyte concentration by location (flume) and season.

Table 1.4 .......... 23
For analytes with no significant *C*-*Q* slope (flat shape), solute coefficient of variation $CV_C$ and the $CV_C/CV_Q$ ratio are presented here to indicate analytes trending towards chemostatic ($CV_C/CV_Q \leq 0.5$) and chemodynamic ($CV_C/CV_Q \geq 1.0$) behavior based on variability.

**CHAPTER 2**

Table 2.1 .......... 60
Soil VWC over the full period of observation and within each season, by ecosystem group.

Table 2.2 .......... 62
Water table position over the full period of observation and within each season, by ecosystem group.

**CHAPTER 3**

Table 3.1 .......... 105
Categorical physical factors that were significant predictors of variation in analyte concentration or water table position.

Table 3.2 .......... 105
Continuous physical factors showing significant correlations with analyte concentration or water table position.

Table 3.3 .......... 106
Summary of surface and shallow groundwater dissolved C concentrations and stable isotopes, $Ca^{2+}$, $Mg^{2+}$, pH and conductivity (mean ± SD) for each sample date.

Table 3.4 .......... 117
Summary of water table position from the surface [cm; median (25$^{th}$, 75$^{th}$ percentile)] by hydrologic group for each sampling time.

# CHAPTER 1

## SEASONAL DYNAMICS AND EXPORTS OF ELEMENTS FROM A FIRST-ORDER STREAM TO A LARGE INLAND LAKE IN MICHIGAN


***Abstract***

Headwater streams are critical components of drainage systems, directly connecting terrestrial and downstream aquatic ecosystems. The amount of water in a stream can alter hydrologic connectivity between the stream and surrounding landscape and is ultimately an important driver of what constituents headwater streams transport. To investigate temporal dynamics and spatial patterns of stream chemistry, we measured stream discharge and chemistry at three points along a forested headwater stream in northern Michigan during the 2015–2016 hydrologic year. We utilized concentration-discharge (*C*-*Q*) relationships to identify dynamics and potential sources of solutes in the stream. Along the headwater stream, surface flow was seasonal in the main stem and perennial flow was spatially discontinuous for all but the lowest reaches. Spring snowmelt was the dominant hydrological event in the year with peak flows an order of magnitude larger at the mouth and upper reaches, and more than twice as large at the mid reach than annual mean discharge. Stream chemistry varied longitudinally along the stream, with measured analyte concentrations generally highest at the mouth. At all flumes, $Ca^{2+}$, $Mg^{2+}$, TSS, DOC, and $SO_4^{2-}$ concentrations were the highest, while concentrations of most anions ($Br^-$, $PO_4^{3-}$, $F^-$, $NO_3^-$) were the lowest. All three *C*-*Q* shapes (positive, negative, flat) were observed at all locations along the stream, with a higher proportion of the analytes showing significant relationships at the mouth than at the mid or upper flumes. At the mouth, positive (flushing) *C*-*Q* shapes were observed for DOC and TSS, while negative (dilution) *C*-*Q* shapes were observed for most cations ($Na^+$, $Mg^{2+}$, $Ca^{2+}$) and biologically cycled anions ($NO_3^-$, $PO_4^{3-}$, $SO_4^{2-}$), as well as $Cl^-$

. Most analytes displayed significant *C-Q* relationships at the mouth, indicating that discharge is a significant driving factor controlling stream chemistry. However, the importance of discharge appeared to decrease moving upstream to the headwaters where other factors, such as parent material and vegetation distribution and groundwater inputs, become more dominant controls on stream chemistry patterns.

### ***Introduction***

Headwater streams are important conduits linking terrestrial and aquatic ecosystems, moving water, nutrients, and energy to downstream surface waters (Gomi et al., 2002; Carpenter et al., 2005; Freeman et al., 2007). Stream discharge is an important driver of the composition of dissolved and particulate matter in the stream and exported from a watershed. Changes in discharge can alter the hydrologic connectivity between streams and the surrounding landscape, as well as connections between ephemeral and perennially flowing stream reaches (Tockner et al., 1999; Pringle, 2003; Freeman et al., 2007; Tetzlaff et al., 2007). While headwater streams may be small in size, they account for at least 70% of the total stream length in typical river networks and are by far the largest proportion (>96%) of streams and rivers in the world (Leopold et al., 1964; Downing et al., 2012; Marx et al., 2017). Inputs from headwater streams can significantly influence the nutrient concentrations and the volume of water in higher order streams (Gomi et al., 2002; Alexander et al., 2007; MacDonald and Coe, 2007). In headwater systems, transport of material from terrestrial to aquatic zones is primarily influenced by runoff and shallow groundwater flow and biogeochemical cycling and transformations occurring in these systems can influence the larger drainage network (Brinson, 1993; McClain et al., 2003; Harvey and Gooseff, 2015; Raymond et al., 2016). Given the significance of these streams to downstream rivers and lakes, we sought to investigate terrestrial-aquatic linkages within headwater watersheds by determining the temporal dynamics and spatial patterns of carbon (C) and dissolved matter.

The relationship between solute concentration and stream discharge has long been used to investigate the transport of river materials and how changing hydrologic conditions impact water quality and nutrient exports (*e.g.,* Edwards, 1973; Foster and Walling, 1978; Walling and Webb, 1983; Williams, 1989). Concentration-discharge (*C*-*Q*) relationships have been used to identify positive (flushing), negative (dilution), and flat (often called chemostatic) solute trends (Godsey et al., 2009; Moatar et al., 2017). Solutes with positive *C*-*Q* relationships are often thought of as being transport-limited, while solutes with negative *C*-*Q* relationships are source-limited (Salmon et al., 2001; Basu et al., 2010; Thomas et al., 2016). For solutes with flat *C*-*Q* shapes, transport- and source-limitation are at an equilibrium, so neither process dominates. *C*-*Q* relationships are thought to be a reflection of solute distribution and availability throughout the watershed, the hydrologic connectivity between solute stores and the stream channel, and in-stream processing or reactivity (Musolff et al., 2015; Moatar et al., 2017). Often, flat *C*-*Q* shapes are observed for solutes that have effectively unlimited stores homogenously distributed throughout the watershed, or where external inputs are high and consistent, such as nutrients in agricultural or urban watersheds (Thompson et al., 2011; Herndon et al., 2015; Musolff et al., 2015; Duncan et al., 2017). Some papers consider all solutes with flat slopes to be chemostatic (*e.g.,* Godsey et al., 2009; Basu et al., 2010). Thompson et al. (2011) and Musolff et al. (2015) delve deeper into the flat slope *C*-*Q* relationship, using the ratio of coefficients of variation of concentration vs. discharge to distinguish solutes with very little variability in concentration (*e.g.,* $Mg^{2+}$, $Ca^{2+}$) from those with higher variability that is not directly related to changes in discharge (*e.g.,* $PO_4^{3-}$).

In *C*-*Q* analyses, dissolved C, suspended sediment, and major cations (*e.g.,* $Na^+$, $K^+$, $Mg^{2+}$,

$Ca^{2+}$) and anions (*e.g.*, $SO_4^{2-}$, $NO_3^-$, $PO_4^{3-}$, $Cl^-$) are often measured. The majority of these analytes are not conservative elements, *i.e.*, they can be bound in soil, biologically cycled, or transformed in the stream or surrounding soil. Because these differences in analyte sources and biogeochemical processing can influence their behavior, understanding their elemental properties can influence how we interpret their *C-Q* shapes. Dissolved organic carbon (DOC) is one of the most commonly measured solutes due to its importance for aquatic ecosystems and the C cycle (Elder et al., 2000; Lottig et al., 2013; Lambert et al., 2014; Marx et al., 2017). Much of the DOC measured in streams comes from terrestrial sources, such as organic rich soil horizons in riparian zones or wetlands (Elder et al., 2000; Inamdar et al., 2004). Carbon can be stored in streams (*e.g.*, sedimentation) and transformed between organic and inorganic forms through microbial or photochemical oxidation or photosynthesis (Schiff et al., 1997; Jonsson et al., 2007; Lottig et al., 2013). Biologically cycled anions include $NO_3^-$, $PO_4^{3-}$, and $SO_4^{2-}$. In temperate forests, $NO_3^-$ is a highly mobile form of a growth-limiting nutrient that is typically present in low concentrations, except where anthropogenic inputs or impacts are high; therefore, $NO_3^-$ in streams is likely produced in riparian zones through nitrification (Galloway and Cowling, 2002; Bernhardt et al., 2005; Dittman et al., 2007; Sebestyen et al., 2008). Not typically considered as growth-limiting as $NO_3^-$, $PO_4^{3-}$ and $SO_4^{2-}$ are also biologically cycled. The primary source of $PO_4^{3-}$ to streams comes from organic matter mineralization or $PO_4^{3-}$ bound to suspended sediments, while $SO_4^{2-}$ can come from atmospheric sources, geologic weathering, or organic matter mineralization (Johnson, 1984; Adams et al., 1989; Achat et al., 2010; Mayer et al., 2010). Major base cations ($Na^+$, $K^+$, $Mg^{2+}$, $Ca^{2+}$) are derived both from parent material weathering, often of carbonate and silicate materials, and mineralization of organic matter. These biologically cycled cations can also be adsorbed onto the cation exchange complex in soil and taken up by vegetation (Likens et al., 1967; Likens et al., 1994; Likens et al., 1998; Williams et al., 2007). Geologic parent material weathering can also be a source of highly soluble anions, such as $Cl^-$ and $F^-$, but typically concentrations are very low unless dominated by an anthropogenic source (*e.g.,* $Cl^-$ due to additions of road salt; Jones and Sroka, 1997; Williams et al., 2007; Musolff et al., 2015).

Recently, *C-Q* relationships have been analyzed across a wide range of watersheds with differing catchment areas, climate conditions, lithologies, land covers, and land management methods (*e.g.,* Burns et al., 2009; Godsey et al., 2009; Basu et al., 2010; Musolff et al., 2015; Thomas et al., 2016; Dupas et al. 2017; Moatar et al., 2017). The *C-Q* relationships for many solutes varied across these studies, with Godsey et al. (2009), Basu et al. (2010), and Thomas et al. (2016) concluding that chemostatic patterns dominated parent material weathering elements such as Si, $Na^+$, $Mg^{2+}$, and $Ca^{2+}$ (Godsey et al., 2009), and vegetation-limiting nutrients, such as $NO_3^-$ and $PO_4^{3-}$, in agricultural watersheds (Basu et al., 2010; Thomas et al., 2016). DOC has widely seen to have a positive, flushing *C-Q* relationship, particularly at high flows (Inamdar et al., 2004; Lambert et al., 2014; Moatar et al., 2017), but seen as chemostatic in some studies (Creed et al., 2015). Even Moatar et al. (2017), who observed significant *C-Q* relationships for elements seen as chemostatic in other studies, observed flat *C-Q* shapes for many solutes at low flows. Across all of these studies, solute concentrations varied less than discharge, suggesting that hydrological controls dominate stream chemistry even across catchments with varying sizes and physical characteristics. In contrast to the summary studies across much larger watersheds where chemostatic *C-Q* trends dominated for many analytes, especially at low flows (*e.g.*, Musolff et al., 2015; Moatar et al., 2017), studies that focused on smaller headwater catchments (80-162 ha) observed significant positive or negative *C-Q* relationships for most analytes measured. Herndon et al. (2015), Hoagland et al. (2017), and Hunsaker and Johnson (2017) did not necessarily observe the same *C*-*Q* shape for all analytes, but they did observe significant *C*-*Q* relationships for Mn, $Ca^{2+}$, $K^+$, $Cl^-$, Fe, Al, DOC, and $NO_3^-$. $Na^+$, $Mg^{2+}$, $SO_4^{2-}$, and Si relationships varied depending on study location. Importantly, the number of studies that explore the *C*-*Q* relationships of a wide range of analytes in temperate watersheds is limited, especially in small forested watersheds where the hydrological and ecological processes that control the processing and export of solutes can be directly investigated. The literature bias towards larger watersheds means that these processes are often likely obscured by multiple land covers, anthropogenic activities, and altered (or even counteracting) natural hydrologic and biogeochemical processes (Burns et al., 2009; Duncan et al., 2017).

Given the importance of headwater streams and this need for additional measurements of stream chemistry dynamics in them, we explored the temporal dynamics and spatial patterns of stream chemistry along a headwater stream in northern Michigan. Our forested 120 ha watershed provides the opportunity to explore how *C*-*Q* relationships vary along a stream that is experiencing the same climatic conditions throughout the watershed, isolating the influence of hydrologic connectivity, and identifying the potential influence of vegetation, and parent material distribution. In this analysis we are addressing three research questions: 1) what are the temporal and spatial patterns of discharge, suspended solids, dissolved C, cations, and anions along a first-order stream, 2) what *C*-*Q* relationships are observed at discrete sampling locations along the stream, and 3) what do these patterns indicate about connections between the stream and surrounding soils and landscape?

## ***Methods***

### *Study Area*

We measured stream discharge and chemistry along Honeysuckle Creek, a headwater stream discharging into Michigan's 4$^{th}$ largest inland lake, Burt Lake (6,900 ha). The 120 ha Honeysuckle Creek watershed is located within the University of Michigan Biological Station (UMBS) land holdings in northern Lower Michigan, USA (45.56°, -84.72°) (Figure 1.1). The climate of the region is continental with a mean annual temperature of 5.5°C and mean annual precipitation of 817 mm, including 294 cm of snow (Nave et al., 2017b). Mixed deciduous and conifer species dominate the forests of this landscape and the broader region, including *Populus* spp., *Acer* spp., *Pinus* spp., and *Quercus rubra,* with *Thuja occidentalis, Abies balsamea,* and *Tsuga canadensis* in the low-lying wetland areas (Nave et al., 2017a). The Honeysuckle Creek watershed and surrounding landscape is characterized by glacial and postglacial landforms that were formed in drift deposited at the end of the Laurentian glaciation (14,000-10,000 years before present) and modified by the large, postglacial Lake Algonquin (11,500-10,500 years before present) and Lake Nippissing (5,000-3,000 years before present; Spurr and Zumberge, 1956; Blewett and Winters, 1995; Lapin and Barnes, 1995). The Silurian limestone and Devonian shale bedrock is overlain by 100-200 m of glacial drift, with wasting ice depositing glacial till as moraines that were later capped by meters of outwash during the final stages of glacial retreat. The Honeysuckle Creek watershed begins at the top of an interlobate moraine (276 m above sea leve, asl), has outwash, till, and lacustrine (dunes, beach ridges) landforms in the middle elevations (255 m to 190 m), and includes an outwash-lake plain wetland (190-181 m) along the shore of Burt Lake. Soils of the upper elevations of the watershed (*i.e.*, the uppermost ~1 km of the watershed) were formed in deep, coarse-textured outwash (Entic and Lamellic Haplorthods) with little water holding capacity. In the middle (about 1 km) of the watershed, soils are finer-textured with restrictive glacial till close to the surface (Alfic Haplorthods, Alfic Epiaqods, Mollic Endoaquents) promoting episaturation and surface water in stream channels. Below 190 m elevation, the outwash-lake plain wetland soils are Terric Haplosaprists with consistent groundwater levels within 10 cm of the surface and perennial surface water in the stream (Nave et al., 2017a). Several seasonal sand tracks run through the watershed and a paved road runs between the mid and mouth flumes roughly parallel to the 190 m contour line (Figure 1.1).

*Field Measurements*

We installed modified Parshall flumes at three locations along Honeysuckle Creek (Figure 1.1) and measured stream stage and calculated stream discharge based on USGS methods (Kilpatrick and Schneider, 1983). We measured stream stage approximately weekly at all three flumes (mouth, mid, upper) from October 2015–September 2016 to capture stream dynamics over the course of an entire hydrologic year. In addition to stream discharge, we measured stream temperature at the mouth of the stream from October 2015–February 2016 (with Onset HOBO Pendant Temperature Data Loggers, Onset Computer Corporation, Bourne, MA) and May 2016–October 2016 (Solinst Levelogger, Solinst Inc., Georgetown, ON, CA). Meteorological (air temperature, precipitation, snow depth) measurements were taken at daily UMBS laboratory facilities approximately 3 km away from the watershed. Weekly chemical composition of precipitation at the UMBS facility (site MI09) was reported as part of the National Atmospheric Deposition Program (NRSP-3, 2018). Stream samples were taken at the same time as stream stage measurements from October 2015–August 2016. We collected water samples at each flume in HDPE bottles, which were kept on ice in the field and transferred to a refrigerator (4°C) within 8 hours of sample collection. Soil samples were taken in the wetland and upland areas of the watershed for separate projects (2014–2017) and are being used in this analysis to provide context for the $\delta^{13}C$ measured in the stream water. Wetland soil sampling and processing methods are described in Nave et al. (2017a). Upland soil samples were taken across the watershed above 255 m elevation with an AMS slide-hammer sampler (split-wall corer 5.2 cm in diameter, 30 cm in length, with clear polycarbonate liners) and two representative profiles were selected for laboratory analysis.

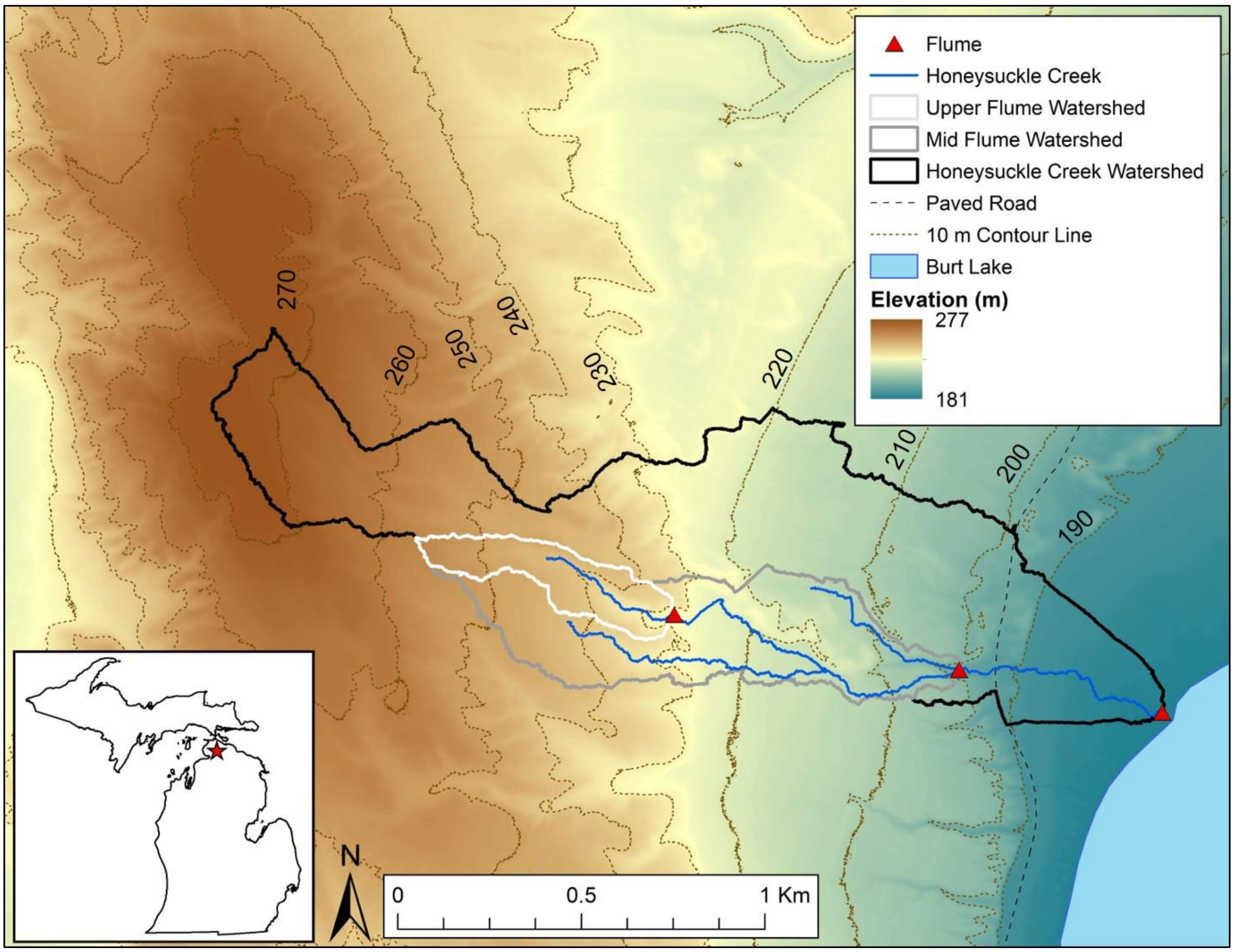


Figure 1.1: Honeysuckle Creek watershed (black outline) and subwatersheds (mid flume is gray, upper flume is white) in northern Lower Michigan (see inset). Three flumes were located along Honeysuckle Creek (mouth at 181 m elevation, mid around 200 m, upper around 230 m). A paved road (dashed line) runs roughly parallel to the 190 m and 200 m elevation contour lines.

*Laboratory Analysis*

In the UMBS Analytical Chemistry Laboratory, stream water samples were filtered through pre-ashed 0.7 µm glass-fiber filters within 24 hours of field collection and were kept refrigerated at 4°C until analysis. Pre and post-filter weights was used to determine total suspended solids (TSS) for each sample. Filtered water samples were analyzed for anions ($Cl^-$, $F^-$, $Br^-$, $NO_3^-$, $PO_4^{3-}$, $SO_4^{2-}$) and cations ($Na^+$, $K^+$, $Mg^{2+}$, $Ca^{2+}$) with an ion chromatogram (Thermo Scientific Dionex Integrion HPLC system, Thermo Fisher Scientific, Inc., Waltham, MA). DOC concentration and stable C isotope signatures were measured with a total organic carbon analyzer (Aurora 1030W TOC Analyzer, OI Analytical, Xylem Inc., College Station, TX) coupled to an isotope ratio mass spectrometer (Thermo Scientific Delta V Advantage IRMS, Thermo Fisher Scientific, Inc., Waltham, MA). Organic soil samples taken in the wetland were processed according to Nave et al. (2017a). Upland mineral soil samples were separated by genetic horizon and then air-dried, weighed, and sieved (2 mm). These soil samples were then density separated in the Carbon, Water and Soils Laboratory at the USDA-Forest Service Northern Research Station (Houghton, MI) as described by Heckman et al. (2014) into free light, occluded light, and heavy fractions. Upland bulk horizons (AE, Bs1, E'Bt) and wetland organic soil horizons (Oa1, Oa2, Oa3) were ball milled and run for C concentration and $\delta^{13}C$ [CHN analyzer (Costech Analytical Technologies, Inc., Valencia, CA) coupled to an isotope ratio mass spectrometer (Finnigan Delta Plus XL IRMS, Thermo Fisher Scientific Inc., Waltham, MA)]. To infer the relative age of the soil C pools contributing to stream water DOC, wetland organic soil horizons and upland soil density fractions were prepared for radiocarbon ($^{14}C$) analysis by graphitization (Vogel et al., 1987), followed by measurement by accelerator mass spectrometry at Lawrence Livermore National Laboratory (Davis et al., 1990). Radiocarbon abundances were normalized by the international radiocarbon standard, oxalic acid 1, and corrected for mass-dependent fractionation according to Stuiver and Polach (1977). Radiocarbon data for the wetland horizons are available in the supplementary table from Nave et al. (2017a). To express radiocarbon values for upland soil horizons in this analysis, we computed bulk upland horizon $^{14}C$ as the weighted average $^{14}C$ values and mass proportions of each density fraction. Raw upland soil fraction $^{14}C$ data are available in supplementary information in Nave et al. (In Review). In this manuscript we report $^{14}C$ values according to $\Delta^{14}C$ notation, as that is the most direct metric of $^{14}C$ abundance, carries fewer assumptions, and has a lower risk of mis-interpretation compared to other notations.

*Data Analysis*

We used non-parametric Kruskal Wallis One-Way ANOVA on Ranks with Dunn's Method of Comparisons tests to compare daily precipitation amounts and weekly precipitation chemical concentrations among seasons to assess potential seasonal differences in precipitation patterns or chemical inputs to the watershed through precipitation. Because we used two different temperature loggers to measure stream temperature at the stream mouth, there was a gap in data collection from February 11, 2016–May 4, 2016. During this period, we used an exponential regression to estimate mean daily stream temperature from 3-day mean air temperature. This relationship between air and stream temperature was strong based on coefficient of determination ($R^2$=0.838) and Nash Sutcliffe Efficiency (NSE=0.811) metrics (data not shown). We used Two-Way ANOVAs to assess temporal and spatial differences in stream chemical concentrations across the watershed. We used season (spring, summer, autumn, winter) and location (the three flumes) as the temporal and spatial factors, respectively. We utilized meteorological seasonal divisions [Spring (MAM), Summer (JJA), Autumn (SON), Winter (DJF)]. We set sample concentrations below analytical detection limit equal to zero and transformed non-normal data using squared, log, and log(x+1) transformations when necessary. We accepted results as statistically significant when $p<0.05$. Due to the very low number of samples where $Br^-$ concentrations were above analytical detection limit, we have excluded $Br^-$ from this analysis.

To assess the influence of stream discharge on chemical concentration, we examined the relationship between concentration ($C$) and discharge ($Q$) at each flume for each analyte. We used the power function that has been used by others (*e.g.*, Basu et al., 2010; Musolff et al., 2015; Moatar et al., 2017) to relate log-transformed $C$ and $Q$. We used log(x+1) transformations of both $C$ and $Q$, to include below detection limit (*i.e.*, zero) values in this analysis. This relationship takes the form:

$$C = aQ^b \qquad (1)$$

where $C$ is concentration, $Q$ is discharge, $a$ is a coefficient with units of concentration, and $b$ is a unit-less exponent representing the slope of the log(x+1)-transformed $C$-$Q$ relationship. The slope ($b$) of the $C$-$Q$ relationship provides insights into the availability, transport capacity, and sources of elements across the watershed. $C$-$Q$ relationships can be divided into positive ($b\geq0$), negative ($b\leq0$), or flat ($b=0$) shapes based on the p-value ($p<0.05$) (Godsey et al., 2009; Musolff et al., 2015; Moatar et al., 2017). Strength of the relationship was assessed on the basis of the coefficient of determination ($R^2$). Positive slopes have been interpreted as enhanced, flushing, or transport-limited elements, while negative slopes have been interpreted as dilution or source-limited materials. Other researchers have observed that many elements exhibit flat $C$-$Q$ shapes ($b=0$ or close to 0) and have described these elements as chemostatic, or as having no change in concentration with discharge (*e.g.*, Godsey et al., 2009; Basu et al., 2010). We have used the divisions proposed by Thompson et al. (2011) and Musolff et al. (2015) to divide analytes with flat $C$-$Q$ shapes into 'chemostatic,' 'chemodynamic,' or 'no trend' groups based on the ratio of coefficients of variation of analyte concentration and discharge ($CV_C/CV_Q$). Analytes with $CV_C/CV_Q \leq 0.5$ are considered chemostatic, $CV_C/CV_Q \geq 1.0$ are considered chemodynamic, and $CV_C/CV_Q$ between these thresholds are considered as having no distinct trend. While other researchers have explored *C-Q* relationships after segmenting their datasets into different flow regimes (*e.g.*, low, high; Herndon et al., 2015; Moatar et al., 2017), we grouped samples from all seasons together to strengthen statistical power for this analysis. We have used point color and shape in *C-Q* relationship figures to group points by season, which for the most part corresponds to different flow regimes. We used a linear regression to relate $\Delta^{14}C$ and $\delta^{13}C$ measured in wetland organic horizons and upland mineral soil density fractions. We have included these data to provide context for the DOC quality (as interpreted from $\delta^{13}C$) in the stream. We used R (Version 3.4.3; R Core Team, 2017) and SigmaPlot (SYSTAT Software, San Jose, CA) to perform statistical analyses.

## ***Results***

### *Stream Discharge and Precipitation Patterns*

Throughout the year of study (October 2015–September 2016) Honeysuckle Creek flow was ephemeral and seasonal, with perennial flow only below 185 m elevation. During the spring snowmelt period (March–April), Honeysuckle Creek flowed continuously for 1.7 km from its headwaters at 236 m elevation to the mouth (181 m). Stream flow was ephemeral at the upper flume (227 m) and for much of the stream reach above 206 m elevation, with surface water beginning to dry up in July and intermittent flow during late summer and autumn after large storm events. At the mid flume (195 m), surface water persisted even in the driest season, although during this time surface water downstream of the flume became disconnected from the perennially flowing stream below 185 m elevation. In the driest season, Honeysuckle Creek surface flow was continuous for an approximately 360 m long reach through the wetland to the confluence with Burt Lake. Stream discharge was highest at the mouth (1,126 ± 809 L $min^{-1}$; mean ± SD), then the middle flume (186 ± 285 L $min^{-1}$), and lowest at the upper flume (47 ± 63 L $min^{-1}$). Across all flumes, discharge was the highest during the spring snowmelt period, ranging from 123 L $min^{-1}$ at the upper flume to 2,627 L $min^{-1}$ at the mouth, and lowest during August when there was no surface water at the upper flume and stream flow was 22-466 L $min^{-1}$ at the other flumes (Figure 1.2). At the mouth, only spring and summer stream flows differed significantly, while at the mid flume, spring discharge was significantly larger than discharge at all other seasons. At the upper flume, stream flow during spring and winter was higher than summer and autumn flows, but not significantly different from each other. Stream temperatures at the mouth were warmest in the summer (13.6° ± 1.6° C) and coldest in the winter (3.6° ± 1.3° C), closely tracking air temperatures.

Precipitation during the study period totaled 1,090 mm, with the most falling during the autumn (327 mm), winter (283 mm), and spring (270 mm) months. The 2015-2016 hydrologic year was wetter than an average year when mean precipitation equals 817 mm. Precipitation during the winter and early spring period typically fell as snow and remained in the watershed until melt began in early March (Figure 1.2). Median daily precipitation amounts were similar in most seasons and only differed between winter and summer months (Figure 1.3). Inputs of cations and $Cl^-$ due to precipitation were likely negligible, as seasonal precipitation concentrations of these analytes were two ($Na^+$, $K^+$, $Cl^-$) to three ($Mg^{2+}$, $Ca^{2+}$) orders of magnitude smaller than seasonal stream concentrations (Table 1.1). Concentrations of $SO_4^{2-}$ in precipitation were only one order of magnitude smaller than concentrations in stream water, while seasonal $NO_3^-$-N concentrations in precipitation (0.11-0.30 mg $L^{-1}$) were only slightly smaller than stream concentrations (0.43-

0.48 mg $L^{-1}$).

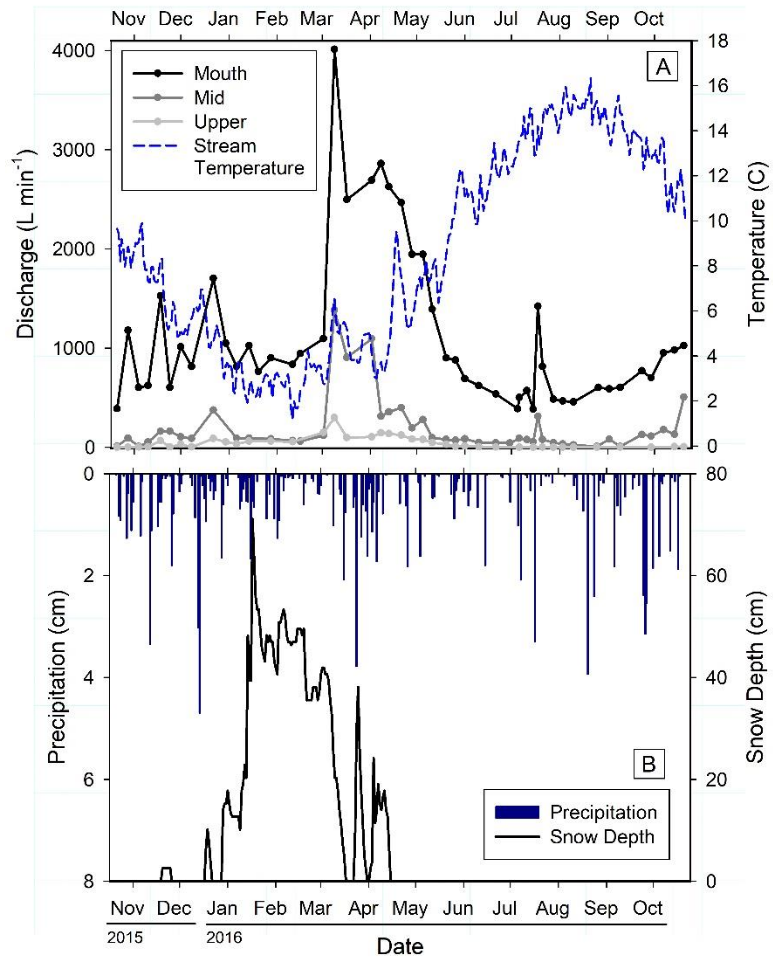


Figure 1.2: Honeysuckle Creek discharge at all three flumes (mouth, mid, upper) and stream temperature at the mouth shown in the top panel (A) during the 2015-2016 hydrologic year. Note: stream temperature during Feb 12-May 4, 2016 was estimated from air temperature as described in the methods. Precipitation and snow depth are shown in the bottom panel (B). Over this time period, discharge was highest at the mouth (1,126 ± 809 L $min^{-1}$; mean ± SD), then the middle flume (186 ± 285 L $min^{-1}$), and lowest at the upper flume (47 ± 63 L $min^{-1}$).

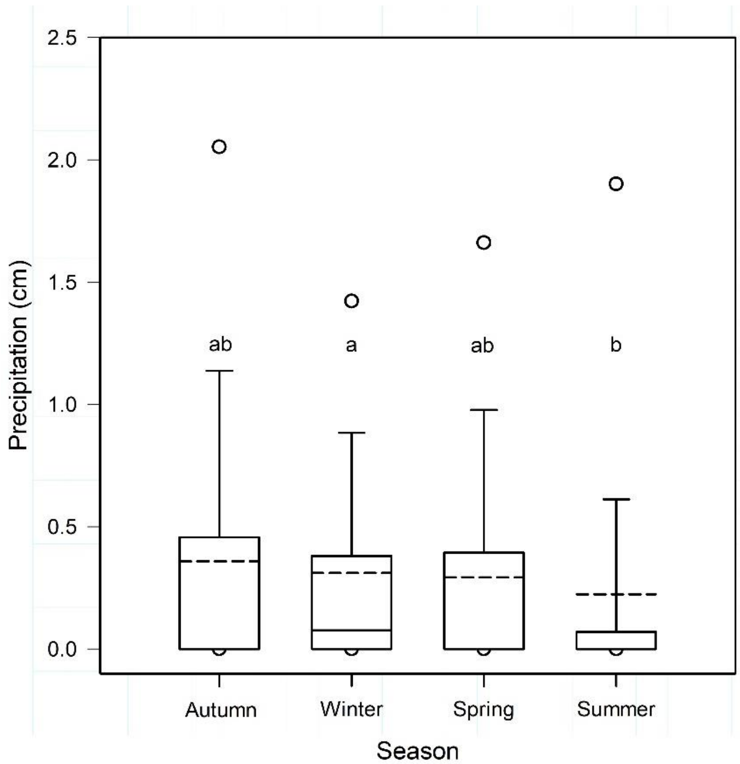


Figure 1.3: Distribution of daily precipitation measured during the study year (October 2015–September 2016), with median values indicated by solid lines and mean values by dashed lines. Whiskers indicate 25th and 75th percentiles and circles indicate 5th and 95th percentiles. Median daily precipitation differed significantly only between winter and summer seasons ($p$<0.05). Statistical significance indicated by different letters.

Table 1.1: Weekly mean precipitation chemistry by season from October 2015–September 2016 (mean ± SD).

| Analyte (mg $L^{-1}$) | Autumn | Winter | Spring | Summer |
|---|---|---|---|---|
| $NO_3^-$-N | 0.11 ± 0.04 | 0.29 ± 0.18 | 0.17 ± 0.10 | 0.28 ± 0.21 |
| $SO_4^{2-}$ | 0.40 ± 0.19 | 0.57 ± 0.38 | 0.56 ± 0.17 | 0.56 ± 0.34 |
| $Na^+$ | 0.03 ± 0.02 | 0.06 ± 0.09 | 0.04 ± 0.03 | 0.03 ± 0.04 |
| $K^+$ | 0.01 ± 0.01 | 0.01 ± 0.01 | 0.02 ± 0.02 | 0.02 ± 0.02 |
| $Mg^{2+}$ | 0.02 ± 0.01 | 0.02 ± 0.02 | 0.03 ± 0.02 | 0.05 ± 0.02 |
| $Ca^{2+}$ | 0.09 ± 0.05 | 0.20 ± 0.30 | 0.22 ± 0.13 | 0.28 ± 0.23 |
| $Cl^-$ | 0.04 ± 0.04 | 0.10 ± 0.14 | 0.05 ± 0.4 | 0.07 ± 0.07 |

*Temporal Dynamics and Spatial Patterns of Stream Chemistry*

Stream chemistry varied longitudinally along the stream, with the highest concentrations of all analytes generally measured at the mouth. The order of analytes with the highest to lowest concentrations varied slightly across flumes, but overall trends were similar. At all flumes, $Ca^{2+}$ (30.6-40.8 mg $L^{-1}$), $Mg^{2+}$ (10.6-13.6 mg $L^{-1}$), TSS (8.5-13.4 mg $L^{-1}$), DOC (3.5-4.5 mg $L^{-1}$), and $SO_4^{2-}$ (3.0-4.3 mg $L^{-1}$) concentrations were the highest, while many anion concentrations were the lowest [$Br^-$ (majority of samples were below detection limit, 0.01 mg $L^{-1}$); $PO_4^{3-}$-P (0.0035-0.0096 mg $L^{-1}$); $F^-$ (0.036-0.048 mg $L^{-1}$); $NO_3^-$-N (0.40-0.49 mg $L^{-1}$)] (Table 1.2).

Table 1.2: Mean stream water analyte concentration ± SD during October 2015–August 2016 sample period. Superscript letters denote significant differences in concentration by location; see Table 1.3 for location, season, and interaction p-values. Asterisks beneath table indicate significant location by season interactions.

| Analyte (mg $L^{-1}$) | Mouth | Mid | Upper |
|---|---|---|---|
| TSS * | 13.05 ± 12.69*a* | 13.44 ± 13.94*a* | 8.45 ± 8.41*b* |
| DOC | 4.5 ± 3.1*a* | 4.3 ± 1.9*a* | 3.5 ± 1.23*a* |
| $NO_3^-$-N | 0.493 ± 0.048*a* | 0.400 ± 0.053*b* | 0.451 ± 0.045*c* |
| $PO_4^{3-}$-P † | 0.01 ± 0.005*a* | 0.004 ± 0.01*b* | 0.003 ± 0.002*b* |
| $SO_4^{2}$ ‡ | 4.31 ± 0.66*a* | 2.98 ± 1.04*b* | 3.28 ± 1.16*c* |
| $Na^+$ | 5.59 ± 1.14*a* | 1.46 ± 0.53*b* | 1.16 ± 0.24*b* |
| $K^+$ § | 1.08 ± 0.48*a* | 1.18 ± 0.41*a* | 1.03 ± 0.37*a* |
| $Mg^{2+}$ | 13.51 ± 2.15*a* | 10.59 ± 2.53*b* | 13.61 ± 4.62*a* |
| $Ca^{2+}$ | 34.85 ± 5.41*a* | 30.58 ± 18.48*b* | 40.79 ± 33.04*a* |
| $Cl^-$ | 6.35 ± 1.29*a* | 0.51 ± 0.15*b* | 0.45 ± 0.13*c* |
| $F^-$ | 0.048 ± 0.027*a* | 0.046 ± 0.027*a* | 0.036 ± 0.026*b* |
| DOC $\delta^{13}C$ ‰ | -25.91 ± 0.46*a* | -26.67 ± 0.43*b* | -26.57 ± 0.27*b* |

* Interaction: Mouth, Mid greater than Upper in spring; no difference between locations in other seasons

† Interaction: Mouth greater than Mid, Upper in autumn, winter; Mouth greater than Mid in spring, summer

‡ Interaction: All locations different in spring, summer; no difference between locations in autumn

§ Interaction: Mid lower than Mouth and Upper in summer; no difference between locations in other seasons

To investigate temporal dynamics and spatial patterns along the stream, we compared analyte concentrations by season and location (flume) (Table 1.3). Concentrations of major elements varied between locations along the stream and between seasons. Overall, concentrations of all analytes except TSS, DOC, and $K^+$ differed between flumes, and all analyte concentrations except $Ca^{2+}$ and $PO_4^{3-}$ had significant seasonal dynamics. Statistically significant season by location interactions were apparent for TSS, $SO_4^{2-}$, $PO_4^{3-}$, and $K^+$ (Table 1.3). Differences in analyte concentrations between flumes depended on the type of analyte (Table 1.2). Biologically cycled analytes ($NO_3^-$, $PO_4^{3-}$, $SO_4^{2-}$) were in higher concentrations at the mouth than the other flumes, along with $Na^+$ and $Cl^-$. The $NO_3^-$, $SO_4^{2-}$, and $Cl^-$ concentrations also differed between the mid and upper flumes, with higher $NO_3^-$ and $SO_4^{2-}$ and lower $Cl^-$ concentrations at the upper flume. The concentrations of some cations derived through parent material weathering and organic matter mineralization ($Ca^{2+}$, $Mg^{2+}$, and $K^+$ in summer) were not different at the mouth or upper flume and were lower at the mid flume (Table 1.2). Seasonal differences in analyte concentrations were not consistent for analytes within the same 'biogeochemical groups.' Specifically, concentrations of some analytes (*e.g,* DOC, $K^+$, $F^-$) varied much more by season than by location, based on their Two-Way ANOVA F statistics (Table 1.3). In contrast, spatial differences in $Na^+$, $Cl^-$, and $PO_4^{3-}$ concentration were much larger than seasonal differences. Only $PO_4^{3-}$, $K^+$, $Ca^{2+}$, and $F^-$ displayed any relationship with stream temperature, with increasing concentration with higher temperatures.

Table 1.3: Two-Way ANOVA results for the comparison of stream analyte concentration by location (flume) and season. F statistic and p-values are given for the location, season, and interaction effects for each analyte.

| Analyte | Location | | Season | | Interaction | |
|---|---|---|---|---|---|---|
| | F | p-value | F | p-value | F | p-value |
| TSS | 0.414 | 0.662 | 4.389 | 0.007 | 2.711 | 0.019 |
| DOC | 0.906 | 0.408 | 18.779 | <0.001 | 0.901 | 0.498 |
| DOC $\delta^{13}C$ | 37.266 | <0.001 | 9.252 | <0.001 | 0.416 | 0.416 |
| $NO_3^-$-N | 21.933 | <0.001 | 4.435 | 0.016 | 0.964 | 0.435 |
| $PO_4^{3-}$-P | 31.004 | <0.001 | 8.786 | 0.092 | 2.298 | 0.044 |
| $SO_4^{2-}$ | 43.741 | <0.001 | 49.106 | <0.001 | 7.838 | <0.001 |
| $Na^+$ | 216.963 | <0.001 | 6.981 | <0.001 | 1.188 | 0.323 |
| $K^+$ | 1.555 | 0.218 | 13.348 | <0.001 | 2.485 | 0.031 |
| $Mg^{2+}$ | 15.728 | <0.001 | 16.533 | <0.001 | 1.249 | 0.292 |
| $Ca^{2+}$ | 5.191 | 0.008 | 2.085 | 0.11 | 0.837 | 0.546 |
| $Cl^-$ | 910.496 | <0.001 | 3.217 | 0.028 | 1.669 | 0.141 |
| $F^-$ | 4.632 | 0.013 | 28.120 | <0.001 | 0.752 | 0.610 |

*Concentration-Discharge Relationships*

Because observed seasonal differences in analyte concentrations might be due to seasonal differences in stream flow, we utilized *C-Q* relationships to better quantify the influence of discharge on chemical concentration in the stream at all three flumes. All three *C-Q* shapes (positive, negative, flat) were observed at all locations along the stream. Moving downstream, a larger proportion of the analytes displayed either a significant positive or negative shape as the contributing area increased from the upper, to the mid, and ultimately to the mouth flume. At the mouth, all analytes displayed either a positive or negative *C-Q* relationship except $K^+$ and $F^-$. Positive (flushing) *C-Q* relationships were observed for DOC and TSS at the mouth and mid flumes, and the DOC *C-Q* relationship showed a positive tendency ($p$=0.063) at the upper flume (Figure 1.4). A negative (dilution) *C-Q* relationship was observed for most cations ($Na^+$, $Mg^{2+}$, $Ca^{2+}$) and biologically cycled anions ($NO_3^-$, $PO_4^{3-}$, $SO_4^{2-}$), as well as $Cl^-$ (Figure 1.5, 1.6). These relationships were most pronounced at the mouth, although dilution shapes were also observed for $NO_3^-$, $Na^+$, and $Mg^{2+}$ at the mid flume and for $Mg^{2+}$ at the upper flume. At the mouth, $K^+$ and $F^-$

displayed flat slopes with a smaller range of concentrations measured than variation in discharge. Moving upstream to the mid flume, more analytes displayed flat *C*-*Q* shapes ($PO_4^{3-}$, $SO_4^{2-}$, $K^+$, $Ca^{2+}$, $Cl^-$, $F^-$) and at the upper flume most analytes had flat slopes ($NO_3^-$, $PO_4^{3-}$, $SO_4^{2-}$, $Na^+$, $K^+$, $Ca^{2+}$, $Cl^-$, $F^-$). For the analytes displaying flat *C*-*Q* slopes, we used the ratio of $CV_C$ to $CV_Q$ to identify strongly chemostatic and strongly chemodynamic elements (Table 1.4). While most of these analytes could be grouped as chemostatic, $PO_4^{3-}$ was chemodynamic at the mid flume and showed no strong trend at the upper flume. The chemostatic analytes included biologically associated elements ($SO_4^{2-}$, $NO_3^-$), minerals weathered from parent material and mineralized from organic matter ($K^+$, $Ca^{2+}$, $Na^+$), and highly mobile anions associated with parent material weathering ($Cl^-$, $F^-$). Some of these analytes had chemostatic characteristics at one flume but had no distinct trend at other flumes, such as $K^+$, $Ca^{2+}$, and $F^-$, which were static at the mid flume, but showed no trend at the upper flume ($Ca^{2+}$, $F^-$) or mouth ($K^+$, $F^-$).

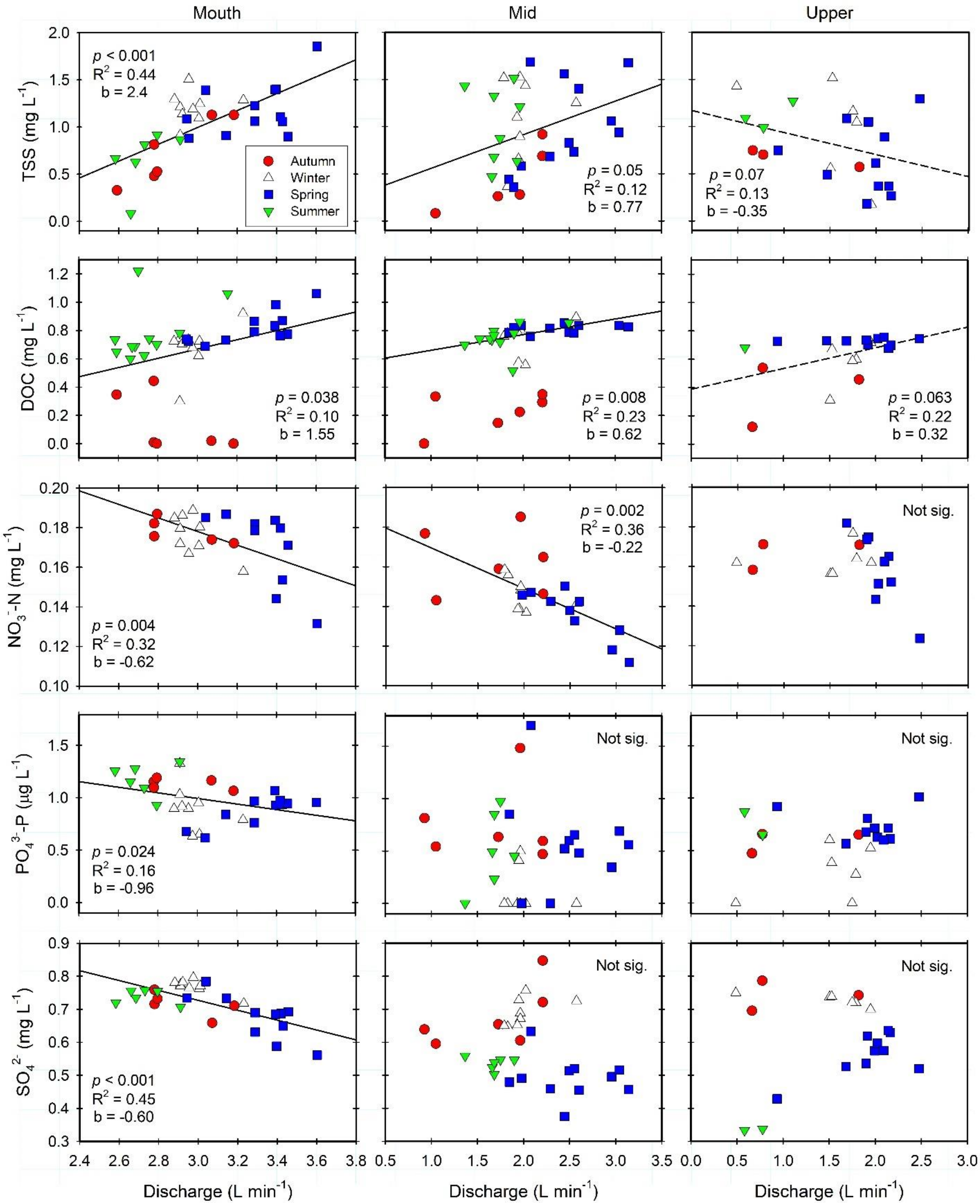


Figure 1.4: *C-Q* relationships for TSS, C, and biologically cycled anions ($NO_3^-$, $PO_4^{3-}$, $SO_4^{2-}$) at all three flumes (mouth, mid, upper), with season indicated by point shape and color. Power relationship significance and strength assessed by p-values and $R^2$ values; slope (*b*) of the relationship is also given.

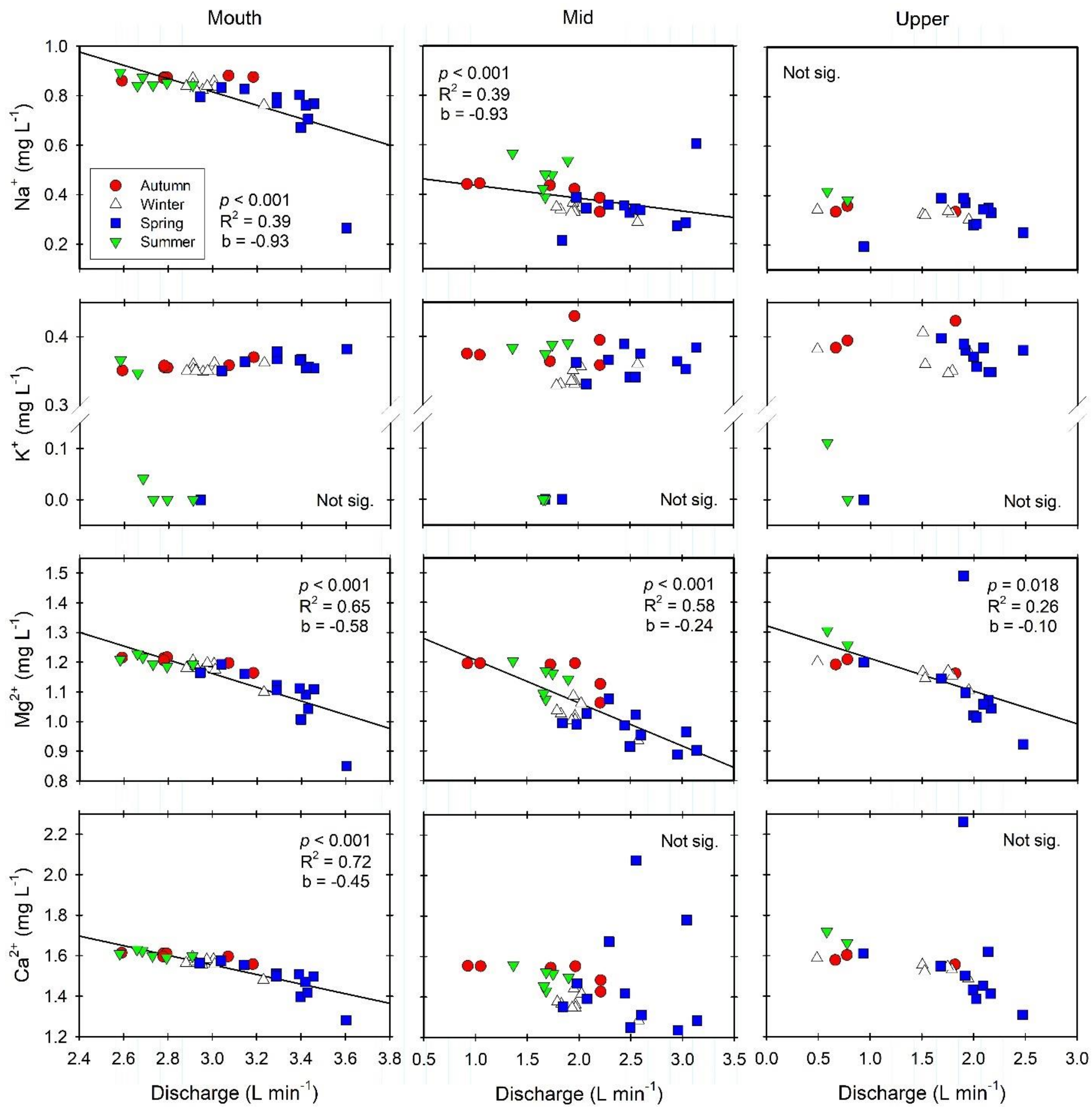


Figure 1.5: *C-Q* relationships for cations ($Na^+$, $K^+$, $Mg^{2+}$, $Ca^{2+}$) at all three flumes (mouth, mid, upper), with season indicated by point shape and color. Power relationship significance and strength assessed by p-values and $R^2$ values; slope (*b*) of the relationship is also given.

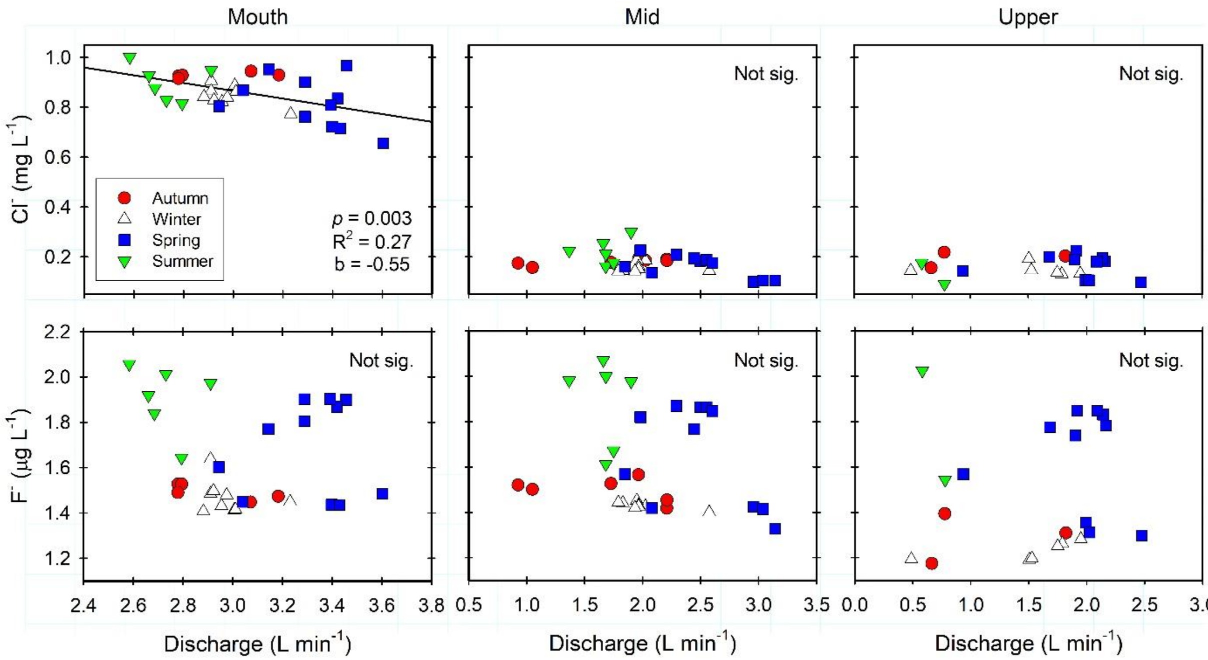


Figure 1.6: *C-Q* relationships for anions ($Cl^-$, $F^-$) associated with parent material weathering at all three flumes (mouth, mid, upper), with season indicated by point shape and color. Power relationship significance and strength assessed by p-values and $R^2$ values; slope (*b*) of the relationship is also given.

Table 1.4: For analytes with no significant *C-Q* slope (flat shape), solute coefficient of variation $CV_C$ and the $CV_C/CV_Q$ ratio are presented here to indicate analytes trending towards chemostatic ($CV_C/CV_Q \leq 0.5$) and chemodynamic ($CV_C/CV_Q \geq 1.0$) behavior based on variability. Analytes are organized by location (flume) and $CV_C/CV_Q$ ratio, beginning with the most variable chemodynamic analytes (noted with a D), followed by analytes with no distinct trend (noted with N), and ending with low-variability chemostatic analytes (noted with S).

| Location | Analyte | $CV_C$ (%) | $CV_C/CV_Q$ | Trend |
|---|---|---|---|---|
| Mouth | $F^-$ | 56 | 0.83 | N |
| | $K^+$ | 43 | 0.61 | N |
| Mid | $PO_4^{3-}$-P | 213 | 1.5 | D |
| | $Ca^{2+}$ | 60 | 0.42 | S |
| | $F^-$ | 60 | 0.41 | S |
| | $K^+$ | 35 | 0.24 | S |
| | $SO_4^{2-}$ | 35 | 0.24 | S |
| | $Cl^-$ | 30 | 0.21 | S |
| Upper | $Ca^{2+}$ | 81 | 0.82 | N |
| | $F^-$ | 71 | 0.72 | N |
| | $PO_4^{3-}$-P | 65 | 0.66 | N |
| | $K^+$ | 40 | 0.40 | S |
| | $SO_4^{2-}$ | 35 | 0.36 | S |
| | $Cl^-$ | 30 | 0.30 | S |
| | $Na^+$ | 21 | 0.21 | S |
| | $NO_3^-$-N | 10 | 0.12 | S |

*Carbon Isotopes in the Stream and Soil*

All flumes displayed similar patterns with respect to DOC $\delta^{13}C$; higher DOC concentrations were more depleted in $\delta^{13}C$. Over the entire sample period the upper (-26.57 ± 0.27‰) and mid flumes (-26.67 ± 0.43‰) had significantly more depleted DOC than the mouth flume (-25.91 ± 0.46‰; Figure 1.7). Seasonally, DOC was most depleted in the spring, followed by winter, and most enriched in summer. There were not DOC $\delta^{13}C$ samples from the autumn. Wetland organic and upland mineral soil $\delta^{13}C$ values were more depleted in surficial horizons (Oa1 compared to Oa2 and Oa3; AE compared to Bs1 and E'Bt). In addition to having more depleted $^{13}C$ signatures, more surficial horizons also had more modern $\Delta^{14}C$ signatures (Figure 1.8). At the upper and mid flumes, higher DOC concentrations (DOC>4.5 mg $L^{-1}$) had $\delta^{13}C$ signatures similar to the fresher organic matter $\delta^{13}C$ present in the surface mineral soil horizon (AE=-26.33 to -27.57‰). High DOC concentrations at the mouth were similar in $\delta^{13}C$ composition surficial wetland organic soils (Oa1=-26.11 to -26.56‰).

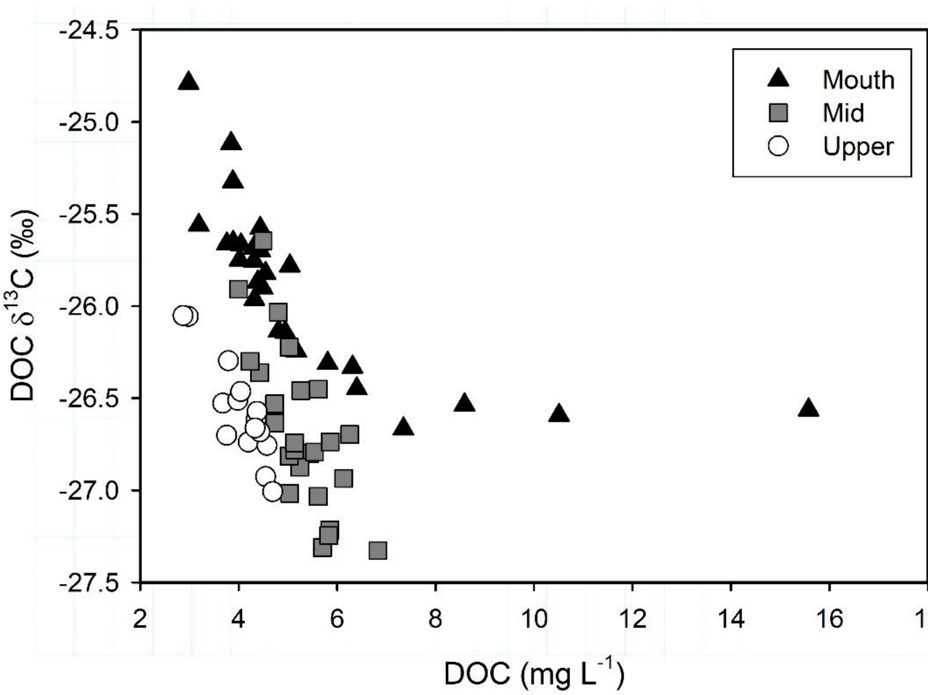


Figure 1.7: Stream DOC and DOC $\delta^{13}C$ at the mouth, mid, and upper flumes. The upper (-26.57 ± 0.27‰) and mid (-26.67 ± 0.43‰) flumes had significantly more depleted DOC $\delta^{13}C$ than the mouth (-25.91 ± 0.46‰). DOC was most depleted in the spring, followed by winter, and most enriched in summer. There are no DOC $\delta^{13}C$ samples from the autumn season.

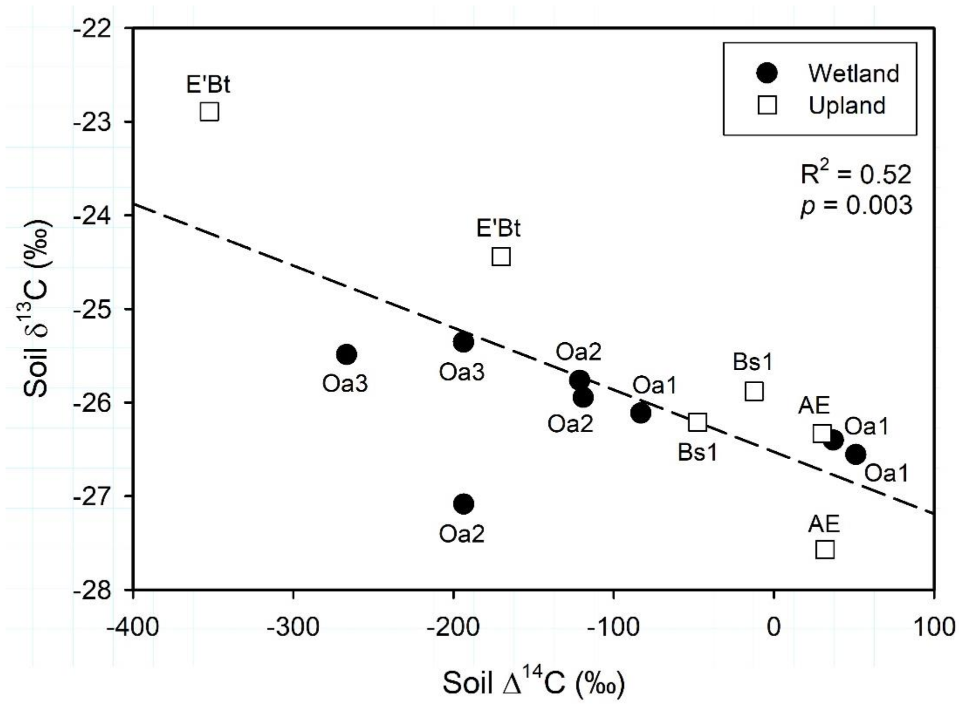


Figure 1.8: Measurements of soil carbon $\Delta^{14}C$ and $\delta^{13}C$ from upland and wetland soil horizons. Soil horizon is indicated above each point. Throughout the watershed, soils with more depleted $\delta^{13}C$ had more modern $\Delta^{14}C$ signatures and came from more surficial soil horizons; linear regression $R^2$=0.52.

***Discussion***

While other researchers have found that many of the analytes they measured displayed chemostatic behavior and had flat *C-Q* shapes with slopes below $|b|<0.2$ (Godsey et al., 2009; Basu et al., 2010; Thompson et al., 2011; Hunsaker and Johnson, 2017; Kim et al., 2017), we found that all Honeysuckle Creek *C-Q* relationships, with the exception of $Mg^{2+}$ at the upper flume, were strongly significant with slopes greater than $|b|>0.2$. Our results did generally agree with the findings of these researchers that solute concentrations vary less than discharge. Most of the analytes we measured displayed both temporal dynamics and spatial patterns, with differences in concentration at flumes and across seasons. Many of the seasonal differences we observed may be due to differences in seasonal stream flow, especially at the mouth, so *C-Q* relationships provided a direct analysis of the influence of discharge on stream chemistry. We observed positive, flushing *C*-*Q* shapes for DOC and TSS, negative, dilution *C*-*Q* shapes for $NO_3^-$, $PO_4^{3-}$, $SO_4^{2-}$, $Na^+$, $Mg^{2+}$, $Ca^{2+}$, and $Cl^-$, with less significant relationships at the mid and upper flumes.

In Honeysuckle Creek, higher stream flows were correlated with higher concentrations of DOC all along the stream and higher concentrations of TSS at the lower flumes. At all flumes higher DOC concentrations were more depleted in $\delta^{13}C$, and over the entire sample period the upper and mid flumes had significantly more depleted DOC than the mouth flume (Figure 1.7). At the upper and mid flumes higher DOC concentrations had $\delta^{13}C$ signatures similar to the fresher organic matter $\delta^{13}C$ present in the surface mineral soil horizon (AE=-26.33 to -27.57‰), while DOC at the mouth was similar in $\delta^{13}C$ composition a mix of litter/fibric and hemic/sapric wetland materials (Oa1 and Oa2; -27.0 to -26.26‰; Nave et al., 2017a). DOC $\delta^{13}C$ trends shifted seasonally, as spring DOC was the most depleted and summer the most enriched, suggesting that in the spring, the stream is transporting more depleted DOC at high concentrations, possibly including soluble C leached from surface soil horizons. DOC concentrations were lower during autumn and had a much shallower *C*-*Q* slopes than in other seasons, indicating a shift in *C*-*Q* relationships from low (autumn) to high flow periods (spring, summer), possibly due to in-stream processing of C, which Herndon et al. (2017) and Moatar et al. (2017) also observed. These results suggest that C is a transport-limited analyte and that concentrations in the stream depend primarily on discharge, not availability, as C sources are widely distributed throughout the watershed. During high flows, the C transported to the stream is likely from surficial soil horizons and is more similar to fresher (*i.e.*, more recently deposited and less decomposed) organic C sources that are near the stream but are not in contact with flowing water during low flow conditions. Other researchers have also observed transport-driven pulses of more depleted $^{13}C$, modern (based on $\Delta^{14}C$) DOC from surficial soil horizons during snowmelt or after large rainfall events (Schiff et al., 1997; Sebestyen et al., 2008; Sanderman et al., 2009; Lambert et al., 2011). More broadly, these increases in DOC concentrations at higher flows have been attributed to an expansion of saturated variable source areas and increased hydrologic connectivity from hillslope areas to riparian zones and stream channels (Boyer et al. 1997; Inamdar et al., 2004; Andrews et al., 2011; Lambert et al., 2014). Increased areal extent of soil saturation and rising water tables allows for flushing of soil DOC to the stream from organic rich soil horizons from distal wetland areas that are disconnected from the stream at lower flows (Hornberger et al., 1994; Brown et al., 1999; Inamdar et al., 2004; Grabs et al., 2012; Lottig et al., 2013; Gannon et al., 2015; Diamond and Cohen, 2018). While some of the DOC reaching the stream may be from upland hillslope sources, such as the DOC $\delta^{13}C$ at the upper and mid flumes that were within the range of upland soil fraction $\delta^{13}C$, most Honeysuckle Creek DOC likely derives from riparian zone soils due to their much larger C stocks compare to upland mineral soils (Elder et al., 2000; Lottig et al., 2013; Lambert et al., 2014). Furthermore, given the large wetland area (10 ha) that the stream flows through to the mouth, it is likely that the DOC entering Burt Lake is most similar in quality to the wetland soil horizons, and that ultimately, this large C reservoir (Nave et al., 2017a) is the primary source for C entering the lake. Lastly, because DOC and TSS both showed positive (flushing) *C-Q* relationships, it is likely that suspended solids account for an additional flux of C into Burt Lake, especially during peak events when high-energy stream flows can transport particulate organic matter.

In contrast to DOC and TSS, expanded connectivity between the stream and shallow soil horizons in riparian areas during high flows did not result in increased concentration of biologically cycled analytes or mineral weathering byproducts. Specifically, negative *C-Q* relationships for $NO_3^-$, $PO_4^{3-}$, and $SO_4^{2-}$ at the mouth and for $NO_3^-$ at the mid flume suggests that the availability of these analytes for in-stream transport is limited by biological activity, with large inputs of snowmelt or precipitation diluting the concentrations. For example, $NO_3^-$ is likely produced primarily in the stream or in very near-stream riparian areas during summer and autumn when low flow conditions favor net $NO_3^-$ production due to increased nitrification and decreased denitrification as the extent of saturated soils shrinks (Burns et al., 2009; Duncan et al., 2017). $NO_3^-$ availability in upland soils is very low, with practically no net nitrification in the top 30 cm of soil and very low concentrations in freely flowing soil water (<100 µg $L^{-1}$ 10 cm below the surface; <50 µg $L^{-1}$ at 60 cm) (Nave et al., 2009, 2011, 2014). With soil water $NO_3^-$ concentrations an order of magnitude less than stream $NO_3^-$, it is likely that in-stream or riparian zone biogeochemical processes and possibly precipitation are the primary sources of $NO_3^-$ to the stream. In a forested watershed Duncan et al. (2017) observed a dilution pattern for $NO_3^-$ when sampling at a weekly time step, however, high frequency sampling during storm events has revealed flushing of $NO_3^-$ with concentrations increasing on the rising limb of storm hydrographs (Inamdar et al., 2004; Duncan et al., 2017; Hunsaker and Johnson, 2017). It is possible that similar phenomena could be occurring in our watershed as near-stream $NO_3^-$ sources are flushed out during storm events and due to the slow production of $NO_3^-$ in those riparian areas, concentrations remain low and are diluted even further, especially during snow melt. A low $CV_C$ for $NO_3^-$ (10-13%) and $SO_4^{2-}$ (15-35%), and the chemostatic $CV_C/CV_Q$ ratio for $SO_4^{2-}$ at the mid and upper flumes and $NO_3^-$ at the upper flume, suggests that the availability of these mobile elements is relatively consistent (Moatar et al., 2017). In contrast, $PO_4^{3-}$ variability was high ($CV_C$ 50-213%) and the $CV_C/CV_Q$ ratio was chemodynamic at the mid flume and did not show a chemostatic trend at the upper flume. $PO_4^{3-}$ also displayed a significant positive relationship with stream temperature, suggesting that biological modulation may be a stronger controlling factor of concentrations than discharge. Higher variability in phosphorus (TP, $PO_4^{3-}$) has also been observed by Thompson et al. (2011), Musolff et al. (2015), Dupas et al. (2017), and Moatar et al. (2017) and this variability could be due to threshold driven variability of sediment-bound P, biological mediation, or to high rates of reactivity in streams.

Negative *C-Q* relationships were also observed for several base cations ($Na^+$, $Mg^{2+}$, $Ca^{2+}$) at the mouth, mid ($Na^+$, $Mg^{2+}$), and even upper ($Mg^{2+}$) flumes. The *C-Q* plots for $Ca^{2+}$ at the mid and $Ca^{2+}$ and $Na^+$ at the upper flumes show a slight, though non-significant dilution tendency. Overall, the abundance of strong dilution patterns ($|b|>0.2$, except for $Mg^{2+}$ at upper flume where $|b|=0.1$) at our site, contrast with findings by Godsey et al. (2009), Hunsaker and Johnson (2017), and Kim et al. (2017), who broadly observed base cations to have chemostatic or negative *C-Q* relationships with slopes close to 0 ($|b|<0.1$). In the Honeysuckle Creek watershed, these major cations are widely available in the soil due to geogenic weathering of the glacial parent materials (Adams and Boyle, 1979, 1982; Williams et al., 2007; Jin et al., 2008). While weathering processes provide a stable source of minerals to be transported through the soil to the stream, the size of the available pool of cations is limited due to cations being bound to soil and taken up by vegetation (Bigelow and Canham, 2015; Herndon et al., 2015; Hoagland et al., 2017). The cation exchange complex and vegetative uptake act as sinks and limit the supply of cations available for transport, resulting in dilution in the stream during snowmelt or large precipitation events. In contrast to the dilution patterns observed for the other major cations, $K^+$ displays a flat *C-Q* shape and chemostatic to neutral $CV_C/CV_Q$ ratio. While parent material weathering is likely a primary source of $K^+$ (Adams and Boyle, 1982), biological processes unique to $K^+$ are likely controlling the availability and distribution of this cation (Likens et al., 1994; Salmon et al., 2001; Tripler et al., 2006). In contrast to the major cations, excluding $K^+$, other parent material weathering byproducts, including the anions $Cl^-$ and $F^-$, show no dilution trends. These anions are not bound up in any sink and are easily mobilized in soil and stream water. While neither $Cl^-$ nor $F^-$ had significant *C-Q* relationships, excepting the negative *C-Q* relationship for $Cl^-$ at the mouth that is likely due to road salt applications to the paved road between the mid and the mouth flumes (Figure 1.1), they did differ somewhat in their levels of variability. $Cl^-$ had lower $CV_C$ (20-30%) and chemostatic $CV_C/CV_Q$ ratios at the mid and upper flumes compared to $F^-$, which was more variable ($CV_C$=56-71%; no trend to slightly chemostatic $CV_C/CV_Q$ ratio) but also measured at much lower concentrations. Musolff et al. (2015), Hunsaker and Johnson (2017), and Moatar et al. (2017) also observed low variability chemostatic trends for $Cl^-$.

At our study site, we observed that from the headwaters to the mouth of the stream, water fluxes and increasing discharge become a more dominant control on stream chemistry as the catchment area increased from 8.5 to 120 ha. Differences in the proportion of analytes with significant *C-Q* relationships (positive, negative) at each location suggest that, as the contributing area increases, stream waters are recording landscape variation in source areas, hydrologic connectivity, residence time, or in-stream biogeochemistry (Singh et al., 2015; Moatar et al., 2017). The degree to which these discrete factors/processes (*e.g.*, connectivity, biogeochemistry) affect *C-Q* relationships is not clear, but may reflect differences in parent material distribution, groundwater inputs, or amount of wetland area in each subwatershed. At the upper flume, the lack of significant *C-Q* relationships for most analytes, suggests that the volume of water (*i.e.*, discharge) is likely not the primary factor controlling analyte concentrations in the stream. As this flume is so near the headwater groundwater source, the amount and chemical characteristics of groundwater sources, parent material distribution, and vegetation are likely significant factors influencing stream chemistry. Moving down Honeysuckle Creek, the influence of discharge appears to increase, as more analytes display significant *C*-*Q* relationships.

Export of C, nutrients, and major ions from the Honeysuckle Creek watershed to Burt Lake is largest during the spring, with pulses during large summer storms. Spring snowmelt is the dominant hydrological event in the year; peak flows at the mouth and upper flumes are an order of magnitude larger than at other times of the year, and more than twice as large at the mid flume than annual mean discharge. During the hydrologic year, mean DOC loading from the mouth of the stream was 3,392 kg $year^{-1}$, with the largest loads in the spring (20 kg $day^{-1}$). Based on our isotopic data, spring DOC inputs to the lake consist of less decomposed, more surficial organic matter than at other times of the year and are likely to be dominated by wetland C with some upland sources mixed in (Elder et al., 2000; Lottig et al., 2013; Lambert et al., 2014; Marx et al., 2017). In the large northern basin of Burt Lake, which is fed only by first- and second-order streams similar to Honeysuckle Creek, DOC inputs from these small streams likely play a key subsidizing role in the C cycle of this aquatic ecosystem. Dissolved and particulate C are essential for maintaining heterotrophic processes within the lake, particularly during the spring when macroinvertebrate populations are booming, and fish are spawning (Carpenter et al., 2005; Frost et al., 2009; Lottig et al., 2013; McLaughlin and Kaplan, 2013; Tanentzap et al., 2017).

### *Conclusions*

Stream discharge and chemistry along Honeysuckle Creek varied widely during the 2015-2016 hydrologic year. Stream discharge increased by an order of magnitude from the headwaters to the mouth, with the largest flows occurring in spring during the snowmelt period and during some large summer storms. Stream chemistry also varied longitudinally along the stream and all analytes were generally in the highest concentrations at the mouth. Many analytes displayed seasonal differences in concentration, likely due to changes in discharge, hydrologic connectivity, biological inputs, or microbial activity.  Overall, the concentrations of all analytes measured displayed much less variation than the measured variation with discharge.  However, all three *C-Q* shapes (positive, negative, flat) were observed at all locations along the stream.  At the mouth, most analytes displayed significant positive or negative *C-Q* relationships, indicating that discharge is a significant driving factor controlling stream chemistry.  The importance of discharge appeared to decrease moving upstream to the headwaters where other factors, such as parent material and vegetation distribution and groundwater inputs, become more dominant controls on stream chemical patterns.  Small streams such as Honeysuckle Creek are an important conduit for energy, nutrients, and ions moving from the upland landscape to inland lakes.

REFERENCES

Achat, D.L., Bakker, M.R., Zeller, B., Pellerin, S., Bienamie, S., & Morel, C. (2010). Long-term organic phosphorus mineralization in Spodosols under forests and its relation to carbon and nitrogen mineralization. *Soil Biology & Biogeochemistry* 42, 1479-1490.

Adams, M.A., Attiwill, P.M., & Polglase, P.J. (1989). Availability of nitrogen and phosphorus in forest soils in northeastern Tasmania. *Biology and Fertility of Soils* 8, 212-218.

Adams, P.W., & Boyle, J.R. (1979). Cation release from Michigan Spodosols leached with aspen leaf extracts. *Soil Science Society of American Journal* 43, 593-596.

Adams, P.W., & Boyle, J.R. (1982). The quantity and quality of nutrient cations in some Michigan Spodosols. *Soil Science* 133, 383-389.

Alexander, R.B., Boyer, E.W., Smith, R.A., Schwarz, G.E., & Moore, R.B. (2007). The role of headwater streams in downstream water quality. *Journal of the American Water Resources Association* 43, 41-59.

Andrews, D.M., Lin, H., Zhu, Q., Jin, L., & Brantley, S.L. (2011). Hot spots and hot moments of dissolved organic carbon export and soil organic carbon storage in the Shale Hills catchment. *Vadose Zone Journal* 10, 943-954.

Basu, N., Destouni, G., Jawitz, J., Thompson, S., Loukinova, N., Darracq, A., Zanardo, S., Yaeger, M., Sivapalan, M., Rinaldo, A., & Rao, R. (2010). Nutrient loads exported from managed catchments reveal emergent biogeochemical stationarity. *Geophysical Research Letters* 37, L23404.

Bernhardt, E.S., Likens, G.E., Hall, R.O. Jr, Buso, D.C., Fisher, S.G., Burton, T.M., Meyer, J.L., McDowell, W.H., Mayer, M.S., Bowden, W.B., Findlay, S.E.G., Maceneale, K.H., Stelzer, R.S., & Lowe, W.H. (2005). Can't see the forest for the stream? In-stream processing and terrestrial nitrogen exports. *BioScience* 55, 219-230.

Bigelow, S.W., & Canham, C.D. (2015). Litterfall as a niche construction process in a northern hardwood forest. *Ecosphere* 6, 1-14.

Blewett, W.L., & Winters, H.A. (1995). The importance of glaciofluvial features within Michigan's Port Huron moraine. *Annals of the Association of American Geographers* 85, 306-319.

Boyer, E.W., Hornberger, G.M., Bencala, K.E., & McKnight, D.M. (1997). Response characteristics of DOC flushing in an alpine catchment. *Hydrological Processes* 11, 1635-1647.

Brinson, M.M. (1993). Changes in the functioning of wetlands along environmental gradients. *Wetlands* 13, 65-74.

Brown, V.A., McDonnell, J.J., Burns, D.A., & Kendall, C. (1999). The role of event water, a rapid shallow flow component, and catchment size in summer stormflow. *Journal of Hydrology* 217, 171-190.

Burns, D.A., Boyer, E.W., Elliott, E.M., & Kendall, C. (2009). Sources and transformations of nitrate from streams draining varying land uses: evidence from dual isotope analysis. *Journal of Environmental Quality* 38, 1149-1159.

Carpenter, S.R., Cole, J.J., Pace, M.L., Van de Bogert, M., Bade, D.L., Bastviken, D., Gille, C.M., Hodgson, J.R., Kitchell, J.F., & Kritzberg, E.S. (2005). Ecosystem subsidies: Terrestrial support of aquatic food webs from 13C addition to contrasting lakes. *Ecology* 86, 2737-2750.

Creed, I.F., McKnight, D.M., Pellerin, B.A., Green, M.B., Bergamaschi, B.A., Aiken, G.R., Burns, D.A., Findlay, S.E.G., Shanley, J.B., Strigel, R.G., Aulenbach, B.T., Clow, D.W., Laudon, H., McGlynn, B.L., McGuire, K.J., Smith, R.A., & Stackpoole, S.M. (2015). The river as a chemostat: fresh perspectives on dissolved organic matter flowing down the river continuum. *Canadian Journal of Fisheries and Aquatic Sciences* 72, 1272-1285.

Davis, J.C., Proctor, I.D., Southon, J.R., Caffee, M.W., Heikkinen, D.W., Roberts, M.L., Moore, T.L., Turteltaub, K.W., Nelson, D.E., Loyd, D.H., & Vogel, J.S. (1990). LLNL/US AMS facility and research program. *Nuclear Instruments and Methods in Physics Research Section B* 52, 269-272.

Diamond, J.S., & Cohen, M.J. (2018). Complex patterns of solute-discharge relationships for coastal plain rivers. *Hydrological Processes* 32, 388-401.

Dittman, J.A., Driscoll, C.T., Groffman, P.M., & Fahey, T.J. (2007). Dynamics of nitrogen and dissolved organic carbon at the Hubbard Brook Experimental Forest. *Ecology* 88, 1153-1166.

Downing, J.A., Cole, J.J., Duarte, C.M., Middelburg, J.J., Melack, J.M., Prairie, Y.T., Kortelainen, P., Striegl, R.G., McDowell, W.H., & Tranvik, L.J. (2012). Global abundance and size distribution of streams and rivers. *Inland Waters* 2, 229-236.

Duncan, J.M., Band, L.E., & Groffman, P.M. (2017). Variable nitrate concentration-discharge relationships in a forested watershed. *Hydrological Processes* 31, 1817-1824.

Dupas, R., Musolff, A., Jawitz, J.W., Rao, P.S.C., Jager, C.G., Fleckenstein, J.H., Rode, M., & Borchardt, D. (2017). Carbon and nutrient export regimes from headwater catchments to downstream reaches. *Biogeosciences* 14, 4391-4407.

Edwards, A.M.C. (1973). The variation of dissolved constituents with discharge in some Norfolk rivers. *Journal of Hydrology* 18, 219-242.

Elder, J.F., Rybicki, N.B., Carter, V., & Weintraub, V. (2000). Sources and yields of dissolved carbon in Northern Wisconsin stream catchments with differing amounts of peatland. *Wetlands* 20, 113-125.

Foster, I.D.L, & Walling, D.E. (1978). Effects of 1976 drought and autumn rainfall on stream solute levels. *Earth Surface Processes* 3, 393-406.

Freeman, M.C., Pringle, C.M., & Jackson, C.R. (2007). Hydrologic connectivity and the contribution of small headwaters to ecological integrity at regional scales. *Journal of the American*

*Water Resources Association* 43, 5-14.

Frost, P.C., Kinsman, L.E., Johnston, C.A., & Larson, J.H. (2009). Watershed discharge modulates relationships between landscape components and nutrient ratios in stream seston. *Ecology* 90, 1631-1640.

Galloway, J.N., & Cowling, E.B. (2002). Reactive nitrogen and the world: 200 years of change. *AMBIO: A Journal of the Human Environment* 31, 64-71.

Gannon, J.P., Bailey, S.W., McGuire, K.J., & Shanley, J.B. (2015). Flushing of distal hillslopes as an alternative source of stream dissolved organic carbon in a headwater catchment. *Water Resources Research* 51, 8114-8128.

Godsey, S.E., Kirchner, J.W., & Clow, D.W. (2009). Concentration-discharge relationships reflect chemostatic characteristics of US catchments. *Hydrological Processes* 23, 1844-1864.

Gomi, T., Sidle, R.C., & Richardson, J.S. (2002). Understanding processes and downstream linkages of headwater systems. *BioScience* 52, 905-916.

Grabs, T., Bishop, K., Laudon, H., Lyon, S.W., & Seibert, J. (2012). Riparian zone hydrology and soil water total organic carbon (TOC): implications for spatial variability and upscaling of lateral riparian TOC exports. *Biogeosciences* 9, 3901-3916.

Harvey, J., & Gooseff, M. (2015). River corridor science: Hydrologic exchange and ecological consequences from bedforms to basins. *Water Resources Research* 51, 6893-6922.

Heckman, K., Throckmorton, H., Clingensmith, C., Vila, F.J.G., Horwath, W.R., Knicker, H., & Rasmussen, C. (2014). Factors affecting the molecular structure and mean residence time of occluded organics in a lithosequence of soils under ponderosa pine. *Soil Biology & Biochemistry* 77, 1-11.

Herndon, E.M., Dere, A.L., Sullivan, P.L., Norris, D., Reynolds, B., & Brantley, S.L. (2015). Landscape heterogeneity drives contrasting concentration-discharge relationships in shale headwater catchments. *Hydrology and Earth System Sciences* 19, 3333-3347.

Hoagland, B., Russo, T.A., Gu, X., Hill, L., Kaye, J., Forsythe, B., & Brantley, S.L. (2017). Hyporheic zone influences on concentration-discharge relationships in a headwater sandstone stream. *Water Resources Research* 53, 4643-4667.

Hornberger, G.M., Bencala, K.E., & McKnight, D.M. (1994). Hydrological controls on dissolved organic carbon during snowmelt in the Snake River near Montezuma, Colorado. *Biogeochemistry* 25, 147-165.

Hunsaker, C.T., & Johnson, D.W. (2017). Concentration-discharge relationships in headwater streams of the Sierra Nevada, California. *Water Resources Research* 53, 7869-7884.

Inamdar, S.P., Christopher, S.F., & Mitchell, M.J. (2004). Export mechanisms for dissolved organic carbon and nitrate during summer storm events in a glaciated forested catchment in New

York, USA. *Hydrological Processes* 18, 2651-2661.

Jin, L., Williams, E., Szramek, K., Walter, L.M., & Hamilton, S.K. (2008). Silicate and carbonate mineral weathering in soil profiles developed on Pleistocene glacial drift (Michigan, USA): Mass balances on soil water geochemistry. *Geochemica et Cosmochimica Acta* 72, 1027-1042.

Johnson, D.W. (1984). Sulfur cycling in forests. *Biogeochemistry* 1, 29-43.

Jones, A.L., & Sroka, B.N. (1997). Effects of highway deicing chemicals on shallow unconsolidated aquifers in Ohio, interim report, 1988-93. U.S. Geological Survey Water-Resources Investigations Report 97-4027, 139 pp.

Jonsson, A., Algesten, G., Bergstrom, A.-K., Bishop, K., Sobek, S., Tranvik, L.J., & Jansson, M. (2007). Integrating aquatic carbon fluxes in a boreal catchment carbon budget. *Journal of Hydrology* 334, 141-150.

Kilpatrick, F.A., & Schneider, V.R. (1983). Use of flumes in measuring discharge: U.S. Geological Survey Techniques of Water-Resources Investigations, Book 3, chap. A14, 46 pp.

Kim, H., Dietrich, W.E., Thurnhoffer, B.M., Bishop, J.K.B., & Fung, I.Y. (2017). Controls on solute concentration-discharge relationships revealed by simultaneous hydrochemistry observations of hillslope runoff and stream flow: The importance of critical zone structure. *Water Resources Research* 53, 1424-1443.

Lambert, T., Pierson-Wickmann, A.-C., Gruau, G., Jaffrezic, A., Petitjean, P., Thibault, J.N., & Jeanneau, L. (2014). DOC sources and DOC transport pathways in a small headwater catchment as revealed by carbon isotope fluctuation during storm events. *Biogeosciences* 11, 3043-3056.

Lambert, T., Pierson-Wickmann, A., Gruau, G., Thibault, J., & Jaffrezic, A. (2011). Carbon isotopes as tracers of dissolved organic carbon sources and water pathways in headwater catchments. *Journal of Hydrology* 402, 228-238.

Lapin, M., & Barnes, B.V. (1995). Using the landscape ecosystem approach to assess species and ecosystem diversity. *Conservation Biology* 9, 1148-1158.

Leopold, L.B., Wolman, M.G., & Miller, J.P. (1964). *Fluvial Processes in Geomorphology*. W.H. Freeman and Company, San Francisco.

Likens, G.E., Bormann, F.H., Johnson, N.M., & Pierce, R.S. (1967). The calcium, magnesium, potassium, and sodium budgets for a small forested ecosystem. *Ecology* 48, 772-785.

Likens, G.E., Driscoll, C.T., Buso, D.C., Siccama, T.G., Johnson, C.E., Lovett, G.M., Fahey, T.J., Reiners, W.A., Ryan, D.F., Martin, C.W., & Bailey, S.W. (1998). The biogeochemistry of calcium at Hubbard Brook. *Biogeochemistry* 41, 89-173.

Likens, G.E., Driscoll, C.T., Buso, D.C., Siccama, T.G., Johnson, C.E., Lovett, G.M., Ryan, D.F., Fahey, T., & Reiners, W.A. (1994). The biogeochemistry of potassium at Hubbard Brook. *Biogeochemistry* 25, 61-126.

Lottig, N.R., Buffam, I., & Stanley, E.H. (2013). Comparisons of wetland and drainage lake influences on stream dissolved carbon concentrations and yields in a north temperate lake-rich region. *Aquatic Sciences* 75, 619-630.

MacDonald, L.H., & Coe, D. (2007). Influence of headwater streams on downstream reaches in forested areas. *Forest Science* 53, 148-168.

Marx, A., Dusek, J., Jankovec, J., Sanda, M., Vogel, T., van Geldern, R., Hartmann, J., & Barth, J.A.C. (2017). A review of $CO_2$ and associated carbon dynamics in headwater streams: A global perspective. *Review of Geophysics* 55, 560-585.

Mayer, B., Shanley, J.B., Bailey, S.W., & Mitchell, M.J. (2010). Identifying sources of stream water sulfate after a summer drought in the Sleepers River Watershed (Vermont, USA) using hydrological, chemical, and isotopic techniques. *Applied Geochemistry* 25, 747-754.

McClain, M.E., Boyer, E.W., Dent, C.L., Gergel, S.E., Grimm, N.B., Groffman, P.M., Hart, S.C., Harvey, J.W., Johnston, C.A., Mayorga, E., McDowell, W.H., & Pinay, G. (2003). Biogeochemical hot spots and hot moments at the interface of terrestrial and aquatic ecosystems. *Ecosystems* 6, 301-312.

McLaughlin, C., & Kaplan, L.A. (2013). Biological lability of dissolved organic carbon in stream water and contributing terrestrial sources. *Freshwater Science* 32, 1219-1230.

Moatar, F., Abbott, B.W., Minaudo, C., Curie, F., & Pinay, G. (2017). Elemental properties, hydrology, and biology interact to shape concentration-discharge curves for carbon, nutrients, sediment, and major ions. *Water Resources Research* 53, 1270-1287.

Musolff, A., Schmidt, C., Selle, B., & Fleckenstein, J.H. (2015). Catchment controls on solute export. *Advances in Water Resources* 86, 133-146.

National Atmospheric Deposition Program (NRSP-3). (2018). NADP Program Office, Wisconsin State Laboratory of Hygiene, 465 Henry Mall, Madison, WI 53706

Nave, L.E., Covarrubias Ornelas, A., Drevnick, P.E., Gallo, A., Hatten, J.A., Heckman, K.A., Matoszuik, L., Sanclements, M., Strahm, B.D., Veverica, T.J., Weiglein, T.L., & Swanston, C.W. In Review. Carbon-mercury interactions in Spodosols assessed through density fractionation, radiocarbon analysis, and soil survey information. *Soil Science Society of America Journal*

Nave, L.E., Drevnick, P.E., Heckman, K.A., Hofmeister, K.L., Veverica, T.J., & Swanston, C.W. (2017a). Soil hydrology, physical and chemical properties and the carbon and mercury in a postglacial lake-plain wetland. *Geoderma* 305, 40-52.

Nave, L.E., Gough, C.M., Maurer, K.D., Bohrer, G., Hardiman, B.S., Le Moine, J., Munoz, A.B., Nadelhoffer, K.J., Sparks, J.P., Strahm, B.D., Vogel, C.S., & Curtis, P.S. (2011). Disturbance and the resilience of coupled carbon and nitrogen cycling in a north temperate forest. *Journal of Geophysical Research* 116, G04016.

Nave, L.E., Gough, C.M., Perry, C.H., Hofmeister, K.L., Le Moine, J., Domke, G.M., Swanston, C.W., & Nadelhoffer, K.J. (2017b). Physiographic factors underlie rates of biomass production during succession in Great Lakes forest landscapes. *Forest Ecology and Management* 397, 157-173.

Nave, L.E., Sparks, J.P., Le Moine, J., Hardiman, B.S., Nadelhoffer, K.J., Tallant, J.M., Vogel, C.S., Strahm, B.D., & Curtis, P.S. (2014). Changes in soil nitrogen cycling in a northern temperate forest ecosystem during succession. *Biogeochemistry* 121, 471-488.

Nave, L.E., Vogel, C.S., Gough, C.M., & Curtis, P.S. (2009). Contribution of atmospheric nitrogen deposition to net primary productivity in a northern hardwood forest. *Canadian Journal of Forest Research* 39, 1108-1118.

Pringle, CM. (2003). What is hydrologic connectivity and why is it ecologically important? *Hydrological processes* 17, 2685-2698.

R Core Team. (2017). R: A language and environment for statistical computing. R Foundation for Statistical Computing, Vienna, Austria. URL https://www.R-project.org/

Raymond, P.A., Saiers, J.E., & Sobczak, W.V. (2016). Hydrological and biogeochemical controls on watershed dissolved organic matter transport: pulse-shunt concept. *Ecology* 97, 5-16.

Salmon, C.D., Walter, M.T., Hedin, L.O., & Brown, M.G. (2001). Hydrological controls on chemical export from an undisturbed old-growth Chilean forest. *Journal of Hydrology* 253, 69-80.

Sanderman, J., Lohse, K.A., Baldock, J.A., & Amundson, R. (2009). Linking soils and streams: Sources and chemistry of dissolved organic matter in a small coastal watershed. *Water Resources Research* 45, 1-13.

Schiff, S.L., Aravena, R., Trumbore, S.E., Hinton, M.J., Elgood, R., & Dillon, P.J. (1997). Export of DOC from forested catchments on the Precambrian Shield of Central Ontario: Clues from $^{13}C$ and $^{14}C$. *Biogeochemistry* 36, 43-65.

Sebestyen, S.D., Boyer, E.W., Shanley, J.B., Kendall, C., Doctor, D.H., Aiken, G.R., & Ohte, N. (2008). Sources, transformations, and hydrological processes that control stream nitrate and dissolved organic matter concentrations during snowmelt in an upland forest. *Water Resources Research* 44, 1-14.

Singh, S., Inamdar, S., & Mitchell, M. (2015). Changes in dissolved organic matter (DOM) amount and composition along nested headwater stream locations during baseflow and stormflow. *Hydrological Processes* 29, 1505-1520.

Spurr, S.H., & Zumberge, J.H. (1956). Late Pleistocene features of Cheboygan and Emmet counties, Michigan. *American Journal of Science* 254, 96-109.

Stuiver, M., & Polach, H.A. (1977). Discussion: reporting of $^{14}C$ data. *Radiocarbon* 19, 355-363.

Tanentzap, A.J., Kielstra, B.W., Wilkinson, G.M., Berggren, M., Craig, N., del Giorgio, P.A., Grey, J., Gunn, J.M., Jones, S.E., Karlsson, J., Solomon, C.T., & Pace, M.L. (2017). Terrestrial support of lake food webs: Synthesis reveals controls over cross-ecosystem resource use. *Science Advances* 3, 1-11.

Tetzlaff, D., Soulsby, C., Bacon, P.J., Youngson, A.F., Gibbins, C., & Malcolm, I.A. (2007). Connectivity between landscapes and riverscapes – A unifying theme in integrating hydrology and ecology in catchment science? *Hydrological Processes* 21, 1385-1389.

Thomas, Z., Abbott, B.W., Troccaz, O., Baudry, J., & Pinay, G. (2016). Proximate and ultimate controls on carbon and nutrient dynamics of small agricultural watersheds. *Biogeosciences* 13, 1863-1875.

Thompson, S.E., Basu, N.B., Lascurain, J., Aubeneau, A., & Rao, P.S.C. (2011). Relative dominance of hydrologic versus biogeochemical factors on solute export across impact gradients. *Water Resources Research* 47, W00J5.

Tockner, K., Penntzdorfer, D., Reiner, N., Schiemer, F., & Ward, J.W. (1999). Hydrological connectivity, and the exchange of organic matter and nutrients in a dynamic river-floodplain system (Danube, Austria). *Freshwater Biology* 41, 521-535.

Tripler, C.E., Kaushal, S.S., Likens, G.E., & Walter, M.T. (2006). Patterns in potassium dynamics in forest ecosystems. *Ecology Letters* 9, 451-466.

Vogel, J.S., Southon, J.R., & Nelson, D.E. (1987). Catalyst and binder effects in the use of filamentous graphite for AMS. Nuclear Instruments and Methods in Physics Research Section B 29, 50-56.

Walling, D.E., & Webb, B.W. (1983). The dissolved load of rivers: A global overview. In *Dissolved Loads of Rivers and Surface Water Quantity/Quality Relationships*, Webb, BW (ed). International Association of Hydrological Sciences: Wallingford, Oxfordshire; Publ 41, 3-20 p.

Williams, G.P. (1989). Sediment concentration versus water discharge during single hydrologic events in rivers. *Journal of Hydrology* 111, 89-106.

Williams, E.L., Szramek, K.J., Jin, L., Ku, T.C.W., & Walter, L.M. (2007). The carbonate system geochemistry of shallow groundwater-surface water systems in temperate glaciated watersheds (Michigan, USA): Significance of open-system dolomite weathering. *GSA Bulletin* 119, 515-528.

# CHAPTER 2

## SOILS AND TOPOGRAPHY CONTROL SEASONAL AND SPATIAL PATTERNS OF FOREST SOIL MOISTURE AND WATER TABLE POSITION


***Abstract***

In forest ecosystems, soil water availability is an important indicator and driver of biogeochemical transformations, pedogenesis, and surface water-groundwater linkages. Given the importance of soil moisture and shallow groundwater to ecosystem processes, field measurements are critical. In this study, we investigated the spatial patterns and temporal dynamics of moisture conditions in a 120 ha forested first-order watershed in northern Michigan. We measured soil volumetric water content (VWC %) and water table levels across a range of glacial parent materials and landforms. We also assessed the utility of using two different spatial frameworks (Landscape Ecosystem classification, Topographic Wetness Index) to represent spatial patterns of and variability in soil moisture and water table levels across the watershed. At the lowest landscape position (outwash-lake plain swamp), saturation was perennial, with a median soil VWC of 53% and the water table position 8 cm below ground surface. Among upland ecosystems, outwash landforms had consistently low VWC (16%) and no evidence of groundwater within 4 m of the surface; moraine ecosystems (till parent material) possessed mixed hydrologic conditions, with VWC ranging from 18-25% and water table levels between 6-65 cm below the surface. In low-variability dry or wet areas with relatively homogenous soils, larger ecosystem classification map units provide good representations of moisture conditions. In the more heterogeneous till soils, a finer scale spatial framework that accounts for local soil variation is optimal. While either spatial framework can be used to estimate moisture conditions, a combination of both is most appropriate in this glaciated landscape.

### *Introduction*

Terrestrial water storage is an important intermediate in the hydrologic cycle between precipitation and receiving surface waters. Soil water storage and availability are important controls for a number of ecosystem processes (Schaetzl et al., 2009; Lin, 2010). In forest landscapes, soil water and groundwater conditions influence biogeochemical processes and nutrient cycling (Burt and Pinay, 2005; Seneviratne et al., 2010; Vidon et al., 2010; Morse et al., 2014). Spatial and temporal variability of soil water can impact carbon and nitrogen cycles by creating favorable conditions for mineralization, leaching, or greenhouse gas production through differing levels of soil saturation and connections between flow paths transporting biogeochemically important substrates (McClain et al., 2003; Porporato et al., 2003; Burt and Pinay, 2005; Castellano et al., 2012; Oswald et al., 2014). The extent of hydrologic connectivity between the landscape and surface waters is dependent upon soil water and shallow groundwater levels, with continuous water tables allowing for the transfer of materials, such as dissolved organic carbon or $NO_3^-$ (Lambert et al., 2014; Duncan et al., 2015) from hillslopes through riparian zones to streams and ultimately exported from a watershed to larger water bodies (Freeman et al., 2007; Jencso et al., 2009; Bracken et al., 2013). In addition, water movement through the soil influences pedogenesis, vertically through soil profiles and laterally along hydrologic flow paths (Lohse and Dietrich, 2005; Bailey et al., 2014). Water availability and storage can influence vegetation growth and distribution (Rodriguez-Iturbe et al., 1999; Tenenbaum et al., 2006; Hwang et al., 2012) and water stress, due to either limited water or excessively saturated soils, can reduce photosynthesis, tree growth, or even changes in phenology (McDowell et al., 2008; Berthelot et al., 2014; Brzostek et al., 2014)

Given the importance of soil moisture and shallow groundwater to ecosystem processes and the transport of material through soil and to surface waters, field measurements of hydrologic conditions are critical. However, field measurements of soil moisture and water table levels can be limited in spatial and temporal resolution due to resource constraints or challenges in accessing the field site throughout the year (Grabs et al., 2009). Developing a relationship between field measurements and easily generated geospatial frameworks can provide a method for estimating moisture conditions across a watershed or scaling field measurements across larger regional scales (Zhu et al., 2012; Ali et al., 2014). Assessing the relationship between terrestrial moisture conditions and landscape or regional spatial frameworks could also potentially provide a method for easily estimating critical areas of soil-ground-surface water linkages, biogeochemical cycling, pedogenesis, or vegetation distribution and productivity.

For this analysis we used two types of spatial frameworks, the first of which is an ecosystem classification. Ecosystem classifications have been developed for a range of landscapes as a way to identify spatial units of recognizable ecosystems using established criteria, such as landform, climate, vegetation, and/or soil (Cleland et al., 1997; Cullum et al., 2016). These types of classifications have been widely used to map plant communities and identify areas to focus conservation efforts (Moores et al., 1996; Ferree and Thompson, 2008; Zenner et al., 2010; Cameron and Williams, 2011; Boyle et al., 2014; Cullum et al., 2016). Hierarchical ecosystem classifications have been previously developed for our northern Michigan study region using physiographic characteristics to define landscape, landform, and ecosystem level map units (Albert et al., 1995; Pearsall et al., 1995). The finest level of this classification hierarchy, the Landscape Ecosystem classification, has been used to identify forest communities (Lapin and Barnes, 1995) and map wetland ecosystems (Zogg and Barnes, 1995), while a more coarsely resolved level of the classification was used to identify bird habitat (Kashian et al., 2003). Utilizing multiple levels of this classification system from the individual ecosystem up to the ecoregion, Nave et al. (2017b) found that physiographic and soil factors can be used to predict forest biomass production rates. While they observed that biomass production rates varied under different moisture conditions (*i.e.*, xeric, mesic, hydric), these moisture groups were based on field observations or estimates, not on quantifiable measurements of soil water. Ecosystem classifications are often based in part on presumed patterns of wetness rather than on measured soil moisture and water table depth, therefore making direct measurements of hydrologic conditions across ecosystems can increase our confidence in the advisability of using ecosystem classifications as representatives of wetness. Mapping hydrologic conditions with existing ecosystem classifications potentially provides a relatively easy way to identify soil moisture status or water table levels across a range of landscapes and regions.

The second type of spatial framework we used is a higher resolution topographic wetness index (TWI), where pixel-level values are calculated based on geospatial inputs. Topographic indices have commonly been correlated with soil moisture (*e.g.,* Lin et al., 2006; James and Roulet, 2007; Ali et al., 2010; Tague et al., 2010; Beaudette et al., 2013; Liang et al., 2017) and water table (*e.g.,* Thompson and Moore, 1996; Monteith et al., 2006; Detty and McGuire, 2010; Grabs et al., 2012; Rinderer et al., 2014) measurements across many study systems. TWIs have been related to hydropedologic unit, soil organic matter, and other soil properties (Moore et al., 1993; Lin et al., 2006; Zinko et al., 2006; Seibert et al., 2007; Pei et al., 2010; Murphy et al., 2011; Grabs et al., 2012; Laamrani et al., 2014; Gillin et al., 2015). TWIs have also been used to map wetland occurrence (Rodhe and Seibert, 1999; Grabs et al., 2009; Rampi et al., 2014) and vegetation distribution (Hwang et al., 2012; Petroselli et al., 2013). While TWIs have been used for various purposes, these indices can be limited in their use at very large scales or across regions due to data limitations or model assumptions (Schaetzl et al., 2009; Rinderer et al., 2014).

The present study, conducted in a first-order watershed possessing high-resolution data amenable to testing both types of spatial frameworks, had two primary objectives. First, we measured patterns of soil moisture and water table position throughout the hydrologic year, contributing to the characterization of watershed-level water distribution and storage across the upper Great Lakes physiographic region. Second, we evaluated the utility of two types of spatial frameworks to represent spatial patterns of and variability in soil moisture and water table levels across the watershed. While numerous other studies have utilized TWIs to describe wetness conditions across watersheds, few have assessed ecosystem classifications against quantitative hydrologic measurements or evaluated soil moisture or groundwater across heterogeneous glacial drift landscape such as ours. The landscape provided the opportunity to evaluate distinct spatial frameworks in settings with diverse parent materials and young topography. A more complete understanding of spatial patterns and temporal dynamics of specific moisture parameters, and identification of spatial frameworks that can be used to represent those moisture patterns, will aid us in determining important sites for hydrologically-influenced processes.

### *Methods*

#### *Study Area*

This research was conducted within the Honeysuckle Creek watershed at the University of Michigan Biological Station (UMBS), in northern Lower Michigan, USA (45.56º, -84.72º) (Figure 2.1). The regional climate is continental with strong local topographic gradients. Mean annual temperature is 5.5ºC and the mean annual precipitation is 817 cm, 294 cm of which is snowfall (Nave et al., 2017b). The approximately 120 ha Honeysuckle Creek watershed drains a small first order stream and several ephemeral channels occupying a variety of glacial and postglacial landforms to Burt Lake, Michigan's 4th largest inland lake.

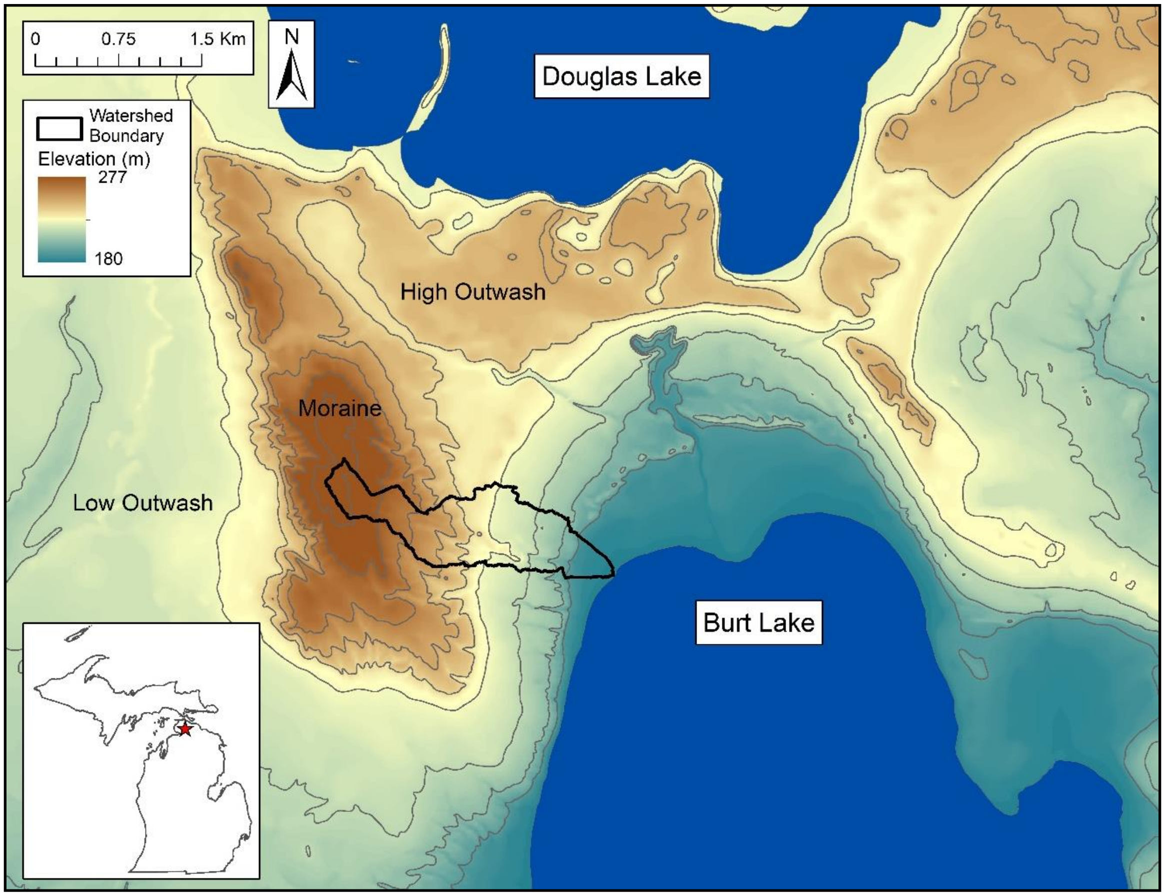


Figure 2.1: Digital Elevation Model (DEM) of the UMBS landscape, with the Honeysuckle Creek watershed outlined in black. Color ramp emphasizes the major glacial landforms (moraine and outwash) and lakes; inset indicates the study area location in northern Lower Michigan.

The UMBS landscape is characteristic of many areas in the northern Lake Michigan and eastern Lake Superior basins. Major landforms were created by the deposition and modification of glacial parent materials at the end of the Laurentian glaciation, between 14,000 and 11,000 years before present (ybp) (Spurr and Zumberge, 1956; Blewitt and Winters, 1995; Lapin and Barnes, 1995). At UMBS, coarse-textured glacial deposits 100-200 m thick overlay Silurian limestone and Devonian shale bedrock. The wasting ice mass deposited till as ground, interlobate, and drumlinized moraines. Much of the till was later capped by meters of outwash deposited during the final stages of glacial retreat from the region. Below an elevation of 255 m above sea level (asl), these landforms were altered by large, postglacial lakes (Lake Algonquin 11,500-10,500 ybp; Lake Nipissing 5,000-3,000 ybp), which resulted in till and outwash features reworked into lacustrine landforms (dunes, beach ridges, lake plains; Spurr and Zumberge, 1956; Blewitt and Winters, 1995). The elevation of the Honeysuckle Creek watershed ranges from 276 m at the top of an interlobate moraine to 181 m at present day Burt Lake.

Within the watershed, soils above 245 m elevation and the northern half of the middle of the watershed (245-190 m) are Entic and Lamellic Haplorthods (Rubicon and Blue Lake series, respectively; Soil Survey Staff, 1991). These are very deep soils (>150 cm) formed in thick sandy or gravelly outwash deposits (Rubicon) or in stratified mixtures of coarse outwash and underlying glacial till (Blue Lake). Blue Lake soils possess loamy lamellae at depth (typically below 80 cm), which impede infiltration. These soil series roughly correspond with soils in the outwash and banded outwash over till Landscape Ecosystem groups (discussed in a later section, Figure 2.2). Soils in the southern half of the middle of the watershed are Alfic Haplorthods and Alfic Epiaquods (Cheboygan and Riggsville series, respectively), which formed in thinner deposits of finer-textured outwash and the underlying dense glacial till. In these soils, the till is laterally extensive and acts as a restrictive layer causing perched water tables. The Cheboygan and Riggsville soil series correspond with soils in the mesic and aquic till Landscape Ecosystem types, respectively. Soils in the mesic till ecosystems have a glacial till restrictive layer between 45-265 cm from the surface and textures that range from medium sand to loamy sand. In the aquic till ecosystems, the glacial till restrictive layer is within 150 cm of the surface and soil textures are predominately loam sand or sit loam. In riparian areas of the middle elevations of the watershed (riparian wetland Landscape Ecosystem type) Mollic Endoaquents (Brevort series) occur; these are mucky mineral soils with redoximorphic features due to persistent saturation from water table perching on top of the glacial till. These soils are finer textured (loamy sand and silt loam) and the glacial till restrictive layer is within 120 cm of the surface. In the lowermost portions of the watershed (below 190 m), saturation and streamflow are perennial, and soils consist of sapric organic materials over underlying sandy outwash-lake plain deposits (Terric Haplosaprists; Tawas and Roscommon series). These soil series correspond to soils in the outwash-lake plain swamp Landscape Ecosystem type, where the mean organic horizon thickness is 0.84 cm (Nave et al., 2017a). Moving downwards in elevation through the watershed, forest composition transitions from xeric-mesic mixtures (*Populus grandidentata, Quercus rubra, Acer rubrum, Pinus strobus*) in the uplands, to mesic-hydric mixtures (*P. grandidentata and P. tremuloides, A.saccharum, Tilia americana, Fraxinus americana, F. nigra*) in the middle elevations, to mixed deciduous-conifer swamp vegetation in the lowlands (*Thuja occidentalis*, *Abies balsamea*, *Tsuga canadensis*; Pearsall et al., 1995).

*Field Measurements*

We measured soil moisture, as volumetric water content (VWC %) of the upper 20 cm of soil, at a minimum biweekly from July–November 2015 and April–November 2016 across the Honeysuckle Creek watershed. We selected sample points (n=97) from a systematic grid of 392 transect points, located 10 m apart (N to S) along transects spaced every 300 m (E to W) across the watershed area. Sample points were selected from a stratified random design to span Landscape Ecosystem types and Topographic Wetness Index (TWI) values present in the watershed (Figure 2.2, 2.3; discussed in later sections). Point locations in the field were marked with a flag to allow for repeated measurements of the exact same point throughout the study period and were georeferenced with a high-resolution GPS unit (~1 m accuracy; Trimble R1 GNSS, Trimble, Inc.). Each time measurements were collected, three Time Domain Reflectometry (TDR;

Hydrosense, Campbell Scientific, Inc.) readings of soil VWC were taken at each point, 2 m from the flag at 0º, 120º, and 240º headings. Each set of soil moisture measurements was taken across the watershed within one day and measurements were not interrupted by rain events. The TDR probe was calibrated with volumetric soil moisture measurements of soil cores taken across a range of wetness conditions throughout the watershed ($R^2$=0.84).

We placed shallow groundwater monitoring wells in areas of the watershed where water tables were observed during soil profile observations and where surface water features indicated that shallow groundwater would likely be present. Throughout this paper we will refer to shallow groundwater, which was groundwater observed within 3 m of the surface due to perching on glacial till restrictive material or consolidated sand in the outwash-lake plain swamp. Shallow wells (n=49) were installed down to the first major parent material unconformity, which was a glacial till restrictive layer (depth ranging from 55-220 cm) in upland ecosystems. In the outwash-lake plain swamp, wells were installed to approximately 160 cm through the organic soil horizons and into the sand C horizon. Slotted PVC wells (3.2-5.1 cm diameter) were deployed in 10 cm diameter boreholes and the void space was filled with a sand pack. Wells were not installed in locations above 240 m elevation because the deep sand outwash soils did not show indication of saturated conditions or shallow groundwater during soil observations. Water table position was measured with a flat tape water level meter (Model 101B, Solinst, Inc., Georgetown, ON, CA) approximately weekly from June 2016–June 2017 in all wells, and from November 2015–June 2017 in wells below 190 m elevation. Readings were corrected for the height of the standpipe such that the water table depth tape measurement was equal to the depth of water below the surface. Pressure transducers (Levelogger, Levelogger Jr., Solinst, Inc., Georgetown, ON, CA) were used to take hourly water table position measurements in a subset of wells (n=12) and were adjusted for atmospheric pressure. These measurements were then aggregated into mean daily water table positions for the subset of wells.

Soil observation, description, and sampling across the watershed was conducted for a soil characterization campaign from September 2014–November 2016 and included field observations made with a 10 cm diameter bucket auger (n=54) and quantitative samples taken by with a slide hammer soil corer (n=33), McCauley gate auger (n=41), or from a pit face (n=13). Observations were made across ecosystem types, landforms, and elevation throughout the watershed. During soil observations, we described horizon thickness and color, made field determinations of texture class, measured depth to glacial till restrictive material or C horizon, and noted depth to water table. For the present study, field determination of soil texture class, depth to glacial till restrictive layer, and depth of water table were the soil characteristics of interest. Soil characteristics were used in the Soil Topographic Index (STI; discussed in a later section).

*UMBS Landscape Ecosystem Classification*

We used a hierarchical, multifactor ecosystem classification as the first of two spatial frameworks for assessing spatial variability in and patterns of water storage (soil VWC, water table depth) across the Honeysuckle Creek watershed. The UMBS Landscape Ecosystem classification defines and maps 125 distinct ecosystem types for the 4,000 ha UMBS property based on landform, microclimate, and soil and vegetation characteristics (Lapin and Barnes, 1995; Pearsall, 1995; Pearsall et al., 1995; Zogg and Barnes, 1995). The ecosystem type map units are at the scale of tens of hectares. The Landscape Ecosystem classification nests within the USDA-Forest Service ECOMAP ecoregional framework below the Subsection level (Cleland et al., 1997). Individual Landscape Ecosystems at UMBS approximate the Landtype phase, which is the most finely resolved spatial unit in the ECOMAP conceptual framework, but which is mapped in very few places in the conterminous U.S. Landscape Ecosystem classifications have been conducted for a variety of landscapes across the upper Midwest region (Albert et al., 2015) including the McCormick Experimental Forest (Pregitzer and Barnes, 1984), the Sylvania Wilderness Area (Spies and Barnes, 1985), and the Huron Mountain Club Reserve Area (Simpson et al., 1990). For this analysis, the Landscape Ecosystem units (originally identified numerically) were given shorthand names that refer to dominant parent material or landform of that ecosystem type. Due to the small spatial extent of some of the ecosystem types within the watershed and our sampling design, some ecosystem types were represented by very few (n=2-3) sample points. Because we wanted to avoid these small sample numbers leveraging our statistical analyses, we grouped ecosystem types with similar parent materials. This resulted in us grouping two banded outwash over till ecosystem types with loamy lamellae within 150 cm of the soil surface, resulting in the banded outwash over till group, and grouping four ecosystem types with at least 150 cm of sandy glaciofluvial or eolian parent materials, resulting in the outwash ecosystem group. After aggregating, we had six landscape ecosystem type groups, which are shown in Figure 2.2: 1) outwash-lake plain swamp, 2) riparian wetland, 3) aquic till, 4) mesic till, 5) banded outwash over till, and 6) outwash [including the outwash, outwash-dune, and outwash-beach ridge ecosystems].

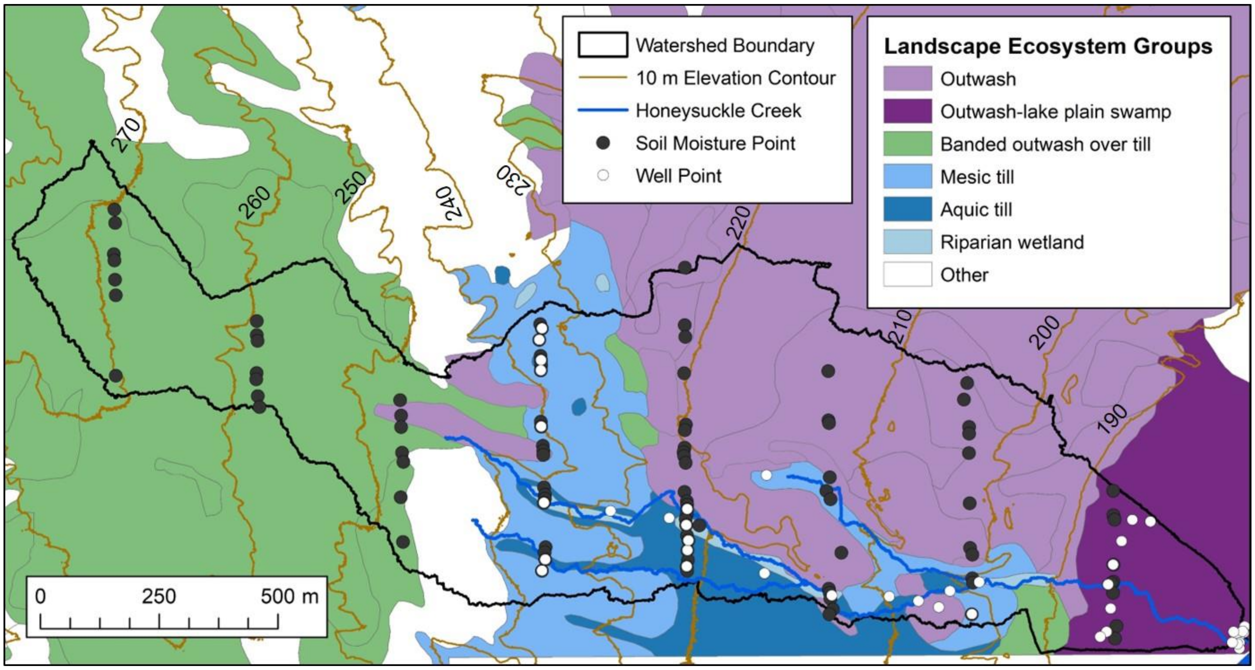


Figure 2.2: Landscape Ecosystem map units of the Honeysuckle Creek watershed. Individual ecosystem types are denoted numerically within the UMBS Landscape Ecosystem classification system; to aid in recognizing their underlying differences, they are grouped and identified here by shorthand names referring to their parent material or landform. Ecosystems on outwash parent materials are shown in purple, deep outwash over glacial till shown in green, and ecosystems with glacial till near the ground surface in blues. Other ecosystems not discussed in this analysis are white. These color groups are the same as the landscape ecosystem types grouped by parent material described in the Methods. Sample points for soil moisture and wells for water table measurements are noted as black and white points, respectively. Brown lines are elevation contours (m above sea level).

*Topographic Wetness Index (TWI) Formulation*

The second type of spatial framework we used to assess the patterns of soil VWC and water table position were topographic wetness indices, one based solely on topographic inputs, the second adding soil properties. These use the continuous variation in elevation and soil transmissivity over space to predict wetness at finer spatial levels than the Landscape Ecosystem map units. These indices, known collectively as TWIs, were initially proposed by Kirkby and Weyman (1974), Beven and Kirkby (1979), and Beven (1986). We generated these two indices with high resolution topographic inputs and soil properties derived from field measurements across the Honeysuckle Creek watershed. The Topographic Index (TI) takes the form:

$$TI = \ln\left(\frac{a}{\tan(\beta)}\right). \qquad (1)$$

where $a$ is the upslope area per unit contour (m) and $B$ is the local slope angle, both determined from a digital elevation model (DEM). We also used the Soil Topographic Index (STI) which adds soil properties to the TI in the form:

$$STI = \ln\left(\frac{a}{K_s D\ tan(\beta)}\right) \qquad (2)$$

where $K_s$ is the mean saturated hydraulic conductivity (m day$^{-1}$) and $D$ is the depth to the glacial till restrictive layer (m). We used both the TI and STI for this analysis, as we wanted to compare how the addition of soil properties to the TWI model impacted the wetness index relationship to field hydrologic measurements.

We used a 0.3 x 0.3 m DEM derived from a 2015 leaf-off aerial LiDAR survey to delineate the Honeysuckle Creek watershed boundary and model flow channels. We resampled the DEM to a 3 m cell size resolution for the topographic input to the wetness indices. Depth to glacial till restrictive layer was measured in the field and mean saturated hydraulic conductivity above the restrictive layer was estimated from field soil texture determinations using the textural triangle and $K_s$ estimates for medium bulk density soil (Schoeneberger et al., 2012). In ecosystems where no restrictive layer was observed, we set 400 cm as the depth value in the outwash upland ecosystems, as this was our maximum sampling depth capability, and 160 cm as the depth value in the outwash-lake plain swamp, which was an average depth to sand C horizon taken from a combination of our soil observations and drinking water well logs from adjacent property owners. Field measurements within each landscape ecosystem were averaged to provide $D$ and $K_s$ values as inputs for the STI. TI and STI maps were generated with the maximum triangle slope calculation (MTS; Tarboton, 1997) and the multiple triangular flow direction algorithm (MD∞; Seibert and McGlynn, 2007), as suggested by Buchanan et al. (2014). The STI map used for this analysis is shown in Figure

2.3. Area-weighted TWI values were extracted within a 3 m buffer around soil moisture sample points and within a 10 m buffer around water table sample points to account for GPS accuracy. ArcGIS (ESRI Inc., Redlands, CA), System for Automated Geoscientific Analyses Geographic Information System (SAGA-GIS), and the RSAGA package in R (Brenning, 2007; R Core Team, 2015) were used to generate the topographic wetness indices.

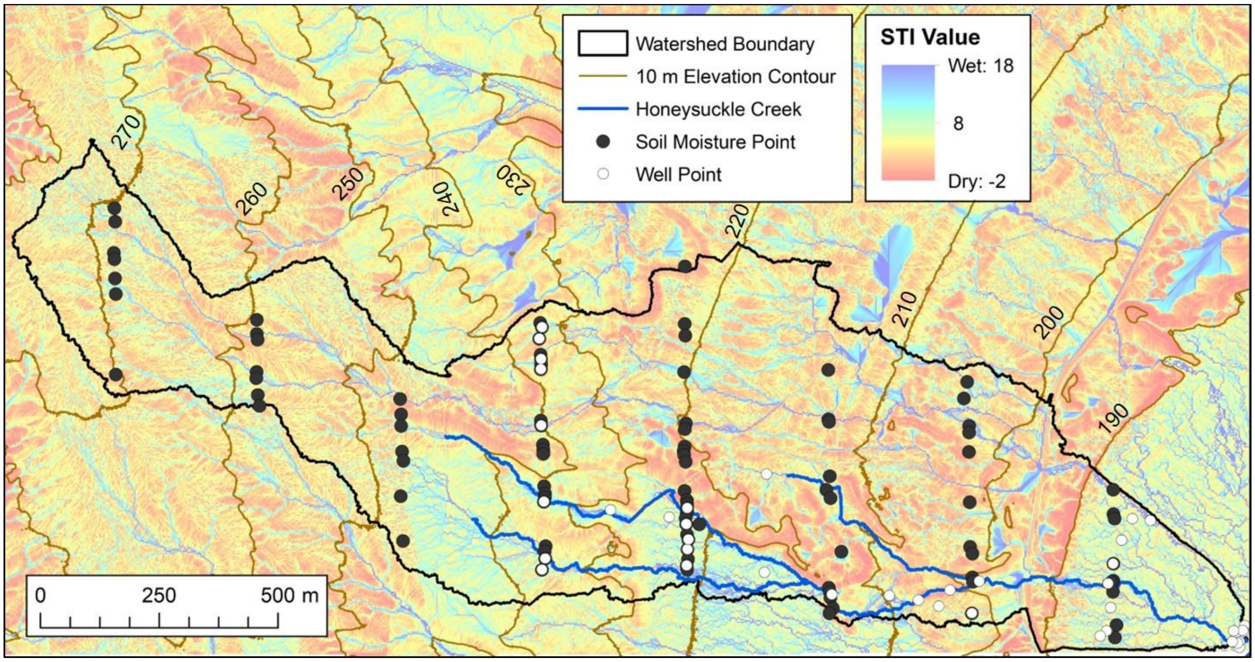


Figure 2.3: STI values across the Honeysuckle Creek watershed. High STI values (blues) indicate areas likely to be wet, while low values (reds) indicate areas likely to be dry. Sample points for soil moisture and wells for water table measurements are noted as black and white points, respectively. Brown lines are elevation contours (m above sea level).

*Point Level Physical Properties*

We summarized a range of physical properties at each sampling point based on field measurements, and digitized elevation and landform GIS data. These properties were: soil texture, depth to restrictive layer, drainage class, basal area, slope class, elevation, and landform. When field observations were not available at a point, we used an average of measurements made within the same landscape ecosystem type. We designated soil texture and measured depth to glacial till restrictive layer in the field. Depth to restrictive layer measurements were grouped at 100 cm intervals for analysis, with 500 cm assigned for points where no restrictive layer was observed. We assigned soil drainage classes (excessively drained to very poorly drained; USDA NRCS, 2016) based on observations of soil profile morphology (*e.g.*, on the basis of redoximorphic features or indications of impeded or lateral drainage) and Landscape Ecosystem classifications (Pearsall et al., 1995). We calculated the basal area of live overstory vegetation from point-quarter vegetation surveys of trees with a DBH (diameter at breast height) greater than 8 cm. Slope was calculated within a 5 m buffer around each point using the high-resolution DEM and grouped by USDA NRCS slope classes (nearly level to steep). Elevation at each point was extracted from the DEM and then points were grouped based on the levels of significant postglacial lakes (*i.e.*, Lake Nipissing below 190 m, Main Lake Algonquin between 190-225 m, Early Lake Algonquin 225-255 m, no lakes with shorelines higher than 255 m). Major and minor landform designations were based on topography and parent material (*e.g.*, outwash, moraine) and are the two levels of the classification hierarchy above ecosystem type (Pearsall et al., 1995).

*Data Analysis*

We performed statistical analyses of soil VWC and water table position to characterize seasonal hydrologic patterns across the Honeysuckle Creek watershed and evaluate whether existing spatial frameworks (Landscape Ecosystem classification, Topographic Wetness Indices) could be used to assess spatial variability and patterns of wetness. Data were examined by meteorological seasons Spring (MAM), Summer (JJA), Autumn (SON), and Winter (DJF). Statistical analyses were conducted with R (R Core Team, 2016) and SigmaPlot (SYSTAT Software, San Jose, CA USA). Histograms and boxplots of soil VWC indicated two distinct soil hydrologic conditions, with the Terric Haplosaprists (below 190 m elevation) being permanently saturated through all seasons, and the mineral soils (Haplorthods, Epiaquods, and Endoaquents) varying seasonally from dry to saturated. Given these fundamental differences in hydrology and matrix material, we separated the Terric Haplosaprists (outwash-lake plain swamp ecosystem) from all other soils in the TWI analyses. Due to non-normally distributed data that could not be transformed into normality, we used nonparametric Kruskal-Wallis One-Way ANOVA on Ranks tests with Dunn's Method of Comparisons to determine which physical properties were significant predictors of median soil VWC and water table position based on H statistic and $p$-value. Statistically significant $p$-values for this analysis were adjusted from $p<0.05$ to $p=0.0063$ by a Bonferroni correction due to repeated Kruskal-Wallis tests for each group (n=8).

To address our second objective, we used two methods to evaluate the ability of the two spatial frameworks to represent spatial patterns of moisture. To evaluate the Landscape Ecosystem classification, we used Kruskal-Wallis tests to determine if soil VWC and water table position differed first by ecosystem group, and then if there were any seasonal differences within each ecosystem. We used daily soil VWC and water table measurements (when water was observed in wells). Due to a small number of sample points in some of the outwash ecosystem types, we compared moisture between the six ecosystem groups described above. In these tests we accepted results as statistically significant when $p<0.0071$ due to Bonferroni correction (n=7). We also assessed individual point-scale variability in measured soil VWC by comparing the mean standard deviation of the 3 measurements taken at each point between landscape ecosystem types with Kruskal-Wallis tests.

Secondly, we used linear regressions to test the relationship between TWI values (TI and STI) and measured soil VWC and water table position in each season. We used seasonal mean soil VWC and water table positions at each point and point-level TWI values. Non-normal data were transformed for this analysis. To assess the utility of TWIs in different soils, we grouped points by parent material (*i.e.*, outwash, till) and tested the relationship between TWI and mean soil VWC for each season. Outwash soils (outwash more than 3 m deep) were compared with till soils (soils with glacial till restrictive material within 3 m of surface). All water table sample points were in till soils. We used dummy variable coding to test for significant differences between the outwash and till regression models as well as the different seasonal regression models.

### *Results*

*Soil Moisture and Water Table Position in Organic versus Mineral Soils*

Soil moisture conditions varied widely throughout the Honeysuckle Creek watershed with generally drier conditions at higher elevations and in glacial outwash landforms and wetter conditions in the lower elevation (especially wetland) ecosystems. Water tables were observed from Burt Lake (181 m) up to 240 m elevation in places where glacial till was within 3 m of the ground surface. Seasonal distributions of soil VWC and water table position indicate two widely different moisture conditions between the organic soils in the outwash-lake plain swamp and the mineral soils of the other ecosystem groups (Figure 2.4). Specifically, the outwash-lake plain swamp organic soils had higher median soil VWC (53%) and shallower depth to water table (8 cm below surface) than the drier mineral soils (17% WC) with deeper water tables (22 cm below surface). Moisture conditions also varied seasonally; in mineral soils, soil moisture was highest and the water table closest to the surface in spring, while organic soils were saturated in both spring and autumn and the water table was within 7 cm of the surface. In both soil types (organic and mineral), soil moisture values were the lowest and water tables furthest from the surface in summer. Setting aside seasonal dynamics, a range of physical factors appeared to influence the soil moisture patters that we observed across the watershed. Drainage class, soil texture, depth to restrictive layer, minor and major landforms, and elevation were all significant predictors of soil VWC in all seasons ($p$<0.0063). These properties were also significant predictors of water table position, but only in the summer and autumn seasons; water table position in spring and winter was not related to any physical factor. Among physical factors, slope class was the only non-significant predictor of soil VWC or water table position in any season. Our metric of forest biomass (live tree basal area) did not have significant predictive capacity for either soil VWC or water table position.

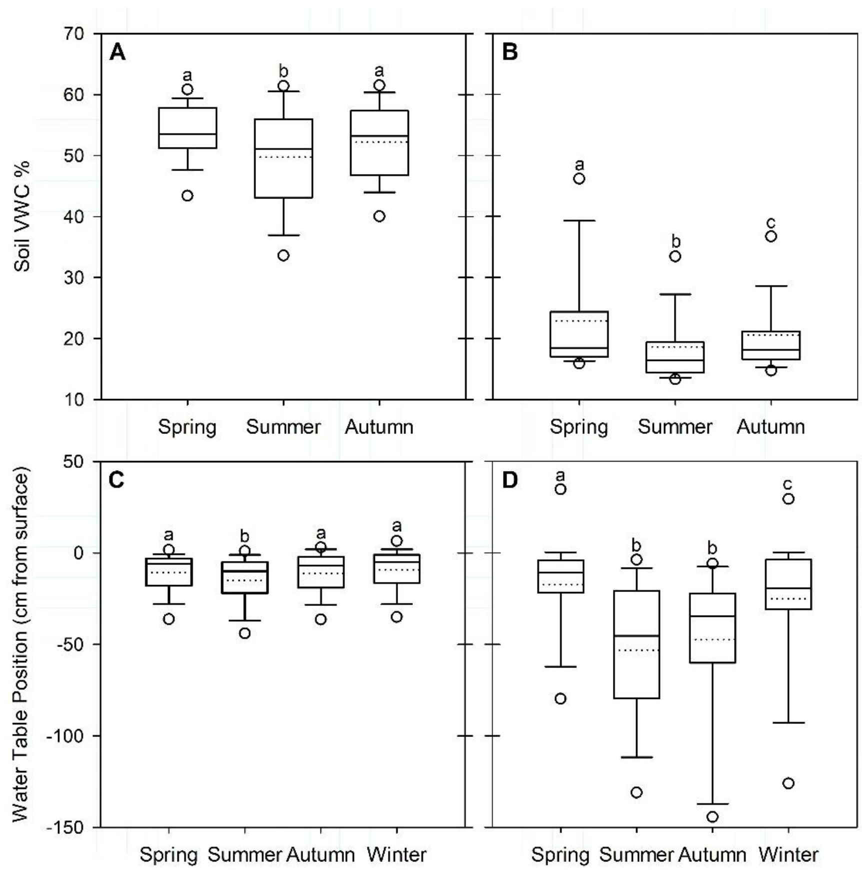


Figure 2.4: Distribution of daily soil VWC and water table position in organic soil from the outwash-lake plain swamp (panels A, C) and mineral soil from the upland ecosystems (panels B, D) by season. Boxes show medians, 25$^{th}$ and 75$^{th}$ percentiles; whiskers are 10$^{th}$ and 90$^{th}$ percentiles; points are outliers beyond the 5$^{th}$ and 95$^{th}$ percentiles. Dotted lines indicate means. Within each panel, letters denote significant seasonal differences in median VWC and water table position.

*Spatial Framework 1: Ecosystem Level Patterns of Wetness*

The Landscape Ecosystem classification was an effective framework to assess significant differences in soil wetness and water table position across ecosystem groups. Specifically, median soil VWC for the entire sampling period differed significantly for all ecosystem groups ($p$<0.0071) except the riparian wetland and aquic till types (Table 2.1). Across the watershed, the wettest soil conditions were observed in the outwash-lake plain swamp ecosystem, where soils were perennially saturated, and the driest conditions were in the outwash and banded outwash over till ecosystems where soils were around field capacity in all seasons. As to differences in mean soil VWC from season to season (Figure 2.5), the riparian wetland and aquic till ecosystems experienced the greatest change in mean VWC across the seasons, changing by 11-12% VWC, while other ecosystems varied by only 1-3% VWC. In the mesic till and outwash ecosystems, soil VWC differed across all seasons, being wettest in spring and driest in summer. In the outwash-lake plain swamp, spring VWC was highest and differed only from summer VWC. In the riparian wetland, aquic till, and banded outwash over till ecosystems, spring soil VWC was higher than summer and autumn measurements.

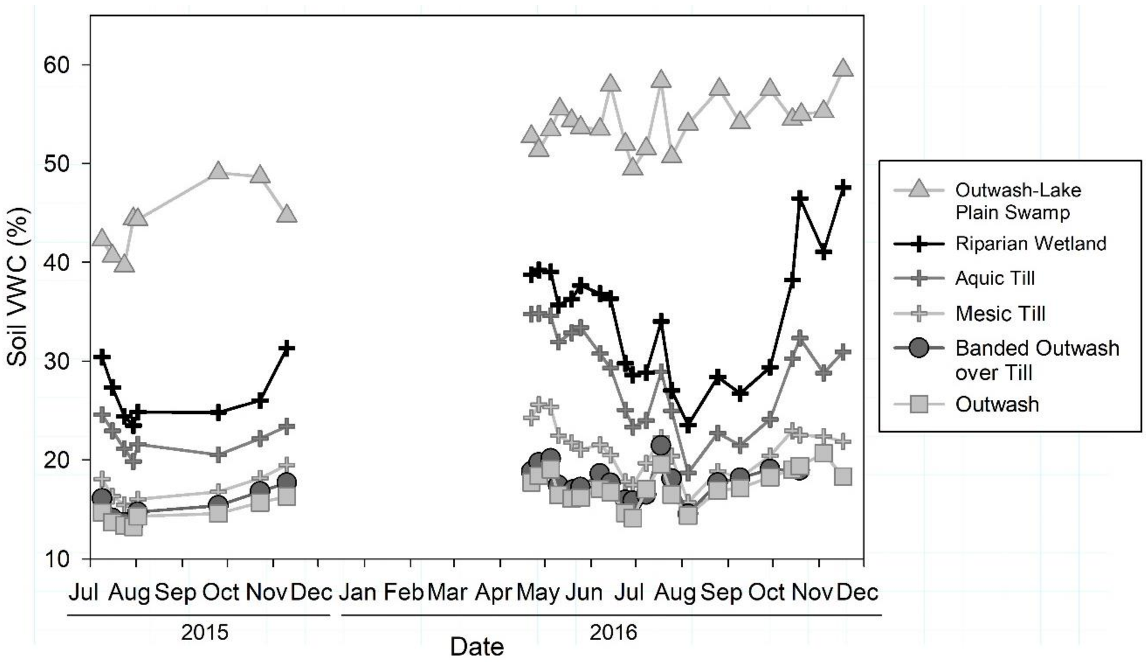


Figure 2.5: Mean soil VWC within Landscape Ecosystem type groups during the period of observation (July–November 2015, April–November 2016). Snow cover existed from December through April.

Table 2.1: Soil VWC over the full period of observation and within each season, by ecosystem groups. Groups consist of individual ecosystem types with similar parent materials; see Methods for group definitions. For each ecosystem group, the table shows the number of sample points (locations) and the median, 25$^{th}$ and 75$^{th}$ percentile of periodic VWC measurements. Significantly different medians among ecosystem groups ($p$<0.0071) are denoted with different letters for the full annual dataset. Seasonal differences within each ecosystem group are discussed in the text.

| Landscape Ecosystem Groups | Sample Points (n) | All Observations | Spring | Summer | Autumn |
|---|---|---|---|---|---|
| | | Soil VWC % | | | |
| Outwash-Lake Plain Swamp | 9 | 53 (47, 57)*a* | 54 (51, 58) | 51 (43, 56) | 53 (47, 57) |
| Riparian Wetland | 9 | 25 (21, 33)*b* | 35 (22, 46) | 23 (17, 34) | 24 (19, 35) |
| Aquic Till | 12 | 25 (19, 38)*b* | 35 (30, 41) | 24 (20, 29) | 24 (21, 28) |
| Mesic Till | 13 | 18 (16, 21)*c* | 20 (18, 29) | 17 (15, 20) | 19 (17, 21) |
| Banded Outwash over Till | 20 | 17 (15, 18)*d* | 18 (17, 19) | 16 (14, 18) | 18 (16, 19) |
| Outwash | 33 | 16 (15, 18)*e* | 18 (16, 18) | 15 (14, 17) | 17 (15, 18) |

In all ecosystems where wells were placed, median water table positions differed significantly (Table 2.2). Across the watershed, water table levels ranged in depth from very near to the ground surface in low topographic positions to meters deep (or even nonexistent) in upland areas (below our deepest wells). Water tables were closest to the ground surface in the outwash-lake plain swamp and riparian wetland, followed by the aquic till ecosystem; these ecosystems had median annual water levels within 25 cm of ground surface. In the mesic till ecosystem, median water table levels were greater than 50 cm below the surface, and the two wells in the outwash ecosystems had water tables more than 100 cm below ground. Although we did place two wells in outwash ecosystems, specifically the outwash-dune and heavily banded outwash ecosystems, these points were at the intersection of outwash and till areas and were not representative of most outwash areas. We did not observe water tables or evidence of saturation in the banded outwash over till ecosystem or at many points within outwash ecosystems during soil profile observations. In all ecosystems where wells were placed median water table positions differed significantly (Table 2.2).

Table 2.2: Water table position over the full period of observation and within each season, by ecosystem groups. Groups consist of individual ecosystem types with similar parent materials; see Methods for group definitions. For each ecosystem group, the table shows the number of sample points (locations) and the median, 25th and 75th percentile of periodic water table measurements. Negative values indicate water below ground surface. Significantly different medians among ecosystem groups ($p$<0.0071) are denoted with different letters for the full annual dataset; seasonal differences within each ecosystem group are discussed in the text.

| Landscape Ecosystem Groups | Sample Points (n) | All Observations | Spring | Summer | Autumn | Winter |
|---|---|---|---|---|---|---|
| | | Water Table Position (cm from surface) | | | | |
| Outwash-Lake Plain Swamp | 26 | -8<br>(-20, -3)*a* | -6<br>(-18, -3) | -10<br>(-22, -5) | -7<br>(-19, -2) | -5<br>(-17, -1) |
| Riparian Wetland | 3 | -6<br>(-10, -1)*b* | -4<br>(-6, 31) | -13<br>(-33, -8) | -10<br>(-21, -7) | -1<br>(-5, 27) |
| Aquic Till | 11 | -25<br>(-39, -17)*c* | -17<br>(-22, -9) | -55<br>(-79, -33) | -35<br>(-57, -32) | -20<br>(-28, -14) |
| Mesic Till | 7 | -65<br>(-123 -37)*d* | -33<br>(-72, -2) | -90<br>(-121, -51) | -140<br>(-145, -55) | -61<br>(-126, -43) |
| Outwash | 2 | -139<br>(-155, -100)*e* | -117<br>(-155, -82) | -152<br>(-155, -123) | -146<br>(-154, -134) | -169<br>(-184, -117) |

Water table position fluctuated widely in the wells, with some wells drying up for weeks to months at a time and others maintaining water levels within a few centimeters throughout the year (Figure 2.6). Generally, water table levels were closer to the surface in the spring and winter seasons, and dropped during the summer and autumn seasons, with some wells even drying up during these seasons. Specific seasonal differences varied within ecosystem types. In the outwash-lake plain swamp, summer median water table position was significantly lower than in the other seasons. In the riparian wetland, winter and spring water levels were significantly higher than summer and autumn levels, with water ponding on the surface in some areas. Similarly, in the aquic till ecosystem water table positions were significantly closer to the surface in spring and winter, with the highest levels in the spring, and the lowest levels in summer and autumn. In the mesic till ecosystem, water tables were highest in spring, lowest in autumn, and did not significantly differ between winter and summer. Water table levels in outwash ecosystems did not differ significantly among seasons.

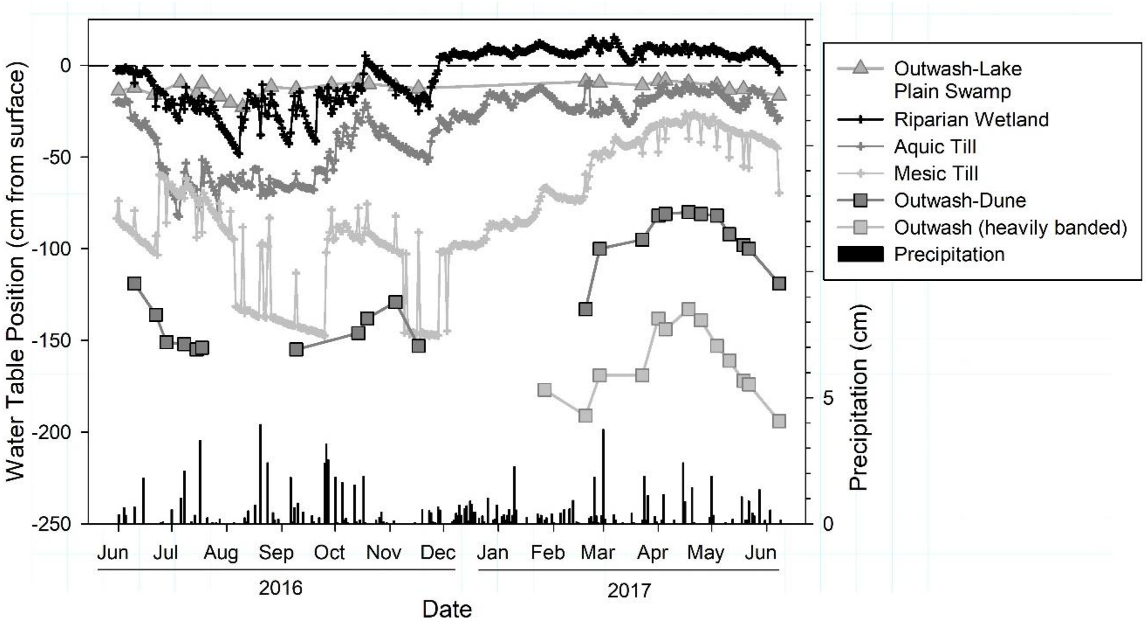


Figure 2.6: Mean daily water table position within Landscape Ecosystem types and precipitation for June 2016–June 2017. Dashed line indicates ground surface. Abrupt, transient fluctuations (peaks) in water level in the riparian wetland, aquic till, and mesic till ecosystems occur when mean values from continuous daily logger measurements are leveraged by periodic measurements of additional wells by hand. These additional, hand-measured wells and the variability they induce in the continuous logger data streams provide an indication of the variation in water level observed within those ecosystems.

*Spatial Framework 2: High Resolution Patterns of Wetness*

Within each 0.07-25.5 ha Landscape Ecosystem map unit in the watershed, a range of local topographic positions, fine scale soil variation, and wetness conditions exist. Within such heterogeneous ecosystems as these, one estimate of soil VWC or water table position might not adequately characterize the range of moisture conditions observed. Ecosystem types with mixed hydrologic conditions (riparian wetland, aquic till, mesic till) had larger standard deviations (4-7% VWC) at each triplicate sampling point than the ecosystems with consistently drier moisture conditions (2% VWC). TWIs, with each pixel covering 9 $m^2$, were tested against field measured moisture conditions to determine if these higher resolution spatial frameworks could account for local variation and provide finer scale estimates of soil VWC and water table depth, which could be especially useful in areas with mixed hydrologic conditions.

Relationships between TWIs and soil VWC revealed that soil parent material created two distinct hydrologic conditions. Across all seasons, point-level soil moisture values in outwash soils (excluding the organic soils of the outwash-lake plain swamp) was below 20% VWC, despite STI values for those points ranging from 0 to 8.2. In contrast, till soils showed increasing VWC (15% to 50%) with increasing STI values. Similar VWC patterns were observed for TI values. Linear regressions with STI values and soil VWC were statistically significant for both the till ($p$<0.001) and outwash soils ($p$=0.005-0.024) in all seasons (Figure 2.7), although the linear models provided better estimates in the till soils ($R^2$=0.25-0.38) than in the outwash soils ($R^2$=0.11-0.16). Linear regressions with TI values and soil VWC were also significant for both parent materials. In outwash soils TI-based models ($p$=0.003-0.021; $R^2$=0.11-0.18) were very similar to STI-based models; however, in till soils the TI-based models explained less of the variation in soil VWC ($p$=0.001-0.018; $R^2$=0.14-0.24) than the STI-based models. Based on dummy variable coding, model slopes were significantly lower for outwash points than till points for both TI and STI models. In addition, all seasonal VWC models were significantly different. In both the till and outwash soils, linear regressions can be used to estimate soil VWC from TI and STI. However, in till soils the STI provides better estimates of VWC than the TI. In outwash soils, the very shallow slopes of the TI and STI models raises questions about the utility of TWIs in very deep and conductive soils.

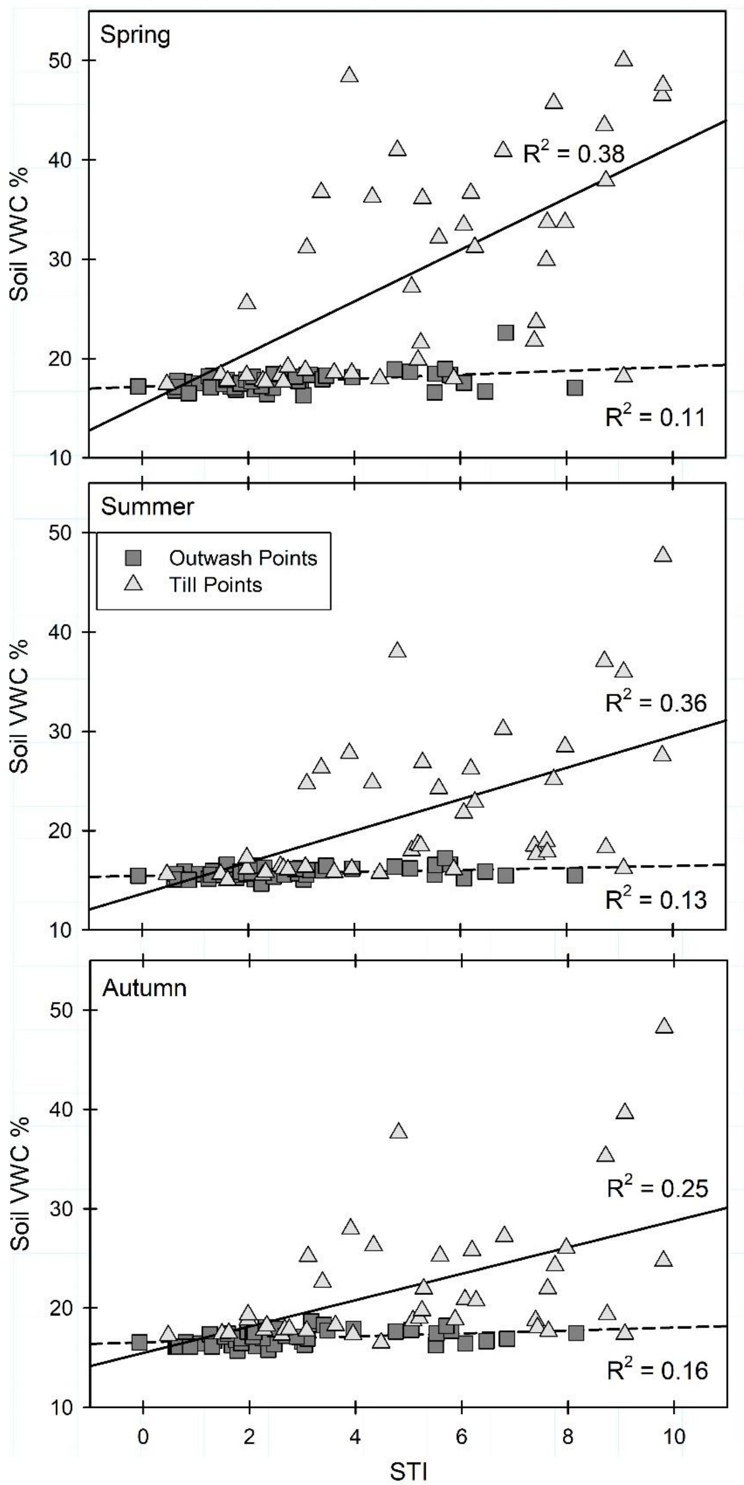


Figure 2.7: Relationships between STI and soil VWC, by season, for sample points grouped by parent material (outwash v. till). Plots exclude sampling points located in the organic soils of the outwash swamp (181-190 m elevation). $R^2$ values are for separate linear regressions fit to till points (solid line) and outwash points (dashed line).

While the STI was the more statistically significant TWI form for estimating soil moisture, especially in till soils, both the STI and TI could be used to estimate water table position from ground surface, when water is present (Figure 2.8). Seasonal mean water table depth was estimated with both TI and STI values for all seasons using linear models ($R^2$=0.17-0.47 for TI models; $R^2$=0.30-0.62 for STI models). Summer and autumn seasons had the strongest linear model fits ($R^2$=0.44, 0.47 for TI; $R^2$=0.60, 0.62 for STI), followed by spring ($R^2$=0.23 for TI; $R^2$=0.33 for STI), and winter ($R^2$=0.17 $p$<0.071 for TI; $R^2$=0.30 for STI). Comparing the seasonal linear models, there were no significant differences between the spring and winter models, or the summer and autumn models based on dummy variable coding. This was true for both the TI- and STI-based models. Both TI and STI values were good predictors of mean water table position, but models using STI values provided a slightly better estimate of water table position.

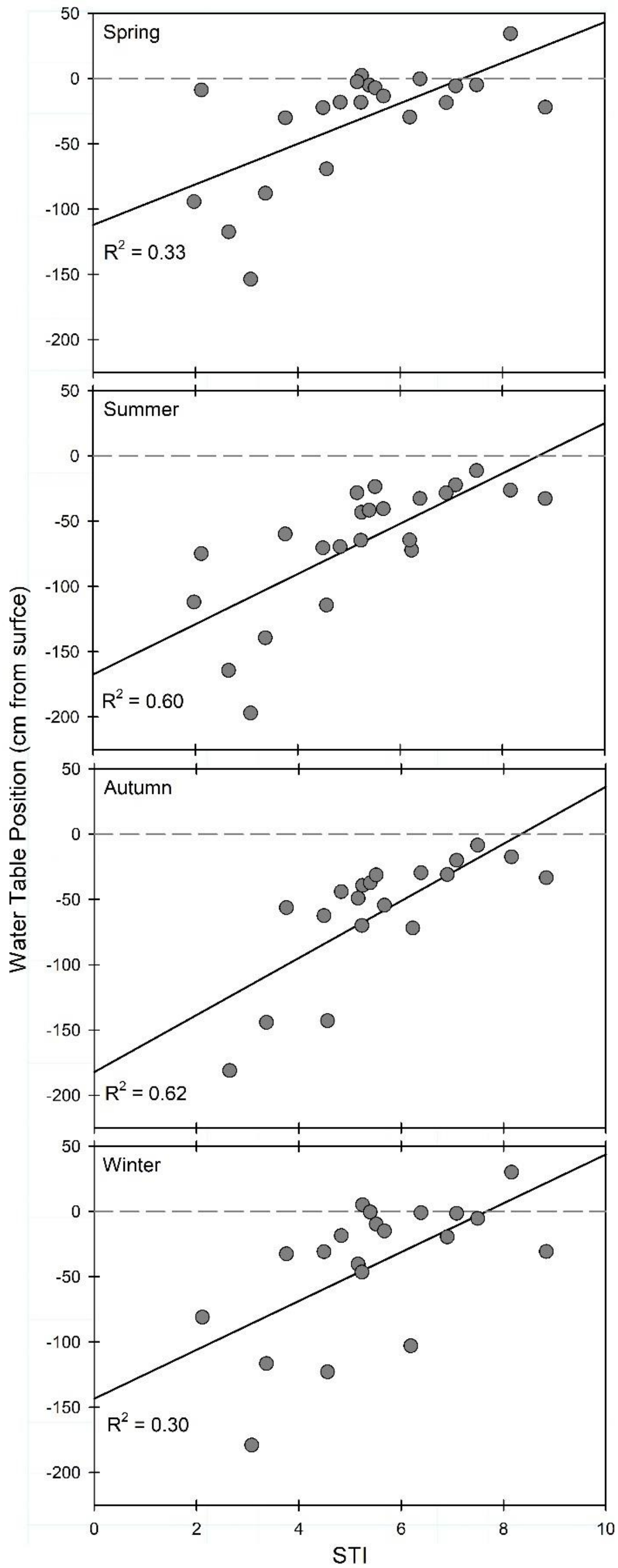


Figure 2.8: Relationships between STI and water table position, by season for individual wells. $R^2$ values are for linear regressions (solid line). Dashed line indicates ground surface.

## ***Discussion***

Topographic position and parent material establish three soil hydrologic regimes (dry, wet, or mixed) across the Honeysuckle Creek watershed. These hydrologic regimes include the dry outwash uplands, the wet outwash-lake plain swamp, and the mixed moisture areas underlain by shallow till. The dry regime is driven primarily by soils with high infiltration rates, the wet regime formed in low topographic areas receiving drainage from uplands, and the mixed moisture regime in areas with both lateral transport of water and soils with a restrictive feature near the surface. Across the watershed, local soil properties have the strongest control over soil moisture conditions, while deeper ground water patterns are driven by both soil properties and topography.

### *Hydrologic Regimes Across the Watershed*

In the outwash ecosystems soils above 190 m elevation, the hydrologic regime was dry, with low soil moisture conditions (15-18% VWC) conditions varying little spatially across the ecosystems or throughout the year. Even in the wettest season (spring, post-snowmelt), soil VWC remained at 18% and no evidence of shallow ground water was observed. These sandy soils continued to dry in summer as vegetation water use peaked (He et al., 2014) and remained dry throughout autumn. In this moisture regime, soil texture and the great depth of outwash material drives consistently dry surface moistures and the limited water holding capacity and lack of restrictive material prevents shallow groundwater retention or perching on shallow restrictive layers.

In contrast, wet moisture conditions were observed in the outwash-lake plain swamp where median soil water remained at or above saturation and varied by only 1-3% VWC throughout the year, and water table levels were persistently within 10 cm of the ground surface. These wet conditions may exist because the low-lying swamp is receiving groundwater draining from higher topographic areas in the mid-elevations of the watershed (Zogg and Barnes, 1995; Nave et al., 2017a). The relatively continuous glacial till parent material in the middle elevations of the watershed (present at elevations from 245 m down to 190 m) provides a surface for shallow water to drain to the outwash-lake plain swamp throughout the year. The low-lying landscape position coupled with the low hydraulic conductivity organic soils in the outwash-lake plain swamp allow for persistent saturation and a wet moisture regime (Bolter, 1969).

Ecosystem types occupying the middle elevations of the watershed possess mixed hydrologic conditions due to glacial till relatively near the surface supporting the lateral transport of water perched on the restrictive material (the mesic till, aquic till, riparian wetland ecosystems). Here, moisture was greatest in the spring, with highest soil VWC and water table positions closest to the surface. In the middle elevations, ecosystems with deeper, more well-drained soils averaged 20% VWC and the water table was 33 cm below the surface; in ecosystems occupying lower topographic areas with shallower soils, spring VWC was 35% and water tables were within 25 cm of the surface or even at the surface in many areas. Summer vegetation transpiration draws down soil VWC and shallow groundwater levels (He et al., 2014), but slow lateral drainage of snow melt, finer textured parent materials with higher water holding capacity, and thicker organic horizons kept likely median soil VWC at 25% and water table levels high throughout the summer and autumn, especially in the lowest topographic positions.

*Applicability of the Two Spatial Frameworks*

In the dry and wet hydrologic regimes, the Landscape Ecosystem classification map units are at a small enough scale (tens of hectares) to represent both soil moisture and shallow ground water conditions and provide estimates of moisture at points not directly measured. In these areas, there was little variation in soil VWC or water table position, either temporally and spatially.

Variation in soil moisture within ach ecosystem group was minimal in the dry uplands (less than 2% VWC). This consistency across the range of elevations, aspects, and slopes suggests that the excessive drainage of the deep, coarse-textured outwash soils overrides any topographic influences on soil wetness in such settings. In the outwash-lake plain swamp, variation in soil moisture content was also relatively low, and very localized, apparently in relation to surface microtopography and the thickness of bryophyte cover. Here, in the outwash-lake plain swamp, the low elevation, level topography, and large contributing area drive consistent conditions that are the opposite extreme from the xeric outwash uplands.

In the mixed hydrologic regime with heterogeneous soils that have formed in the unsorted glacial till, both soil and topography are important factors controlling moisture. While the Landscape Ecosystem classification was able to distinguish significant differences in moisture among these ecosystems (mesic till, aquic till, riparian wetland), within ecosystem soil VWC varied from 15% to 46%, very local variation (*i.e.*, among triplicate sampling points) was as high as 6% VWC, and VWC varied by over 10% seasonally in till ecosystems. As the till itself is comprised of a wider range of glacial sediments, distributed in a non-uniform manner (*i.e.*, as compared to water-sorted glacial deposits), the finer scale integration of soil and topographic properties afforded by the TWIs was needed to represent spatial patterns of wetness. While both the TI and STI could be used to estimate soil VWC and water table position, the inclusion of soil properties in the wetness index was essential for optimal estimates of soil VWC, and slightly improved estimates of water table position.

*Broader Relevance of TWIs*

While not intended to be globally representative, our study area has sufficient variation in parent material and topography to assess the ability of TWIs to represent moisture conditions across a wide range of physical factors that control wetness in glacial drift landscapes. Our analysis suggests that TWIs provide the most accurate estimates of soil moisture and water table position and are most appropriate in areas of the watershed with restrictive material within 3 m of the ground surface. Many other studies have also observed good relationships between soil moisture and groundwater level and TWIs in primarily forested study areas with shallow soils above restrictive layers or bedrock (*e.g.*, Gburek et al., 2006; Lin et al., 2006; Penna et al., 2009; Detty and McGuire, 2010; Beaudette et al., 2013; Rinderer et al., 2014). However, in areas with conductive soils or relatively flat topography with low hydraulic gradients, the observed relationships between TWIs and moisture conditions have been weaker, possibly because surface topography is not a strong control on groundwater under such conditions (*e.g.,* Barling et al., 1994; Case et al., 2005; Grabs et al., 2009; Bachmair and Weiler, 2012). In glaciated areas with both till and deeper alluvial soils, Grabs et al. (2012) observed good predictions of water table depth from a TI in both till and alluvial sediment in Sweden, although the TI provided better estimates of riparian zone carbon characteristics in the till areas compared to the alluvial sediment areas. Approximately 170 km north of our study area, Monteith et al. (2006) observed a positive relationship between TI and water table depth in two glacial drift watersheds, although this positive relationship was only true for wells in basal till and they observed no relationship in ablation till areas. Our study strengthens and extends the inference of that work, by indicating that dense, impermeable glacial till has a controlling influence on wetness and a functional role similar to bedrock, even in landscapes where its distribution is discrete and interrupted by other types of glacial parent materials.

In these heterogeneous glacial landscapes, we must consider landform and parent material when deciding where to use TWIs to identify moisture patterns. Where there is low hydraulic conductivity glacial till restrictive material, perched shallow water tables can form above this horizon, connecting shallow groundwater and surface soil water vertically, as well as connecting these points to others along hillslopes and into riparian zones (Detty and McGuire, 2010; Ali et al., 2011). The distribution of perched water tables can activate surface and subsurface flow pathways, resulting in expanded hydrologic connectivity between the landscape and the stream network (Gburek et al., 2006; Jencso et al., 2009; Tetzlaff et al., 2014; Gillin et al., 2015). Given our full annual period of observation, we have observed that seasonal variation is generally lower than spatial variation within all three hydrologic regimes, although, shorter-term fluctuations in wetness did occur, particularly in the mixed hydrologic regime. These peaks in soil moisture and water table level due to storm events could be important for element processing and transporting material through the watershed (Brown et al., 1999; Inamdar et al., 2004; Sebestyen et al., 2014; Duncan et al., 2015). Snowmelt and rain can cause the lateral and vertical expansion of variable source areas across the watershed and into organic rich near-surface soil horizons that are only connected to the stream at lower flows (Boyer et al., 1997; Lambert et al., 2014; Tetzlaff et al., 2014). Both TWIs and the Landscape Ecosystem classification can be used to identify the areas, such as riparian zones and topographic lows, likely to respond to precipitation events, and be sources of carbon or nitrate (Andrews et al., 2011; Duncan et al., 2013; Gannon et al., 2015) flushed from terrestrial to aquatic ecosystems. In places with deep outwash lacking some restrictive component to create a perched water table and connect surface soil and groundwater, topographic indices are likely not the most appropriate spatial framework for identifying moisture patterns. This analysis indicates that in ecosystems where VWC and water table position do not vary much, such as ecosystems with outwash parent materials, ecosystem classifications can be used instead of TWIs to estimate moisture patterns. In the mineral outwash soils, flow paths identified by the TWIs had no relationship between moisture conditions or soil profile observations. However, in the outwash-lake plain swamp TWI flow paths were able to identify subtle, topographically driven differences in water movement that induced spatial patterns in soil morphology and distribution of elements (Nave et al., 2017a).

***Conclusions***

Our measurements of soil water and shallow groundwater through a hydrologic year provide a baseline for understanding the spatial patterns and temporal dynamics of terrestrial water in the Honeysuckle Creek watershed. We have been able to identify three dominant hydrologic regimes across the watershed and the spatial frameworks that are most appropriate to estimate moisture conditions at points we are unable to sample. While either spatial framework (ecosystem classification or TWI) can be used to estimate soil VWC and water table position, a combination of both approaches is most appropriate in this region. In areas with minimal soil moisture variation (dry or wet) with relatively homogenous soils, larger ecosystem classification map units provide good estimates of moisture conditions. In areas with very heterogeneous till soils, finer scale spatial frameworks that account for local soil variation are optimal for characterizing spatial patterns. Utilizing both spatial frameworks in future research will aid in identifying biogeochemically important sites, assessing hydrologic connectivity throughout the watershed, and informing sampling campaigns. Provided parent material and soil characteristic data, watersheds with similar geologic and climatic conditions can be stratified into units differing in wetness and variability using ecosystem classification, such as the ECOMAP framework, and TWI spatial frameworks.

## REFERENCES


Albert, D.A., M. Lapin, and D.R. Pearsall. 2015. Knowing the territory: Landscape Ecosystem classification and mapping. The Michigan Botanist 54:34-41.

Albert, D.A. 1995. Regional landscape ecosystems of Michigan, Minnesota and Wisconsin: A working map and classification. General Technical Report NC-178. St. Paul, Minnesota: U.S. Dept. of Agriculture, Forest Service, North Central Forest Experiment Station.

Ali, G.A., C.L'Heureux, A.G. Roy, M. Turmel, and F. Courchesne. 2011. Linking spatial patterns of perched groundwater storage and stormflow generation processes in a headwater forested catchment. Hydrol Process 25:3843-3857.

Ali, G.A., C. Birkel, D. Tetzlaff, C. Soulsby, J.J. McDonnell, and P. Tarolli. 2014. A comparison of wetness indices for the prediction of observed connected saturated areas under contrasting conditions. Earth Surf. Process. Landforms 39:399-413.

Ali, G.A., A.G. Roy, and P. Legendre. 2010. Spatial relationships between soil moisture patterns and topographic variables at multiple scales in a humid temperate forested catchment. Water Resour. Res. 46:1-18.

Andrews, D.M., H. Lin, A. Zhu, L. Jin, and S.L. Brantley. 2011. Hot spots and hot moments of dissolved organic carbon export and soil organic carbon storage in the Shale Hills catchment. Vadose Zone J. 10:943-954.

Bachmair, S. and M. Weiler. 2012. Hillslope characteristics as controls of subsurface flow variability. Hydrol. Earth Syst. Sci. 16:3699-3725.

Bailey, S.W., P.A. Brousseau, K.J. McGuire, and D.S. Ross. 2014. Influence of landscape position and transient water table on soil development and carbon distribution in a steep, headwater catchment. Geoderma 226-227:279-289.

Barling, R.D., I.D. Moore, and R.B. Grayson. 1994. A quasi-dynamic wetness index for characterizing the spatial distribution of zones of surface saturation and soil water content. Water Resour. Res. 30:1029-1044.

Beaudette, D.E., R.A. Dahlgren, and A.T. O'Geen. 2013. Terrain-shape indices for modeling soil moisture dynamics. Soil Sci. Soc. Am. J. 77:1696-1710.

Berthelot, J., Saint-Laurent, D., Gervais-Beaulac, V., Savoie, D. 2014. Assessing the effects of periodic flooding on the population structure and recruitment rates of riparian tree forests. Water 6:2614-2633.

Beven, K.J. 1986. Runoff production and flood frequency in catchments of order n: An alternative approach. In: V.K. Gupta, I. Rodriguez-Iturbe, and E.F. Wood, editors, Scale Problems in Hydrology. D. Water Science and Technology Library, vol 6. Springer, Dordrecht. p. 107-131.

Blewett, W.L. and H.A. Winters. 1995. The importance of glaciofluvial features within Michigan's

Port Huron moraine. Ann. Assoc. Am. Geogr. 85:306-319.

Bolter, D.H. 1969. Physical properties of peats as related to decomposition. Soil Science Society of America Proceedings 33:606-609.

Boyer, E.W., G.M. Hornberger, K.E. Bencala, and D.M. McKnight. 1997. Response characteristics of DOC flushing in an alpine catchment. Hydrol. Processes 11:1635-1647.

Boyle, M.F., S.R. Abella, and V.B. Shelburn. 2014. An ecosystem classification approach to assessing forest change in the southern Appalachian Mountains. For. Ecol. Manage. 323:85-97.

Bracken, L.J., J. Wainwright, G.A. Ali, D. Tetzlaff, M.W. Smith, S.M. Reaney, and A.G. Roy. 2013. Concepts of hydrological connectivity: Research approaches, pathways and future agendas. Earth-Science Reviews 119:17-34.

Brenning, A 2007. RSAGA: SAGA geoprocessing and terrain analysis in R. http://cran.r-project.org/web/packages/RSAGA/index.html.

Brown, V.A., J.J. McDonnell, D.A. Burns, and C. Kendall. 1999. The role of event water, a rapid shallow flow component, and catchment size in summer stormflow. J. Hydrol. 217:171-190.

Brzostek, E.R., D. Dragoni, H.P. Schmid, A.F. Rahman, D. Sims, C.A. Wayson, D.J. Johnson, and R.P Phillips. 2014. Chromic water stress reduces tree growth and the carbon sink of deciduous hardwood forests. Global Change Biol. 20:2531-2539.

Buchanan, B.P., M. Fleming, R.L. Schneider, B.K. Richards, J. Archibald, Z. Qiu, and M.T. Walter. Evaluating topographic wetness indices across central New York agricultural landscapes. Hydrol. Earth System Sci. 18:3279-3299.

Burt, T.P. and Pinay, G. 2005. Linking hydrology and biogeochemistry in complex landscapes. Prog. Phys. Geogr. 29:297-316.

Cameron, R.P. and D. Williams. 2011. Completing an ecosystem classification system for Nova Scotia. Natural Areas Journal 31:92-96.

Case, B.S., F. Meng, and P. Arp. 2005. Digital elevation modelling of soil type and drainage within small forested catchments. Can. J. Soil Sci. 85:127-137.

Castellano, M.J., D.B. Lewis, D.M. Andrews, and M.D. McDaniel. 2012. Coupling Biogeochemistry and Hydropedology to Advance Carbon and Nitrogen Cycling Science. In: Lin, H., editors, Hydropedology, p. 711-735.

Cleland D.T., P.E. Avers, W.H. McNab, M.E. Jensen, R.G. Bailey, T. King, and W.E. Russell. 1997. National hierarchical framework of ecological units. In: Boyce, M.S. and A. Haney, editors, Ecosystem Management: Applications for sustainable forest and wildlife resources, p. 181-200. New Haven, CT: Yale University Press.

Cullum, C., K.H. Rogers, G. Brierley, and E.T.F. Witkowski. 2016. Ecological classification and mapping for landscape management and science: Foundations for the description of patterns and processes. Progress in Physical Geography 40:38-65.

Detty, J.M. and K.J. McGuire. 2010. Topographic controls on shallow groundwater dynamics: Implications of hydrologic connectivity between hillslopes and riparian zones in a till mantled catchment. Hydrol. Processes 24:2222-2236.

Duncan, J.M., L.E. Band, P.M. Groffman, and E.S. Bernhardt. 2015. Mechanisms driving the seasonality of catchment scale nitrate export: Evidence for riparian ecohydrologic controls. Water Resour. Res. 51:6.

Duncan, J.M., P.M. Groffman, and L.E. Band. 2013. Towards closing the watershed nitrogen budget: Spatial and temporal scaling of denitrification. J. Geophys. Res. Biogeosci. 118:1105-1119.

Ferree, C. and E. Thompson. 2008. Land type association description for Vermont. Report to Vermont Department of Forests, Parks, and Recreation, Vermont Agency of Natural Resources, Waterbury, Vermont.

Freeman, M.C., C.M. Pringle, and C.R. Jackson. 2007. Hydrologic connectivity and the contribution of stream headwaters to ecological integrity at regional scales. JAWRA 43:5-14.

Gannon, J.P., S.W. Bailey, K.J. McGuire and J.B. Shanley. 2015. Flushing of distal hillslopes as an alternative source of stream dissolved organic carbon in a headwater catchment. Water Resour. Res. 51:8114-8128.

Gburek, W.J., B.A. Needelman, and M.S. Srinivasan. 2006. Fragipan controls on runoff generation: Hydropedological implications at landscape and watershed scales. Geoderma 131:330-344.

Gillin, C., S.W. Bailey, K.J. McGuire, and J.P. Gannon. 2015. Mapping of hydropedological spatial patterns in a steep headwater catchment. Soil Sci. Soc. Am. J. 79:440-453.

Grabs, T., K. Bishop, H. Laudon, S.W. Lyon, J. Seibert. 2012. Riparian zone hydrology and soil water total organic carbon (TOC): implications for spatial variability and upscaling of lateral riparian TOC exports. Biogeosciences 9:3901-3916.

Grabs, T., J. Seibert, K. Bishop and H. Laudon. 2009. Modeling spatial patterns of saturated areas: A comparison of the topographic wetness index and a dynamic distributed model. J. Hydrol. 373:15-23.

He, L., V.Y. Ivanov, G. Bohrer, K.D. Mauer, C.S. Vogel, and M. Moghaddam. 2014. Effects of fine-scale soil moisture and canopy heterogeneity on energy and water fluxes in a northern temperate mixed forest. Agricu. For. Meteorol. 184:243-256.

Hwang, T., L.E. Band, J.M. Vose, and C. Tague. 2012. Ecosystem processes at the watershed scale: Hydrologic vegetation gradient as an indicator for lateral hydrologic connectivity of headwater catchments. Water Resour. Res. 48:W06514.

Inamdar, S.P., S.F. Christopher, and M.J. Mitchell. 2004. Export mechanisms for dissolved organic carbon and nitrate during summer storm events in a glaciated forested catchment in New York, USA. Hydrol. Processes 18:2652-2661.

James, A.L. and N.T. Roulet. 2007. Investigating hydrologic connectivity and its association with threshold change in runoff response in a temperate forested watershed. Hydrol. Processes 21:3391-3408.

Jencso, K.G., B.L. McGlynn, M.N. Gooseff, S.M. Wondzell, K.E. Bencala, and L.A. Marshall. 2009. Hydrologic connectivity between landscapes and streams: Transferring reach- and plot-scale understanding to the catchment scale. Water Resour. Res. 45:W04428.

Kashian, D.M., B.V. Barnes, and W.S. Walker. 2003. Landscape ecosystems of northern Lower Michigan and the occurrence and management of the Kirtland's warbler. Forest Science 49:140-159.

Kirkby, M.J. and D.R. Weyman. 1974. Measurements of contributing area in very small drainage basins. Seminar Series B, No. 3. Department of Geography, University of Bristol, Bristol, England.

Laamrani, A., O. Valeria, Y. Bergeron, N. Fenton, and L.Z. Cheng. 2014. Distinguishing and mapping permanent and reversible paludified landscapes in Canadian black spruce forests. Geoderma 237:88-97.

Liang, W., S. Li, and F. Hung. 2017. Analysis of the contributions of topographic, soil, and vegetation features on the spatial distributions of surface soil moisture in a steep natural forested headwater catchment. Hydrol. Processes 31:3796-3809.

Lambert, T., A.-C. Pierson-Wickmann, G. Gruau, A. Jaffrezic, P. Petitejean, J.N. Thibault, and I. Jeanneau. 2014. DOC sources and DOC transport pathways in a small headwater catchment as revealed by carbon isotope fluctuation during storm events. Biogeosciences 11:3043-3056.

Lapin, M. and B.V. Barnes. 1995. Using the landscape ecosystem approach to assess species and ecosystem diversity. Conservation Biology 9:1148-1158.

Lin, H.S. 2010. Earth's critical zone and hydropedology: Concepts, characteristics, and advances. Hydrol. Earth System Sci. 14: 25-45.

Lin, H.S., W. Kogelmann, C. Walker, and M.A. Burns. 2006. Soil moisture patterns in a forested catchment: A hydropedological perspective. Geoderma 131:345-368.

Lohse, K.A. and W.E. Dietrich. 2005. Contrasting effects of soil development on hydrological properties and flow paths. Water Resour. Res. 41:W12419.

McClain, M.E., E.W. Boyer, C.L. Dent, S.E. Gergel, N.B. Grimm, P.M. Groffman, S.C. Hart, J.W. Harvey, C.A. Johnston, E. Mayorga, W.H. McDowell, and G. Pinay. 2003. Biogeochemical hot spots and hot moments at the interface of terrestrial and aquatic ecosystems. Ecosystems 6:301-312.

McDowell, N., W.T. Pockman, C.D. Allen, D.D. Breshears, N. Cobb, T. Kolb, J. Plaut, J. Sperry, A. West, D.G. Williams, and E.A. Yepez. 2008. Mechanisms of plant survival and mortality during drought: Why do some plants survive while others succumb to drought? New Phytologist 178:719-739.

Monteith, S.S., J.M. Buttle, P.W. Hazlett, F.D. Beall, R.G. Semkin, and D.S. Jeffries. 2006. Paired-basin comparison of hydrological response in harvested and undisturbed hardwood forests during snowmelt in central Ontario: I. Streamflow, groundwater and flowpath behavior. Hydrol. Processes 20:1095-1116.

Moore, I.D., P.E. Gessler, G.A. Nielsen, and G.A. Peterson. 1993. Soil attribute prediction using terrain analysis. Soil Sci. Soc. Am. J. 57:443-452.

Moores, L.J., B. Pittman, and G. Kitchen. 1996. Forest ecological classification and mapping: Their application for ecosystem management in Newfoundland. Environmental Monitoring and Assessment 39:571-577.

Morse, J.L., S.F. Werner, C.P. Gilin, C.L. Goodale, S.W. Bailey, K.J. McGuire, and P.M. Groffman. 2014. Searching for biogeochemical hot spots in three dimensions: Soil C and N cycling in hydropedologic settings in a northern hardwood forest. Journal of Geophysical Research: Biogeosciences 119:1596-1607.

Murphy, P.N.C., J. Ogilvie, F. Meng, B. White, J.S. Bhatti, and P.A. Apr. 2011. Modelling and mapping topographic variations in forest soils at high resolution: A case study. Ecological Modelling 222:2314-2332.

Nave, L.E., P.E. Drevnick, K.A. Heckman, K.L. Hofmeister, T.J. Veverica, and C.W. Swanston. 2017a. Soil hydrology, physical and chemical properties and the distribution of carbon and mercury in a postglacial lake-plain wetland. Geoderma 304:40-52.

Nave, L.E., C.M. Gough, C.H. Perry, K.L. Hofmeister, J.M. Le Moine, G.M. Domke, C.W. Swanston, and K.J. Nadelhoffer. 2017b. Physiographic factors underlie rates of biomass production during succession in Great Lakes forest landscapes. For. Ecol. Manage. 397:157-173.

Oswald, C.J. and B.A. Branfireun. 2014. Antecedent moisture conditions control mercury and dissolved organic carbon concentration dynamics in a boreal headwater catchment. Water Resour. Res. 50: 6610-6627.

Pearsall, D.R. 1995. Landscape Ecosystems of the University of Michigan Biological Station: Ecosystem diversity and ground-cover diversity. School of natural Resources and Environment, University of Michigan, Ann Arbor. Dissertation, 396pp, plus maps.

Pearsall, D.R., B.V. Barnes, G.R. Zogg, M. Lapin, and R.R. Ring. 1995. Landscape Ecosystems of the University of Michigan Biological Station. School of Natural Resources and Environment, University of Michigan, Ann Arbor, p. 66. Technical Report.

Pei, T., C. Qin, A. Zhu, L. Yang, M. Luo, B. Li, and C. Zhou. 2010. Mapping soil organic matter using the topographic wetness index: A comparative study based on different flow-direction algorithms and kriging methods. Ecological Indicators 10:610-619.

Penna, D., M. Borga, D. Norbiato, and G.D. Fontana. 2009. Hillslope scale soil moisture variability in a steep alpine terrain. J. Hydrol. 364: 311-327.

Petroselli, A., F. Vessella, L. Cavagnuolo, G. Piovesan, and B. Schirone. 2013. Ecological behavior of Quercus suber and Quercus ilex inferred by topographic wetness index (TWI). Trees 27:1201-1215.

Porporato, A., P. D'Odorico, F. Laio, and I. Rodriguez-Iturbe. 2003. Hydrologic controls on soil carbon and nitrogen cycles. I. Modeling scheme. Adv. Water Resour. 26:45-58.

Pregitzer, K.S., and B.V. Barnes. 1984. Classification and comparison of the upland hardwood conifer ecosystems of the Cyrus H. McCormick Experimental Forest, Upper Michigan. Can. J. For. Res. 14:362-375.

Rampi, L.P., J.F. Knight, and C.F. Lenhart. 2014. Comparison of flow direction algorithms in the application of the CTI for mapping wetlands in Minnesota. Wetlands 34:513-525.

Rinderer, M., H.J. van Meerveld, and J. Seibert. 2014. Topographic controls on shallow groundwater levels in a steep, prealpine catchment: When are the TWI assumptions valid? Water Resour. Res. 50: 6067-6080.

Rodhe, A. and J. Seibert. 1999. Wetland occurrence in relation to topography: A test of topographic indices as moisture indicators. Agric. For. Meteorol. 98-99:325-340.

Rodriguez-Iturbe, I., P. D'Odorico, A. Porporato, and L. Ridolfi. 1999. On the spatial and temporal links between vegetation, climate, and soil moisture. Water Resour. Res. 35:3709-3722.

Schaetzl, R.J., F.J. Krist, K. Stanley, and C.M. Hupy. 2009. The Natural Soil Drainage Index: An ordinal estimate of long-term soil wetness. Physical Geography 30:383-409.

Schoenenberger, P.J., D.A. Wysocki, E.C. Benham, and Soil Survey Staff. 2012. Field book for describing and sampling soils, Version 3.0. Natural Resources Conservation Service, National Soil Survey Center, Lincoln, NE.

Sebestyen, S.D., Shanley, J.B., Boyer, E.W., Kendall, C., Doctor, D.H. 2014. Coupled hydrological and biogeochemical processes controlling variability of nitrogen species in streamflow during autumn in an upland forest. Water Resour. Res. 50:1569-1591.

Seneviratne, S.I., T. Corti, E.L. Davin, M. Hirschi, E.B. Jaeger, I. Lehner, B. Orlowsky, and A.J. Teuling. 2010. Investigating soil moisture-climate interactions in a changing climate: A review. Earth-Science Reviews 99:125-161.

Seibert, J. and B.L. McGlynn. 2007. A new triangular multiple flow direction algorithm for computing upslope areas from gridded digital elevation models. Water Resour. Res. 43:W04501.

Seibert, J., J. Stendahl, and R. Sorensen. 2007. Topographical influences on soil properties in boreal forests. Geoderma. 141:139-148.

Simpson, T.A., P.E. Stuart, and B.V. Barnes. 1990. Landscape ecosystems and cover types of the Reserve Area and adjoining lands of the Huron Mountain Club, Marquette Co., MI. Huron Mountain Wildlife Foundation Occasional Paper No. 4.

Soil Survey Staff, 1991. Natural Resources Conservation Service, United States Department of Agriculture. Soil Survey of Cheboygan County, Michigan.

Spies, T.A. and B.V. Barnes. 1985. A multi-factor ecological classification of the northern hardwood and conifer ecosystems of the Sylvania Research Area, Upper Peninsula, Michigan. Can. J. For. Res. 15:949-960.

Spur, S.H. and J.H. Zumberge. 1956. Late Pleistocene features of Cheboygan and Emmet counties, Michigan. Am. J. Sci. 254:96-109.

Tague, C., L. Band, S. Kenworthy, and D. Tenebaum, D. 2010. Plot- and watershed-scale soil moisture variability in a humid Piedmont watershed. Water Resour. Res. 46:W12541.

Tarboton, D.G. 1997. A new method for the determination of flow directions and upslope areas in grid digital elevation models. Water Resour. Res. 33:309-319.

Tenebaum, D.E., L.E. Band, S.T. Kenworthy, and C.L. Tague. 2006. Analysis of soil moisture patterns in forested and suburban catchments in Baltimore, Maryland, using high-resolution photogrammetric and LIDAR digital elevation datasets. Hydrol. Processes 20:219-240.

Tetzlaff, D., C. Birkel, J. Dick, J. Geris, and C. Soulsby. 2014. Storage dynamics in hydropedological units control hillslope connectivity, runoff generation, and the evolution of catchment transit time distributions. Water Resour. Res. 50:969-985.

Thompson, J.C. and R.D. Moore. 1996. Relations between topography and water table depth in a shallow forest soil. Hydrol. Processes 10:1513-1525.

Vidon, P., C. Allan, D. Burns, T.P. Duval, N. Gurwick, S. Inamdar, R. Lowrance, J. Okay, D. Scott, and S. Sebestyen. 2010. Hot spots and hot moments in riparian zones: Potential for improved water quality management. J. Am. Water Resour. Assoc. 46:278-298.

R Core Team. 2016. R: A language and environment for statistical computing. Vienna, Austria: R Foundation for Statistical Computing. Retrieved from http://www.R-project.org

Zenner, E.K., J.E. Peck, K. Brubaker, B. Gamble, C. Gilbert, D. Heggenstaller, J. Hickey, K. Stitch, and R. Withington. 2010. Combining ecological classification systems and conservation filters could facilitate the integration of wildlife and forest management. J. For. 108:296-300

Zhu, Q., K. Liao, Y. Xu, G. Yang, S. Wu, and S. Zhou. 2012. Monitoring and prediction of soil moisture spatial-temporal variations from a hydropedological perspective: A review. Soil Research 50:625-637.

Zinko, U., M. Dynesius, C. Nilsson, and J. Seibert. 2006. The role of soil pH in linking groundwater flow and plant species density in boreal forest landscapes. Ecograph 29:515-524.

Zogg, G.P. and B.V. Barnes. 1995. Ecological classification and analysis of wetland ecosystems, northern Lower Michigan, USA. Can. J. For. Res. 25:1865-1875.

## CHAPTER 3

LANDSCAPE HYDROLOGIC UNITS, WATER CONNECTIVITY, AND CHEMISTRY IN A GREAT LAKES GLACIAL DRIFT WATERSHED

***Abstract***

Water movement through the landscape to streams provides a fundamental linkage between terrestrial and aquatic environments in headwater systems. Water and material inputs from terrestrial ecosystems are important for downstream rivers and lakes as well as local and regional biogeochemical cycles. Identifying hydrologic connections between upland forests, riparian areas and wetlands, and surface waters can reveal how and when water movement connects the landscape units that make up a watershed. Here, we sought to characterize the spatial distribution, connectivity, and chemistry of ground and surface water within a forested watershed, and to identify landscape units that play potentially significant roles in the terrestrial-aquatic interface. We conducted this work for a headwater stream and large inland lake in a forested glacial drift landscape in northern Michigan, U.S.A., using precipitation, shallow groundwater, and stream water chemistry to identify the origins of water in the ground and stream, and reveal which portions of the landscape were traversed by those waters. During the spring, surface water was mixture of snowmelt-fed shallow groundwater and recent precipitation. However, in summer and autumn, isotopic and chemical similarity between shallow groundwater, surface water, and precipitation increased, indicating that recent precipitation became the increasingly dominant source of both shallow groundwater and stream water in these seasons. Emergent, fundamentally distinct landscape hydrologic units were useful representations of vertical and spatial hydrologic connectivity within this headwater system and identified unique source contributions of carbon to the stream. The riparian areas and the outwash-lake plain wetland likely have a much stronger

influence on stream chemistry and discharge than the upland disconnected or periodically connected landscape units, due to the perennial connections between shallow groundwater from the consistently connected areas and surface water.

### *Introduction*

In fluvial networks across the Great Lakes region, as well as across the globe, headwater streams are the smallest and most abundant streams (Bishop et al., 2008; Downing et al., 2012; Fergus et al., 2017). Water movement from hillslopes through riparian zones to streams provides a fundamental linkage between terrestrial and aquatic environments in headwater systems (Freeman et al., 2007; Covino, 2017). Streams receive particulate and dissolved organic matter and nutrients from the landscape and connect important terrestrial and aquatic biogeochemical cycles (*e.g.*, carbon [C] cycling; Fasching et al., 2016), storing, transforming or exporting matter to rivers and lakes (Leibowitz et al., 2018), and influencing the nutrient dynamics of downstream ecosystems (Gomi et al., 2002; Alexander et al., 2007; MacDonald and Coe, 2007). Although riparian areas may be a small fraction of the total watershed area, they can have a significant impact on the water quality of streams and the transport of material. This is due to generally saturated conditions and organic matter rich soils compared to upland areas as well as their physical position at the interfaces of terrestrial and aquatic ecosystems (Ballinger and Lake, 2006; Seibert et al., 2009; Lidman et al., 2017). These material transfers can be reciprocal; terrestrial organic matter can be important for maintaining stream and lake ecosystem structure and function and emerging insects can be important sources of energy and nutrients for terrestrial food webs (Baxter et al., 2005; Soininen et al., 2015; Fasching et al., 2016). The biogeochemical link between the terrestrial and aquatic ecosystems is to a large extent driven by hydrology, as subsurface flow transports material through the landscape and impacts soil moisture, which in turn affects soil microbial redox reactions (McClain et al., 2003; Covino, 2017; Fritz et al., 2018). These terrestrial-aquatic linkages are important for local and regional biogeochemical cycles, but to understand their dynamic interactions, we must first investigate the spatial and temporal hydrologic connections between the terrestrial environment and streams that define which areas are connected to surface waters and under what conditions.

Water movement through the landscape and the hydrologic connectivity between hillslopes, riparian zones, and the stream channel can be spatially and temporally variable (Covino, 2017; Fritz et al., 2018). The variability in the spatial distribution of water storage across watersheds can result in differing runoff responses, presenting challenges in predicting when and where runoff will occur (Bracken et al., 2013). The connectivity between streams and runoff source areas can vary laterally, vertically, and longitudinally in space, as well as through time (Freeman et al., 2007; Covino, 2017). Hydrologic connectivity can be dependent upon precipitation inputs or antecedent storage conditions, climatic conditions, topography, geology, soil characteristics, vegetation, and land use (Soulsby et al., 2006; Ali et al., 2011; Jencso and McGlynn, 2011; Emanuel et al., 2014). Connectivity across a watershed has often been inferred from soil moisture or shallow groundwater measurements (*e.g.,* Western et al., 2001; Jencso et al., 2009; Penna et al., 2015), although spatial patterns of soil water do not always reflect the hydrologic responses being observed in the stream (*e.g.*, Tromp-Van Meerveld and McDonnell, 2006; James and Roulet, 2009). In landscapes dominated by glacial drift materials, the heterogeneous distribution of parent material and topography can create complex hydrologic connections. In low-lying topographic positions with poorly draining riparian and wetland areas, saturated areas can expand and contract, affecting connectivity (*e.g.*, Soulsby et al., 2006; Tetzlaff et al., 2014). Hillslopes with impervious till layers can act like bedrock controlling threshold mediated subsurface flow (*e.g.*, Gburek et al., 2006; Ali et al., 2011); and thick unsaturated soils can promote vertical infiltration of water and recharge of deep groundwater (*e.g.,* Hinton et al., 1993; Naylor et al., 2016).

Groundwater is a primary water source for many headwater streams (Gomi et al., 2002; Covino, 2017; Buttle, 2018), and variability in connections between land units with differing hydrologic responses can influence the magnitude and timing of streamflow (Jencso et al., 2009; Ali et al., 2011; Bachmair and Weiler, 2014). While direct hydrologic measurements (*i.e.*, soil moisture, water table) can provide insights into which portions of a watershed are contributing water to a stream, the chemical signatures of water can be used to investigate water storage and mixing, flow paths, and distinct water sources to a stream (McGuire et al., 2005; James and Roulet, 2006; Inamdar et al., 2013; Tetzlaff et al., 2014). The natural chemical tracers in water, especially water isotopes ($\delta^{18}O$, $\delta D$) can be used to distinguish between the baseflow maintaining consistent streamflow and runoff from storm events (Klaus and McDonnell, 2013). Chemical tracers have been used to help constrain sources of runoff and groundwater and their temporal dynamics and can be useful for clarifying observed hydrological responses (Kirchner et al., 2010; Shanley et al., 2015). Chemical properties of the groundwater can act as fingerprints of land units or physical properties (*e.g.*, parent material, recent organic matter), as different materials impart identifiable chemical characteristics to the water (Ali et al., 2010; Lessels et al., 2016; Covino, 2017). Mixing models use chemical and isotopic tracers to identify discrete hydrologic source areas and flow paths contributing water to streams (Hooper, 2003; Liu et al., 2008; Singh et al., 2015). These methods have been useful for identifying important landscape source areas controlling stream chemistry, such as dissolved organic carbon (DOC) concentrations and quality ($\delta^{13}C$; Inamdar and

Mitchell, 2006; Sebestyen et al., 2008; Lambert et al., 2014) and water sources maintaining streamflow (Klaus et al., 2015; Peng et al., 2015; Ala-aho et al., 2018).

In the upper Great Lakes region of North America, heterogeneous surface geology, abundant precipitation, and widely varying vegetation types and land uses create complex conditions for the movement of water through landscapes. Some of these landscapes have been very well studied in terms of terrestrial ecosystem structure (*e.g.*, Hardiman et al., 2013), and functions such as C cycling (Gough et al., 2007) and vegetation water use (He et al., 2014), but investigations of hydrologic linkages and connectivity lag behind in many areas. Landscapes comprised of deep, conductive glacial till and aggrading forests pose a specific problem, in that observed terrestrial C sinks may in fact be exporting a substantial, but as yet accounted portion of their sequestered C to aquatic ecosystems. Given the potential importance of hydrologic and material fluxes from terrestrial to aquatic ecosystems in groundwater-driven headwater systems such as these, we investigated a well-studied landscape in northern Michigan, U.S.A., seeking to identify land units with potentially important terrestrial aquatic linkages for a headwater stream and large inland lake. In the present study, we aim to address these goals through the following research objectives: 1) identify the origin of the water flowing in shallow groundwater and the stream, 2) characterize the occurrence and chemistry of groundwater across the watershed, 3) identify landscape hydrologic units contributing to surface water at three locations along the stream, and 4) use temporal variation in stream flow and shallow groundwater to infer how spatial connectivity changes seasonally.

### ***Methods***

*Study Area*

This research was conducted in a forested headwater watershed, the Honeysuckle Creek watershed, at the University of Michigan Biological Station (UMBS), which is located in northern Lower Michigan, USA (45.56°, -84.72°). The regional climate is continental with a mean annual temperature of 5.5°C and mean annual precipitation of 817 mm, including 294 cm of snow (Nave et al., 2017a). This analysis is part of a larger project to characterize water, soil, major elements, and their interactions throughout the 120 ha Honeysuckle Creek watershed and export to Burt Lake, the 4$^{th}$ largest of Michigan's ~11,000 inland lakes. Measurements of streamflow and chemistry as well as soil moisture and water table levels have been reported in other publications (Hofmeister et al., In Revision; Hofmeister et al., In Prep, Nave et al., 2017a). The watershed drains to a small first order stream, approximately 1.7 km in length at its maximum extent during the spring snowmelt period (Hofmeister et al., In Prep). The topography of the UMBS landscape is determined by the landforms formed in glacial drift deposited at the end of the Laurentian glaciation (14,000-10,000 years before present, ybp) and subsequently modified by large, postglacial lakes (Lake Algonquin, 11,500-10,500 ybp; Lake Nippissing, 5,000-3,000 ybp; Spurr and Zumberge, 1956; Blewitt and Winters, 1995; Lapin and Barnes, 1995). Moraine, outwash plain, and lacustrine (dunes, beach ridges) landforms are all present in the Honeysuckle Creek watershed. The upper elevations of the Honeysuckle Creek watershed (277-245 m above sea level, asl) are dominated by deep, coarse-textured outwash soils (Entic and Lamellic Haplorthods). Along the stream channels in the middle elevations of the watershed (245-190 m), finer-textured soils with restrictive glacial till close to the surface can be found (Alfic Haplorthods, Alfic Epiaqods, Mollic Endoaqents). The outwash-lake plain wetland along the shore of Burt Lake is characterized by Terric Haplosaprists.

*Field Measurements*

We installed 44 shallow groundwater monitoring wells below 240 m elevation in the watershed to the mouth (Figure 3.1). Shallow groundwater is defined as groundwater measured within 3 m of the ground surface. Shallow wells (n=22) were installed down to the first major parent material unconformity, which was a glacial till restrictive layer (55-220 cm below the surface) in upland ecosystems. In the outwash-lake plain wetland, wells (n=20; approximately 160 cm deep) were installed through the organic soil horizons and into the sand C horizon. Slotted PVC wells (3.2-5.1 cm diameter) were deployed in 10 cm diameter boreholes and the void space was filled with a sand pack. Two stainless steel drive point wells were also installed at the headwaters of the stream (210 cm deep) and at the mid flume (360 cm deep) into the glacial restrictive material. Water table position was measured with a flat tape water level (Model 101B, Solinst, Inc., Georgetown, ON, CA) approximately weekly from June 2016–November 2017. Pressure transducers (Levelogger, Levelogger Jr., Solinst, Inc., Georgetown, ON, CA) were deployed to take hourly water table position measurements in a subset of wells (n=12). Hourly measurements were adjusted for atmospheric pressure and aggregated into mean daily water table position measurements. As part of a different project in the Honeysuckle Creek watershed, soil volumetric water content (VWC %) in the upper 20 cm of soil was measured at points across the watershed, including at 23 of the shallow groundwater wells. At each point, three Time Domain Reflectometry (TDR; Hydrosense, Campbell Scientific, Inc.) readings of soil VWC were taken. At the well locations, soil VWC was measured at minimum biweekly from June–November 2016 and April–June 2017.

We installed modified Parshall flumes at three locations along Honeysuckle Creek (Figure

3.1) and measured stream stage and calculated stream discharge based on USGS methods (Kilpatrick and Schneider, 1983). Stream stage at the mouth and mid flumes was measured approximately weekly by hand from October 2015–May 2016. Beginning May 2016 for the mouth and February 2017 for the mid flume through November 2017, the height of water in the stream was measured hourly with pressure transducers (Levelogger, Solinst, Inc., Georgetown, ON, CA). Stream stage measurements at the upper flume were taken approximately weekly by hand from October 2015–November 2017.

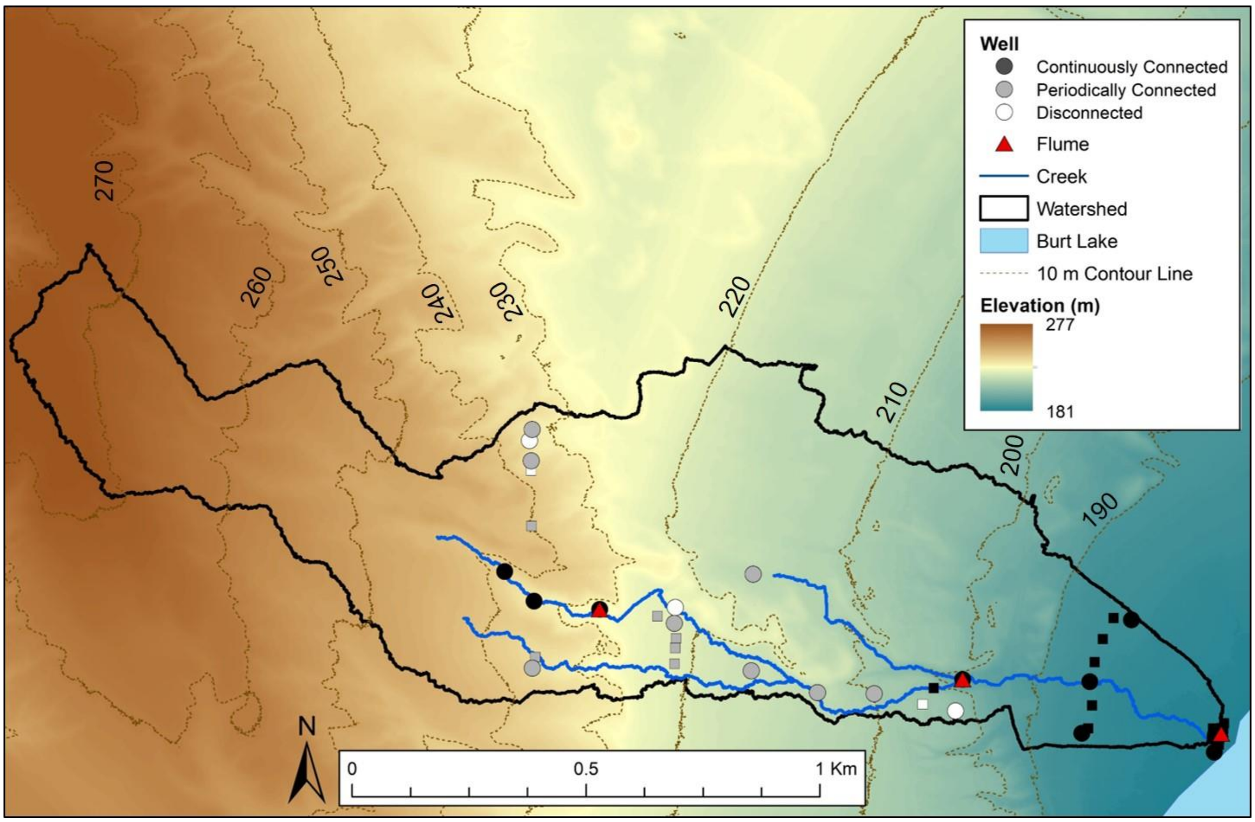


Figure 3.1: Shallow groundwater wells (circle or square points) and stream flumes (triangle points) across the Honeysuckle Creek watershed. Wells sampled for chemistry are represented as circles; their colors represent correspondence to discrete landscape hydrologic groups (continuously connected, periodically connected, disconnected). Wells measured only for water table position are shown as squares but follow the same color scheme for the hydrologic groups, given in the legend. Where disconnected wells (white) are very close to periodically or continuously connected wells (gray and black, respectively), the disconnected wells were located 20-40 m upslope.

Meteorological measurements were taken daily at UMBS laboratory facilities approximately 3 km away from the watershed. Weekly chemical composition of precipitation at the UMBS facility (site MI09) was reported as part of the National Atmospheric Deposition Program (NRSP-3, 2018). As part of another project at UMBS, precipitation samples were collected frequently to capture event-scale water isotope dynamics, and these have been used to constrain meteoric contributions to ground and stream water in the Honeysuckle Creek watershed. These precipitation samples were collected at the AmeriFlux and FASET flux towers (~3 km from watershed; Nave et al., 2014), which are at a similar elevation (236-239 m) to the middle of the watershed. The AmeriFlux site is a long-term study site with an eddy covariance and meteorological tower. Samples were collected in plastic buckets with a layer of mineral oil to prevent evaporation following the methods of Friedman et al. (1992) and Scholl et al. (1996). Samples were transferred to HDPE vials and the bucket was emptied, cleaned, dried, and the mineral oil was replaced for the next sample. The UMBS Local Meteoric Water Line (LMWL; $\delta D=7.89*\delta^{18}O+14.4$) parallels the Global Meteoric Water Line (GMWL; $\delta D=8*\delta^{18}O+10$; Craig, 1961), but has a slightly higher intercept due to the incorporation of evaporated water from Lake Michigan in precipitation falling at UMBS. (Gat et al., 1994; Bowen et al., 2012)

For this analysis, shallow groundwater and surface water samples were collected in late April, early June, and early November of 2017. These sampling times were chosen to represent the spring snowmelt period, beginning of summery dry down, and storm driven autumn wet-up. We selected a subset (n=18) of all the shallow wells across the watershed to sample for water chemistry. The selected wells were chosen to represent a range of landscape positions, soils, depth to glacial restrictive material, and position along the stream. At each sampling time (April, June, November) we collected water samples at 15-17 wells depending on if water was present and the three flumes in HDPE bottles, which were kept on ice in the field and transferred to a refrigerator (4°C) within 8 hours of sample collection.

*Laboratory Analysis*

In the UMBS Analytical Chemistry Laboratory, shallow groundwater and stream water samples were filtered through pre-ashed 0.7 µm glass-fiber filters within 24 hours of field collection and were kept refrigerated at 4°C until analysis. The specific conductivity (Hanna Instruments, HI8733 Conductivity meter, Hanna Instruments, Inc., Woonsocket, RI) and pH (Mettler Toledo SevenCompact pH meter, Mettler-Toledo, LLC, Columbus, OH) of unfiltered water samples was measured prior to filtration. Filtered water samples were analyzed for anions ($Cl^-$, $F^-$, $Br^-$, $NO_3^-$, $PO_4^{3-}$, $SO_4^{2-}$) and cations ($Na^+$, $K^+$, $Ca^{2+}$, $Mg^{2+}$) with an ion chromatogram (Thermo Scientific Dionex Integrion HPLC system, Thermo Fisher Scientific, Inc., Waltham, MA). Dissolved inorganic and organic C (DIC, DOC) concentration and stable isotope signatures were measured with a total organic carbon analyzer (Aurora 1030W TOC Analyzer, OI Analytical, Xylem Inc., College Station, TX) coupled to an isotope ratio mass spectrometer (Thermo Scientific Delta V Advantage IRMS, Thermo Fisher Scientific, Inc., Waltham, MA). Local precipitation, shallow groundwater, and surface water isotope analyses were performed on a Picarro L2130-i Cavity Ringdown Spectrometer with an A0212 high-precision vaporizer and attached autosampler (Picarro Inc., Santa Clara, CA). The Picarro ChemCorrect software was used to monitor for organic contamination. While we analyzed water samples for this wide range of analytes (conductivity, pH, anions, cations, C, water isotopes), in this manuscript we focused only on the conductivity, pH, $Ca^{2+}$, $Mg^{2+}$, C, and water isotope analytes for reasons addressed in the results.

*Physical Factors and Hydrologic Groups*

At each well location we summarized a range of physical properties based on field measurements and topographic and physiographic metrics. These physical factors were selected to identify topographic, hydrologic, landform, and soil characteristics and used to determine if physical landscape features could be used to predict groundwater chemistry. Categorical physical factors included major landform, landscape ecosystem type, hydrologic group, soil texture, and well depth. Major landform and landscape ecosystem type assignments come from a hierarchical, multifactor ecosystem classification created for UMBS. This ecosystem classification defines and maps 125 distinct ecosystem types across the UMBS property based on landform, microclimate, soil, and vegetation (Pearsall et al., 1995), and has been found to describe meaningful spatial units in terms of wetland characteristics, forest growth rates, and soil textures (Zogg and Barnes, 1995; Nave et al., 2017b). Major landforms designated within the Honeysuckle Creek watershed include outwash plain and moraine landforms. Individual ecosystem types are given numerical names in the original classification, and for this analysis we have given them shorthand names that refer to the dominant parent material or landform of each ecosystem type. Within the Honeysuckle Creek watershed, we placed shallow groundwater wells in dune (type 74), outwash over till upland (types 113, 116), outwash over till riparian (type 118), and outwash-lake plain wetland (type 55) ecosystems.

Paired measurements of soil VWC and water table position were taken from June 2016–2017 at a subset of wells (n=23) and used to classify the degree of vertical connectivity between surface soil moisture and shallow groundwater at each point. Hydrologic groups were developed to describe three different vertical connectivity patterns. These connectivity patterns include a disconnected pattern, a periodically connected pattern, and a consistently connected pattern (Figure 3.2). These patterns can be observed utilizing data from all 23 wells as well as with data solely from the wells sampled for chemistry. Focusing on the wells sampled for chemistry, the disconnected hydrologic group displayed relatively little change in soil VWC for changes in water table position; VWC was low (mean=19 ± 2%), water table levels were below 100 cm, and many of the wells dried up in summer and autumn. The periodically connected group displayed a strong positive linear relationship between VWC and water table position, with mean a VWC of 31 (± 10%), water table levels within 50 cm of the ground surface (-43 ± 34 cm), and some wells going dry for a period of time. In the consistently connected group, soils were reliably saturated (mean VWC=53 ± 6%), water tables were around 10 cm below the surface (± 4 cm), and wells very rarely went dry (Figure 3.2, 3.3).

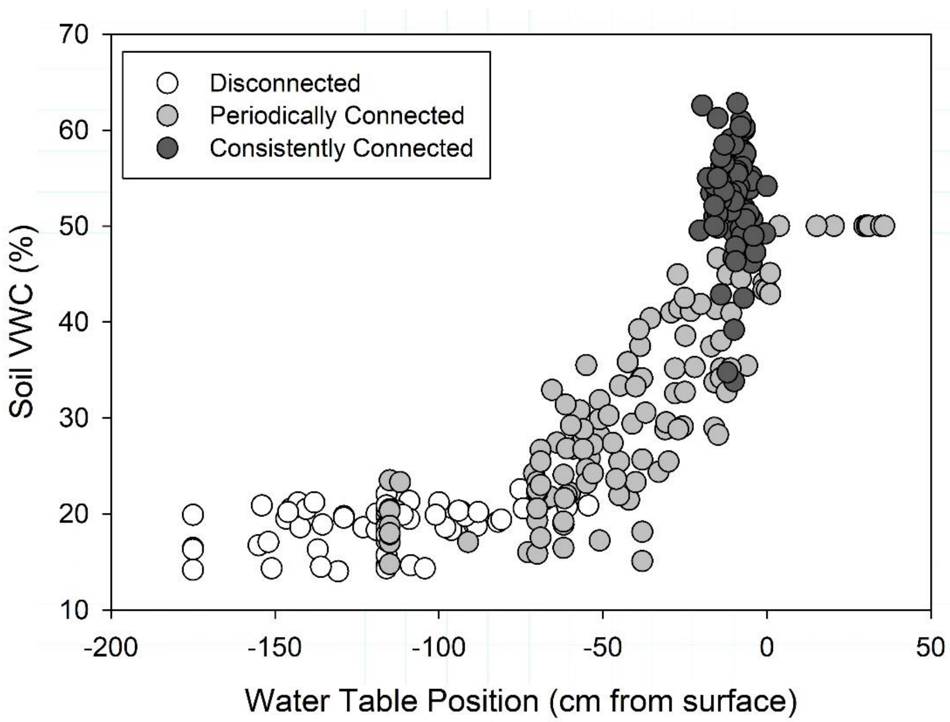


Figure 3.2: Paired soil VWC and water table position measurements for 18 of the shallow groundwater wells sampled for chemistry. Three hydrologic groups (disconnected, periodically connected, consistently connected) were developed to describe three fundamental relationships between soil water in the top 20 cm of the profile and shallow groundwater. The same patterns were observed when all 23 locations across the watershed with paired VWC and water table measurements were included.

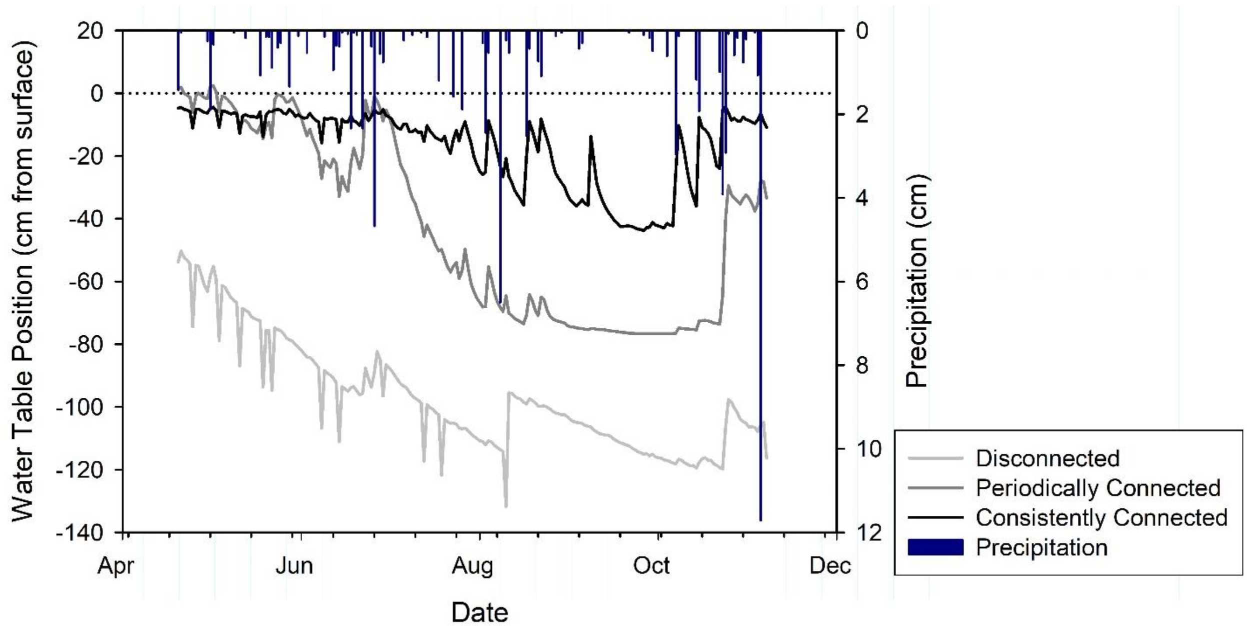


Figure 3.3: Precipitation and water table position for each hydrologic group during April–November 2017. Water table levels in the consistently connected group remained within 45 cm of the ground surface throughout the sampling period, while in the disconnected group water levels were highest in the spring and dropped throughout the summer and autumn with the majority of the wells drying up. The periodic group displayed similarities to both of the other groups, with water tables within 20 cm of the ground surface in the spring and water levels furthest from the surface in the summer and early autumn, with some wells even drying up during that time.

Soil texture class above the glacial till restrictive layer at each well point was determined in the field as part of the soil observation, description, and sampling campaigns that took place in 2014-2016 to sample soils across the watershed. For this analysis, soil texture classes included sand, loamy sand, sandy loam, and sapric muck groups. Wells were also grouped by depth into 0-100 cm, 100-200 cm, and deeper than 200 cm groups. All wells in the 0-100 cm and 200+ cm groups are located in the upland ecosystems. The 100-200 cm wells were divided into upland and outwash-lake plain wetland groups given the distinct differences in the moisture regimes of mineral and organic soils observed by Hofmeister et al. (In Revision).

Topographic factors including elevation, slope, and topographic wetness indices were extracted or derived from a high resolution (0.3 m x 0.3 m) DEM. Elevation was extracted at each well point and slope was calculated within a 5 m buffer around each point. Two topographic wetness indices, a topographic index (TI) based solely on topographic inputs, and a soil topographic index (STI) based on topography and soil characteristic inputs, were used for this analysis. These wetness indices can be used to identify areas likely to be saturated (high index value) or dry (low index value) based on the upslope contributing area and slope at each point, as well as the soil depth and saturated hydraulic conductivity if soil properties are included. Hofmeister et al. (In Revision) describe how these indices were generated for the Honeysuckle Creek watershed. At each point, basal area of live overstory vegetation was calculated from point-quarter vegetation surveys of trees with a DBH (diameter at breast height) greater than 8 cm. The final physical factor utilized to identify chemical patterns was the water table position at the time of sampling (*i.e.*, April, June, or November).

*Data Analysis*

For this analysis, we report water table and stream stage measurements taken between April and November 2017. All statistical analyses were conducted with R (R Core Team, 2017) and SigmaPlot (SYSTAT Software, San Jose, CA, USA) and are considered significant when $p<0.05$. A simple water balance was estimated for the Honeysuckle Creek watershed as well as the mid and upper flume subwatersheds based on two full hydrologic years of data (October 2015–2017). A water balance can provide information about how much of the precipitation is going to stream discharge, evapotranspiration, and groundwater storage. We used a simple water balance where precipitation (input) is equal to the sum of evapotranspiration, discharge, and net storage (outputs). Precipitation and stream discharge were measured during the study period and evapotranspiration was estimated by Fatichi and Ivanov (2014). We also estimated the daily contribution of baseflow to the stream at the mouth and mid flumes as well as the mean baseflow contribution (baseflow index; BFI) to the stream during the April–November 2017 sampling period. We utilized the digital filter hydrograph separation proposed by Nathan and McMahon (1990) with three filter passes and a filter parameter of 0.925 (Fuka et al., 2014). We compared seasonal median BFI values for both flumes with Kruskal-Wallis One-Way ANOVA on Ranks test due to the non-normal nature of the BFI data.

We utilized water isotopes from the precipitation samples taken at the UMBS AmeriFlux tower to identify the origin of the water found the shallow groundwater wells and in the stream. The relationship between $\delta D$ and $\delta^{18}O$ from precipitation, shallow groundwater, and surface water samples was tested with linear regressions. Precipitation, shallow groundwater, and surface water linear regressions were performed on data from all seasons together (April, June, November data combined), as well as each season separately for precipitation and shallow groundwater samples only. Given the limited number of surface water samples from the individual sampling times (n=3), linear regressions were not conducted for individual seasons. Dummy variable coding was used to test for significant differences between the precipitation, shallow groundwater, and surface water linear models. Deuterium excess (D-excess), calculated as D-excess=$\delta D$-8*$\delta^{18}O$, is associated with kinetic isotopic fractionation and can be used to distinguish between evaporation or condensation processes (Dansgaard, 1964). D-excess values equal to 10 indicate samples along the GMWL, while D-excess values below 10 indicate evaporation (Matheny et al., 2017; Ala-aho et al., 2018). One-Way ANOVAs were used to compare precipitation, shallow groundwater, and surface water D-excess values for each sampling time. Along with the water isotope regressions, we used D-excess values to compare precipitation, shallow groundwater, and surface water sources and distinguish between evaporated and non-evaporated waters.

We utilized One-Way ANOVAs to determine if the categorical physical factors (major landform, landscape ecosystem type, hydrologic group, soil texture class, well depth) could predict variation in the shallow groundwater chemical concentrations. For the continuous physical factors (elevation, slope, basal area, TI, STI, water depth at sampling), we used Pearson Product Moment Correlations to test for significant relationships between these physical factors and shallow groundwater chemical concentrations. For these analyses, data from all three sampling times were combined to improve the statistical power of these tests. In addition, non-normal data were transformed closer to normality. We generated scatter plots of physical factor group means with standard error bars for the categorical factors that were significant predictors of shallow groundwater chemistry. For the continuous factors, scatterplots and linear regressions were generated between the physical factor and selected analytes. With measurements from all wells across the watershed we used Kruskal-Wallis tests to compare seasonal water table positions (April, June, November) within each hydrologic group. We also used Kruskal-Wallis tests compared the duration of dry periods for each hydrologic group (*i.e.*, when no shallow groundwater was present in wells) during April–November 2017.

To identify the contributions of shallow groundwater sources to the stream, we used a mixing analysis that takes the form:

$$Q_{surface}C_{surface} = Q_{G1}C_{G1} + Q_{G2}C_{G2} + Q_{G3}C_{G3} \quad (1)$$

where $Q$ is discharge of the stream (*surface*) or groundwater sources (*G1*, *G2*, *G3*) and $C$ is the concentration of a select analyte in the stream or groundwater sample. For this type of mixing analysis, two chemical analytes are required, and the groundwater sources must be distinct. We used the hydrologic groups discussed above to represent three separate sources of shallow groundwater as they were the most consistently significant physical sources of variation in water chemistry and water table position. We have measured stream discharge ($Q_{surface}$), stream water ($C_{surface}$) and shallow groundwater ($C_{G1}$, $C_{G2}$, $C_{G3}$) chemical concentrations but must calculate the shallow groundwater contributions ($Q_{G1}$, $Q_{G2}$, $Q_{G3}$). When the surface water sample falls within the mixing space, the percentage contributed from each shallow groundwater source can be calculated. Shallow groundwater source contributions to surface water were calculated when shallow groundwater was the sole source and there were no additional external water sources. We conducted this mixing analysis for all the samples together, as well as separately by season to identify whether source contributions are temporally dynamic. Given the importance of C to both aquatic and terrestrial ecosystems, DOC and DIC were chosen for this analysis to provide insights into the origins of dissolved C in the stream. Carbon and water isotopes were selected to provide insights into the potential origins of the water transporting the C.

## ***Results***

### *Hydrologic Metrics*

The water balances for each subwatershed reveal that the amount of water available for storage as soil water, shallow groundwater, or deep groundwater decreased as the watershed area increased. Mean annual precipitation measured at UMBS from October 2015–2017 was 1,016 mm year$^{-1}$ and evapotranspiration was estimated to be 600 mm year$^{-1}$ by Fatichi and Ivanov (2014) using data from the nearby AmeriFlux tower. Mean annual stream discharge was 40 L min$^{-1}$ at upper flume (252 mm year$^{-1}$ of runoff reaching upper flume), 237 L min$^{-1}$ at mid flume (342 mm year$^{-1}$ of runoff), and 1,156 L min$^{-1}$ (506 mm year$^{-1}$ of runoff) at the mouth. At the upper and mid flumes, precipitation inputs were sufficient to account for water losses from the watershed due to evapotranspiration and stream discharge, leaving a net surplus of water that could be stored in some form in the ground at the upper (164 mm year$^{-1}$) and mid (75 mm year$^{-1}$) flumes. At the upper flume this surplus water was approximately 65% of annual discharge, and at the mid flume the surplus was 22% of annual discharge. However, precipitation alone was not sufficient to account for both evapotranspiration and discharge at the mouth of the stream, falling 18% short of the estimated annual stream discharge. Streamflow at both the mid and mouth flumes along Honeysuckle Creek was primarily baseflow. During the April–November 2017 sample period the mean baseflow index (BFI) value at the mouth was 0.79, while the mean BFI value was higher at the mid flume (BFI=0.89). BFI values at the upper flume could not be calculated due to the periodic sampling design. While daily BFI values fluctuated based on precipitation events, seasonal baseflow contributions to the stream were smallest in the spring, increasing in the summer, and largest in the autumn at both the mid and mouth flumes. (Figure 3.4, 3.5)

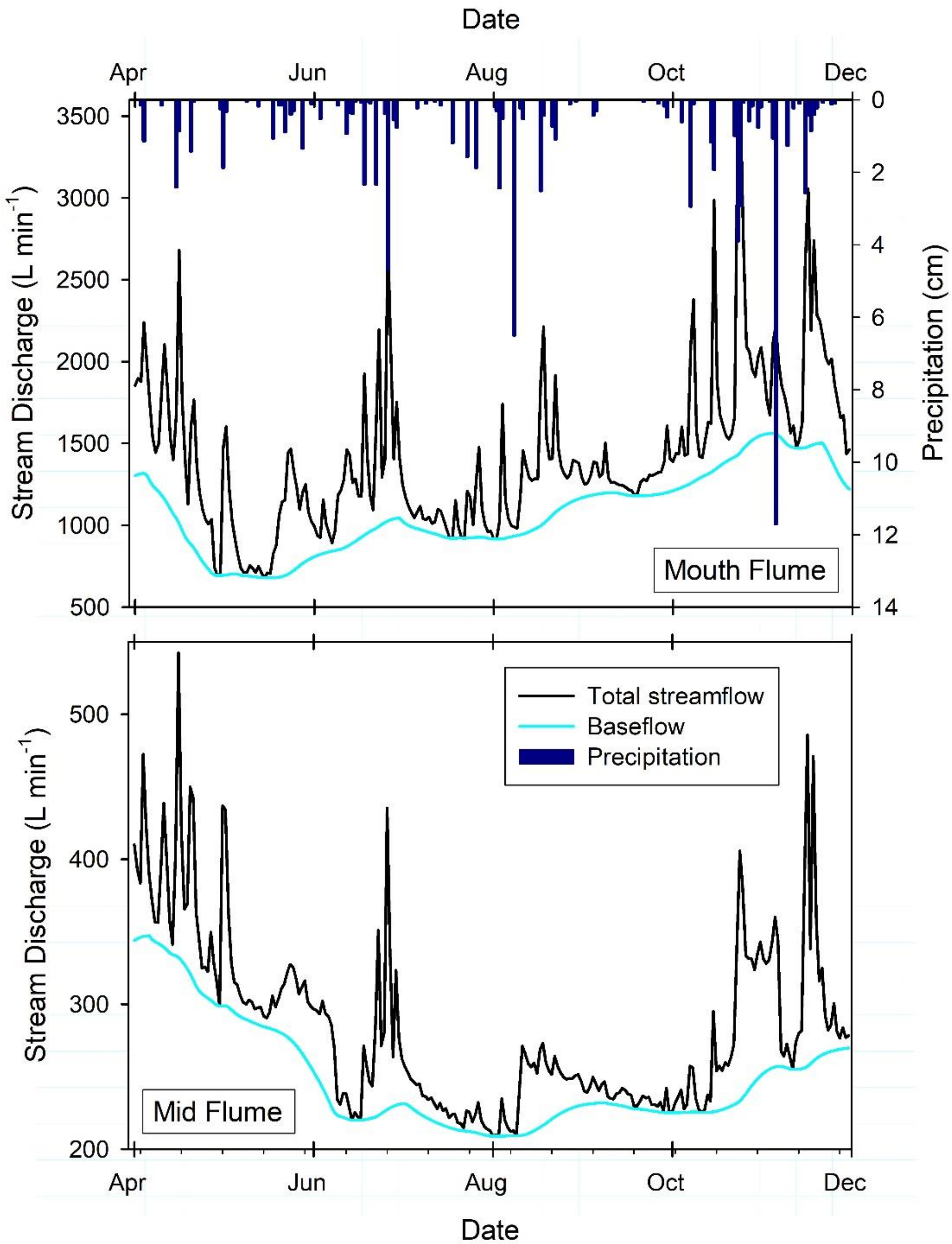


Figure 3.4: Total streamflow at the mouth (top panel) and mid flumes (bottom panel) along Honeysuckle Creek (black line), the estimated baseflow contribution (light blue line) to the stream, and precipitation for the April–November 2017 sampling period. During the sampling period shown, the mean BFI was 0.79 at the mouth and 0.89 at the mid flume.

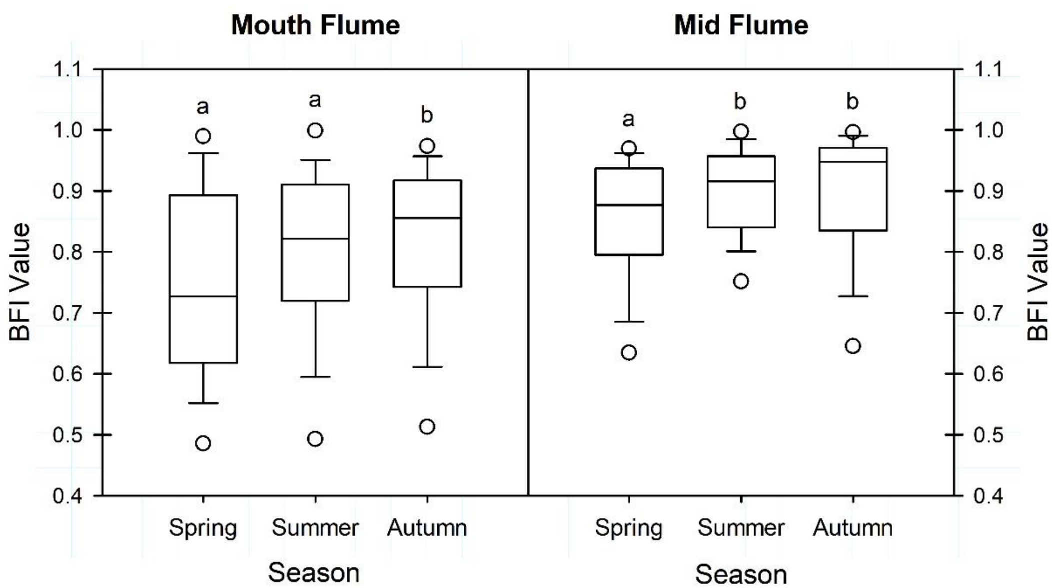


Figure 3.5: Seasonal BFI values for the mouth and mid flumes during 2017. At both flumes, seasonal median baseflow contributions were significantly lower in the spring and higher in the autumn seasons. Significant differences between seasons are denoted by different letters for each flume individually.

*Origin of Shallow Groundwater, Surface Water*

Throughout the April to November 2017 sampling period, shallow groundwater and surface water isotopic signatures were very similar. A comparison of water isotope linear regressions (δD versus $\delta^{18}O$) demonstrated that over all the seasons, surface water isotopes ($r^2$=0.69) did not differ from precipitation isotopes ($r^2$=0.96; $p$=0.299) or from shallow groundwater isotopes ($r^2$=0.59; $p$=0.337), although groundwater and precipitation isotopes did differ significantly ($p$=0.001; Figure 3.6). This difference between precipitation and groundwater appears to be driven primarily by the April sampling time, where shallow groundwater and precipitation regressions differed significantly ($p$<0.001; Figure 3.7). In June, there was a marginally significant difference between shallow groundwater and precipitation regressions ($p$=0.05) and in November there was no difference between shallow groundwater and precipitation regressions ($p$=0.237). April shallow groundwater samples had more depleted δD values (-77.45 to -62.82‰) compared to precipitation (-76.88 to -10.46‰) and the groundwater samples D-excess were below 10 and significantly lower than the precipitation D-excess values (Figure 3.7). Surface water D-excess values were above 10 and were not significantly different from either precipitation or shallow groundwater. D-excess values did not significantly differ between water sources in either summer or autumn. The similarity between shallow groundwater, surface water, and precipitation increased in June and was very strong in November (Figure 3.7).

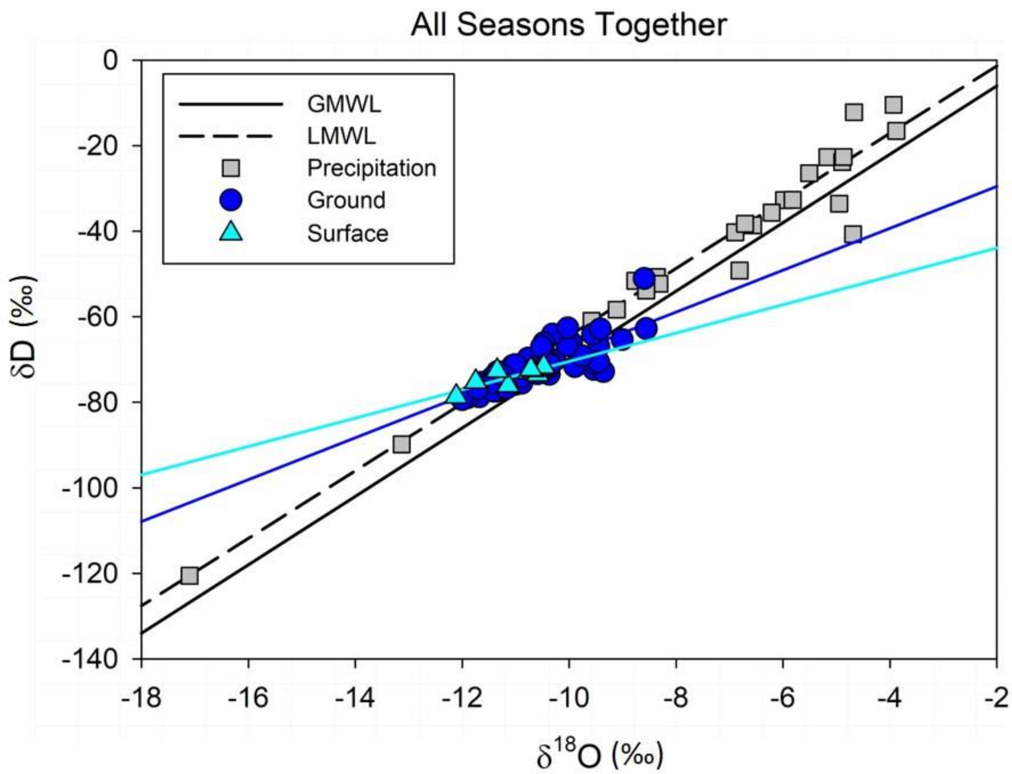


Figure 3.6: Precipitation, shallow groundwater, and surface water isotopes ($\delta^{18}O$, $\delta D$) for the spring, summer, and autumn seasons combined. Linear regressions for precipitation (n=27, $r^2$=0.96), surface water (n=9, $r^2$=0.69), and shallow groundwater (n=50, $r^2$=0.64) are shown. Comparisons of these regressions indicate that there is no significant difference between precipitation and surface water models ($p$=0.299) or surface water and shallow groundwater models ($p$=0.337), although the precipitation and shallow groundwater models do differ significantly ($p$=0.001). The Global Meteoric Water Line (GMWL; $\delta D=10+8*\delta^{18}O$) and Local Meteoric Water Line (LMWL; $\delta D=14.4+7.89*\delta^{18}O$) are also plotted.

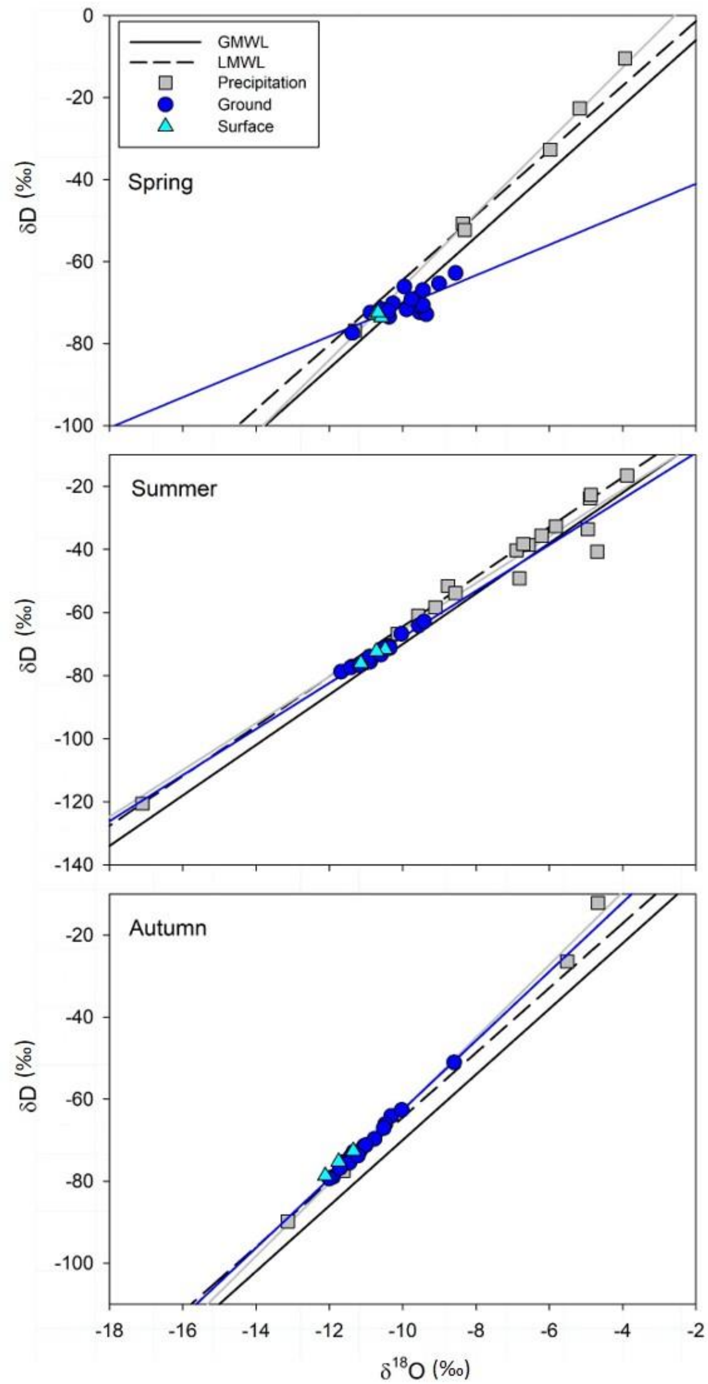


Figure 3.7: Precipitation, shallow groundwater, and surface water isotopes ($\delta^{18}O$, $\delta D$) for the spring, summer, and autumn seasons. Linear regressions for precipitation (spring n=6, $r^2$=0.99; summer n=17, $r^2$=0.96; autumn n=4, $r^2$=0.99) and shallow groundwater (spring n=17, $r^2$=0.54; summer n=15, $r^2$=0.97; autumn n=18, $r^2$=0.99) are shown for each season. Surface water linear regressions were not conducted for individual seasons due to the small sample size (n=3) for each sample time. Precipitation and shallow groundwater models were significantly different in spring ($p$<0.001), marginally different in summer ($p$=0.05), and not different in autumn ($p$=0.237). The Global Meteoric Water Line (GMWL) and Local Meteoric Water Line (LMWL) are also plotted.

*Landscape Characteristics Determining Groundwater Chemistry*

Physical characteristics of the watershed, particularly physiographic, hydrologic, and soil factors, were significant sources of variation in groundwater chemistry. Physical factors included those derived from ecosystem classifications (major landform, landscape ecosystem type) and topography (elevation, slope, TI, STI), as well as field observations, including soils (soil texture class) above ground vegetation (basal area), well depth, and measurements of shallow groundwater and soil VWC (water depth at sampling, hydrologic group) (Table 3.1, 3.2). Landscape characteristics were able to predict variation in concentrations of C, major cations ($Na^{+}$, $Ca^{2+}$, $Mg^{2+}$) and $Cl^{-}$, C and water isotope signatures, pH, and conductivity. Measurements of these analytes in surface and shallow groundwater samples are summarized in Table 3.3. No physical factors were significant predictors of variation in the concentrations of major biologically cycled analytes ($NO_3^{-}$, $SO_4^{2-}$, $PO_4^{3-}$, $K^{+}$) or $F^{-}$ and $Br^{-}$ ions.

Table 3.1: Categorical physical factors that were significant predictors of variation in analyte concentration or water table position. P-values considered significant when $p<0.05$ are bolded.

| | DIC | DOC | DIC $\delta^{13}C$ | DOC $\delta^{13}C$ | Cl- | Na+ | $Mg^{2+}$ | $Ca^{2+}$ | pH | Conductivity | Water Table Position | $\delta^{18}O$ | $\delta D$ |
|---|---|---|---|---|---|---|---|---|---|---|---|---|---|
| Major landform | 0.215 | 0.109 | 0.269 | 0.113 | **<0.001** | **<0.001** | 0.381 | 0.069 | 0.305 | 0.095 | 0.934 | 0.095 | 0.137 |
| Landscape Ecosystem Type | **<0.001** | 0.287 | 0.192 | 0.096 | **<0.001** | **<0.001** | **<0.001** | **<0.001** | 0.245 | **<0.001** | **<0.001** | **0.027** | **<0.001** |
| Hydrologic Group | **<0.001** | 0.139 | 0.213 | **0.041** | **<0.001** | **<0.001** | **<0.001** | **<0.001** | **0.002** | **<0.001** | **<0.001** | 0.077 | **0.01** |
| Soil Texture | **<0.001** | 0.436 | 0.291 | 0.207 | **<0.001** | **<0.001** | **<0.001** | **0.001** | 0.082 | **<0.001** | **<0.001** | 0.11 | 0.073 |
| Well Depth | 0.445 | **<0.001** | 0.249 | **0.004** | **<0.001** | **<0.001** | 0.171 | 0.231 | **0.016** | 0.229 | **<0.001** | **0.024** | **0.004** |

Table 3.2: Continuous physical factors showing significant correlations with analyte concentration or water table position. Cell contents are P-values and correlation coefficients (r); significant results ($p<0.05$) are bolded.

| | DIC | DOC | DIC $\delta^{13}C$ | DOC $\delta^{13}C$ | Cl- | Na+ | $Mg^{2+}$ | $Ca^{2+}$ | pH | Conductivity | Water Table Position | $\delta^{18}O$ | $\delta D$ |
|---|---|---|---|---|---|---|---|---|---|---|---|---|---|
| Elevation | 0.169, -0.2 | **0.05, -0.281** | 0.609, -0.075 | 0.401, -0.123 | **<0.001, -0.686** | **<0.001, -0.658** | 0.492, -0.101 | **0.05, -0.281** | 0.916, -0.015 | 0.079, -0.253 | 0.774, -0.045 | **0.026, 0.318** | **0.033, -0.306** |
| Slope | 0.075, -0.257 | 0.342, -0.139 | 0.617, -0.073 | 0.155, -0.206 | 0.104, -0.235 | 0.051, -0.281 | 0.085, -0.249 | 0.144, -0.212 | 0.753, 0.046 | 0.119, -0.225 | **<0.001, -0.583** | 0.473, 0.105 | 0.872, -0.024 |
| Basal Area | 0.85, 0.034 | 0.562, 0.103 | 0.86, 0.031 | 0.978, -0.005 | **0.0436, 0.348** | **0.0287, 0.375** | 0.543, 0.108 | 0.407, 0.147 | 0.395, -0.151 | 0.513, 0.116 | 0.395, 0.151 | 0.658, -0.079 | 0.739, 0.059 |
| TI | 0.076, 0.308 | 0.259, 0.199 | 0.567, 0.102 | 0.684, 0.073 | 0.912, -0.020 | 0.525, 0.113 | 0.458, 0.132 | 0.265, 0.197 | 0.404, -0.148 | 0.233, 0.210 | **0.001, 0.582** | 0.521, -0.114 | 0.902, 0.022 |
| STI | **0.006, 0.460** | 0.207, 0.222 | 0.426, 0.141 | 0.580, 0.098 | 0.958, 0.009 | 0.528, 0.112 | 0.126, 0.268 | **0.025, 0.384** | 0.353, -0.164 | **0.025, 0.384** | **<0.001, 0.649** | 0.706, -0.067 | 0.960, -0.009 |
| Water Depth at Sampling | **0.015, 0.37** | 0.109, 0.248 | **<0.001, 0.506** | 0.275, 0.17 | 0.709, 0.059 | 0.982, 0.004 | 0.069, 0.28 | 0.069, 0.28 | 0.964, 0.007 | **0.043, 0.31** | - | 0.997, -0.004 | 0.409, 0.129 |

Table 3.3: Summary of surface and shallow groundwater dissolved C concentrations and stable isotopes, $Ca^{2+}$, $Mg^{2+}$, pH, and conductivity (mean ± SD) for each sample date.

| | Source | DIC (mg $L^{-1}$) | DOC (mg $L^{-1}$) | DIC δ13C (‰) | DOC δ13C (‰) | $Ca^{2+}$ (mg $L^{-1}$) | $Mg^{2+}$ (mg $L^{-1}$) | pH | Conductivity (μS $cm^{-1}$) |
|---|---|---|---|---|---|---|---|---|---|
| April | Surface | 26.4 ± 7.5 | 6.2 ± 1.4 | -7.04 ± 0.61 | -27.02 ± 0.5 | 24.62 ± 7.4 | 10.15 ± 2.72 | 7.75 ± 0.02 | 190 ± 52 |
| | Ground | 27.4 ± 16.1 | 5.9 ± 3.3 | -6.65 ± 1.83 | -26.69 ± 1.18 | 24.13 ± 15.47 | 11.34 ± 7.19 | 7.54 ± 0.43 | 191 ± 104 |
| June | Surface | 36.6 ± 10.7 | 5.2 ± 1.2 | -9.82 ± 1.76 | -26.8 ± 0.9 | 33.98 ± 10.01 | 13.54 ± 3.27 | 7.78 ± 0.13 | 273 ± 83 |
| | Ground | 34.8 ± 14.7 | 6.3 ± 5.3 | -10.62 ± 1.72 | -26.8 ± 1.03 | 30.66 ± 13.72 | 13.08 ± 5.87 | 7.28 ± 0.37 | 252 ± 121 |
| November | Surface | 25.2 ± 4.1 | 4.5 ± 0.9 | -12.15 ± 1.09 | -27.87 ± 0.4 | 36.63 ± 5.39 | 14.56 ± 1.47 | 7.5 ± 0.22 | 231 ± 27 |
| | Ground | 25.4 ± 12.3 | 7. 4 ± 5.5 | -14.36 ± 4.18 | -27.92 ± 0.63 | 37.05 ± 13.76 | 14.41 ± 5.28 | 7.08 ± 0.33 | 244 ± 88 |

Each hydrologic group differed significantly from the other two in its DIC concentrations and conductivity (Figure 3.8). The continuously connected group had significantly higher $Ca^{2+}$ and $Mg^{2+}$ concentrations than the periodic or disconnected groups. Natural abundance DOC $\delta^{13}C$ signatures differed significantly between the continuously connected and periodically connected groups, with more isotopically enriched values in continuously connected wells (Figure 3.8). In addition, water table levels also differed significantly within each hydrologic group, with mean (± SD) water table levels significantly closer to the surface in the consistently (-13 ± 8 cm) and periodically connected (-15 ± 24 cm) groups compared to the disconnected group (-77 ± 47 cm; Figure 3.3). Landscape ecosystem type and soil texture class were also significant predictors of DIC, $Ca^{2+}$, $Mg^{2+}$, conductivity and water table depth (Table 3.1). Wells in the mesic outwash over till upland ecosystem (113) had significantly lower concentrations of DIC and $Mg^{2+}$, lower conductivity, and water table levels further from the surface compared to wells in the aquic outwash over till upland ecosystem (116), outwash over till riparian ecosystem (118), or outwash-lake plain wetland ecosystem (55). Ecosystem type 113 also had significantly lower $Ca^{2+}$ concentrations than the upland and outwash-lake plain wetland ecosystems (types 118, 55). The dune ecosystem type (74) was excluded from this statistical test due to a very small sample size (n=1 well in November sampling event).

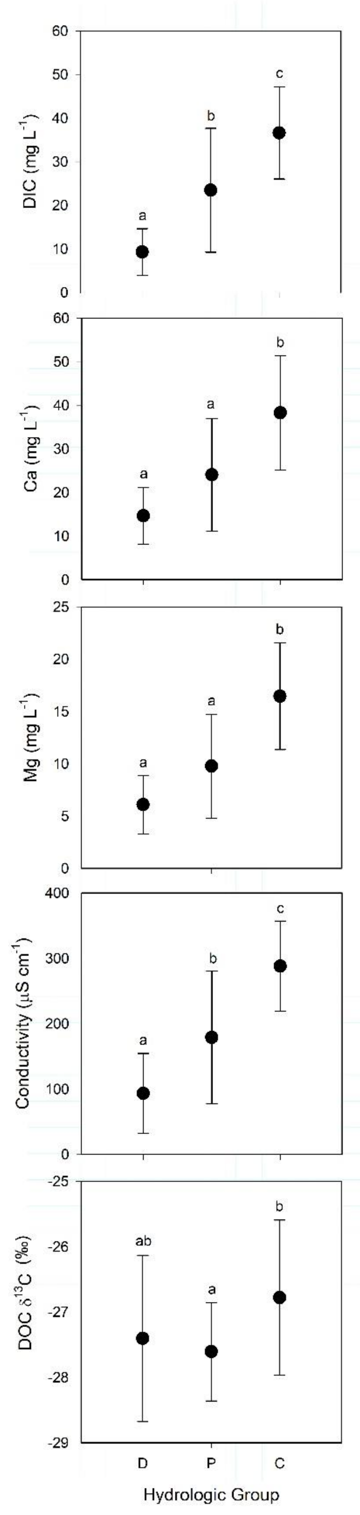


Figure 3.8: Mean DIC, $Ca^{2+}$, $Mg^{2+}$ concentrations, conductivity, and DOC $\delta^{13}C$ signatures by hydrologic group (D=disconnected, P=periodically connected, C=continuously connected). Error bars indicate standard deviation. Significant differences between groups are denoted by different letters.

Soil texture also affected groundwater chemistry; DIC, $Ca^{2+}$, and $Mg^{2+}$ concentrations and conductivity were significantly lower in the sand and loamy sand soils than in the sandy loam and sapric muck soils (Figure 3.9). Water table levels were also significantly lower in the sand soils than the other soils. While well depth was not a significant predictor of DIC, $Ca^{2+}$, $Mg^{2+}$ or conductivity, it was a significant predictor of DOC, DOC $\delta^{13}C$, and pH (Table 3.1; Figure 3.10). In the upland areas of the watershed, shallow groundwater DOC concentrations were significantly lower, and pH was more alkaline in the deepest wells (200+ cm) compared to the shallow wells (0-100 cm). DOC concentrations did not differ between the shallowest upland wells (0-100 cm) and the outwash-lake plain wetland wells (100-200 swamp), although the quality of the C did differ with more isotopically depleted DOC $\delta^{13}C$ in the shallow upland wells (0-100 cm) compared to the outwash-lake plain wetland wells (Figure 3.10).

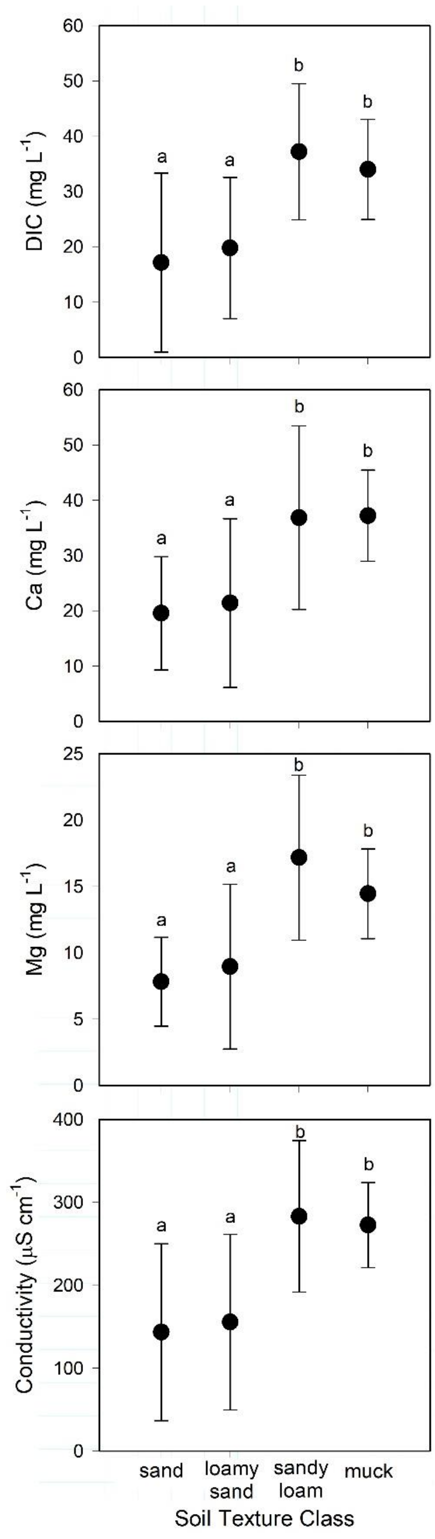


Figure 3.9: Mean DIC, $Ca^{2+}$, $Mg^{2+}$ concentrations and conductivity by soil texture class (whole profile). Error bars indicate standard deviation. Significant differences between groups are denoted by different letters.

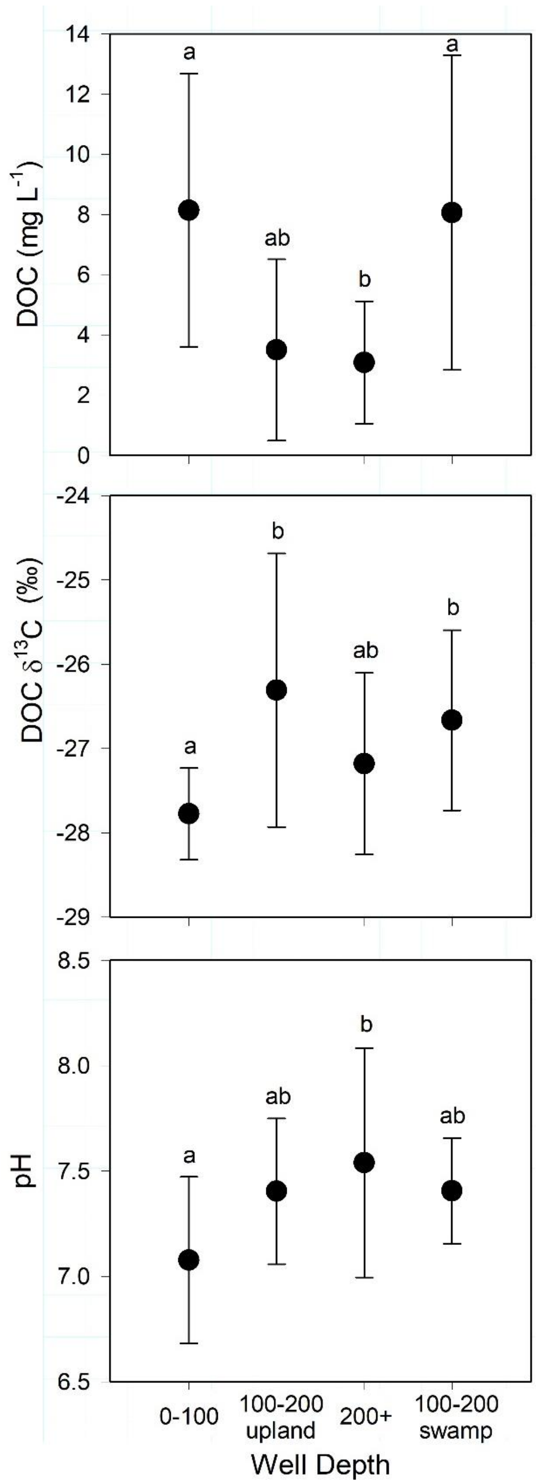


Figure 3.10: Mean DOC concentration, DOC $\delta^{13}C$, and pH by well depth. Well depth groups include wells 0-100 cm, 100-200 cm, and 200+ cm deep. The 100-200 cm wells were divided into upland (100-200 upland) and outwash-lake plain wetland (100-200 swamp) groups due to inherent differences between mineral and organic soils. Error bars indicate standard deviation. Significant differences between groups are denoted by different letters.

Of the continuous physical factors, elevation had a significant correlation with DOC, $Ca^{2+}$, $Cl^-$, and $Na^+$ concentrations and water isotopes (Table 3.2). Basal area was only correlated with $Cl^-$ and $Na^+$, although natural $Cl^-$ and $Na^+$ concentrations were likely modified by road salt applications in the lower portion of the watershed. Slope and TI had significant correlations with water depth at sampling, as did STI, which was also correlated with DIC and $Ca^{2+}$ concentrations and conductivity (Figure 3.11). At higher STI values, DIC and $Ca^{2+}$ concentrations were higher, conductivity was greater, and water table levels were closer to the surface. Hofmeister et al. (In Revision) also observed that both TI and STI could be used to estimate water table position across the watershed using measurements from all 22 upland wells during June 2016-2017.

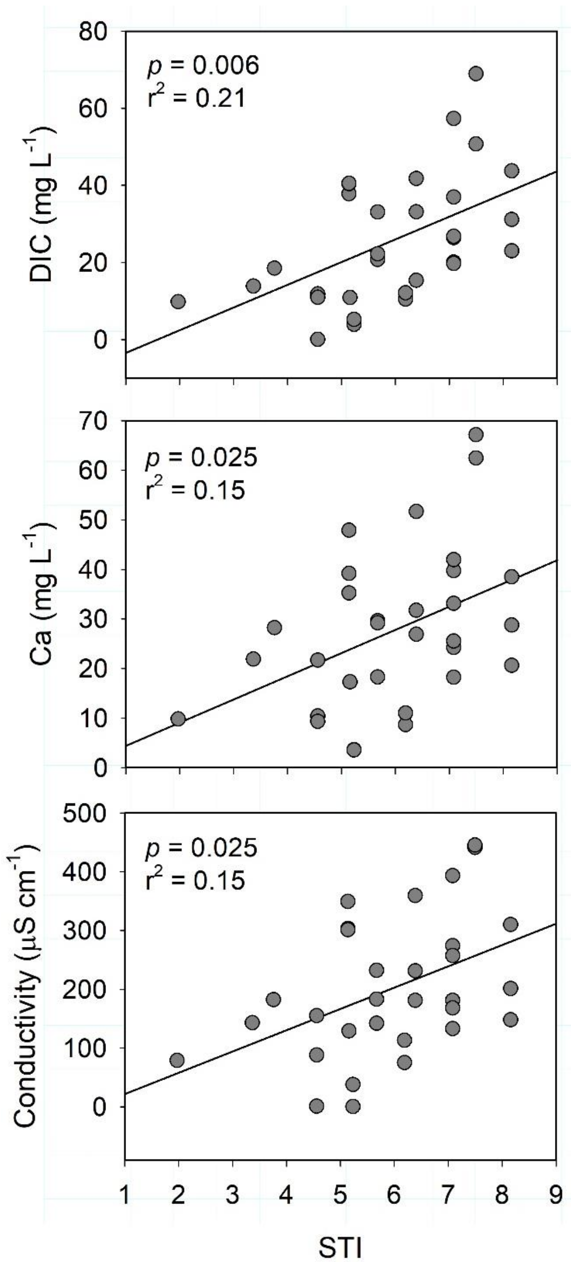


Figure 3.11: Relationship between STI and DIC, $Ca^{2+}$, and conductivity. Linear regressions were significant for all analytes shown ($p$<0.05).

*Shallow Groundwater Contributions to Stream*

We utilized mixing diagrams and analyses to identify the potential contributions of shallow groundwater C and water sources to the stream at each flume. With the hydrologic groups representing three shallow groundwater sources, mixing diagrams for DIC and DOC concentrations and DIC $\delta^{13}C$ and $\delta D$ are presented in Figure 3.12. Averaged across all seasons, concentrations of DIC and DOC in surface water fell within the standard errors of the mixing space established by the three shallow groundwater hydrologic groups (Figure 3.12). Surface water DIC and deuterium isotopic signatures also generally fell within the shallow groundwater envelopes, although the mouth flume was consistently more depleted in $\delta D$ and often more enriched in DIC $\delta^{13}C$ than the shallow groundwater. Surface water DOC concentrations were generally lower and DIC $\delta^{13}C$ more enriched than the shallow groundwater, falling at the margins (but within the standard errors).

Looking across seasons, the best fits of observed surface waters with the predicted shallow groundwater envelopes occurred in the spring, and surface water points generally fell further outside the predicted source area as the year went on. In June, stream DOC was slightly below the shallow groundwater predictions and DIC $\delta^{13}C$ was slightly more enriched, and in November, stream DOC concentrations were substantially lower and DIC $\delta^{13}C$ were further enriched relative to the predictions. Surface water at the mouth was consistently more depleted in $\delta D$ than the other surface water samples and more depleted than any of the shallow groundwater samples, except the disconnected group in June. Where surface water observations fell within the mixing space, it was possible to compute shallow groundwater contributions to stream C concentrations and isotope signatures. In April, all surface water samples were within standard errors of both the C concentrations and both the upper and mid flumes were within the standard errors of the isotope envelopes. In June at the mid flume, C concentrations were contributed equally from the periodically connected and disconnected groups (40% from each), along with a 20% contribution from the consistently connected group. At the upper flume surface water originated primarily from the periodically connected group (61%), with contributions from the consistently connected (22%) and disconnected (16%) groups. Surface water at all flumes in November were outside the mixing space defined by C concentration and the upper and mid flumes were at the margins of the C and water isotope envelope while the mouth was more depleted in δD and enriched in DIC $\delta^{13}C$.

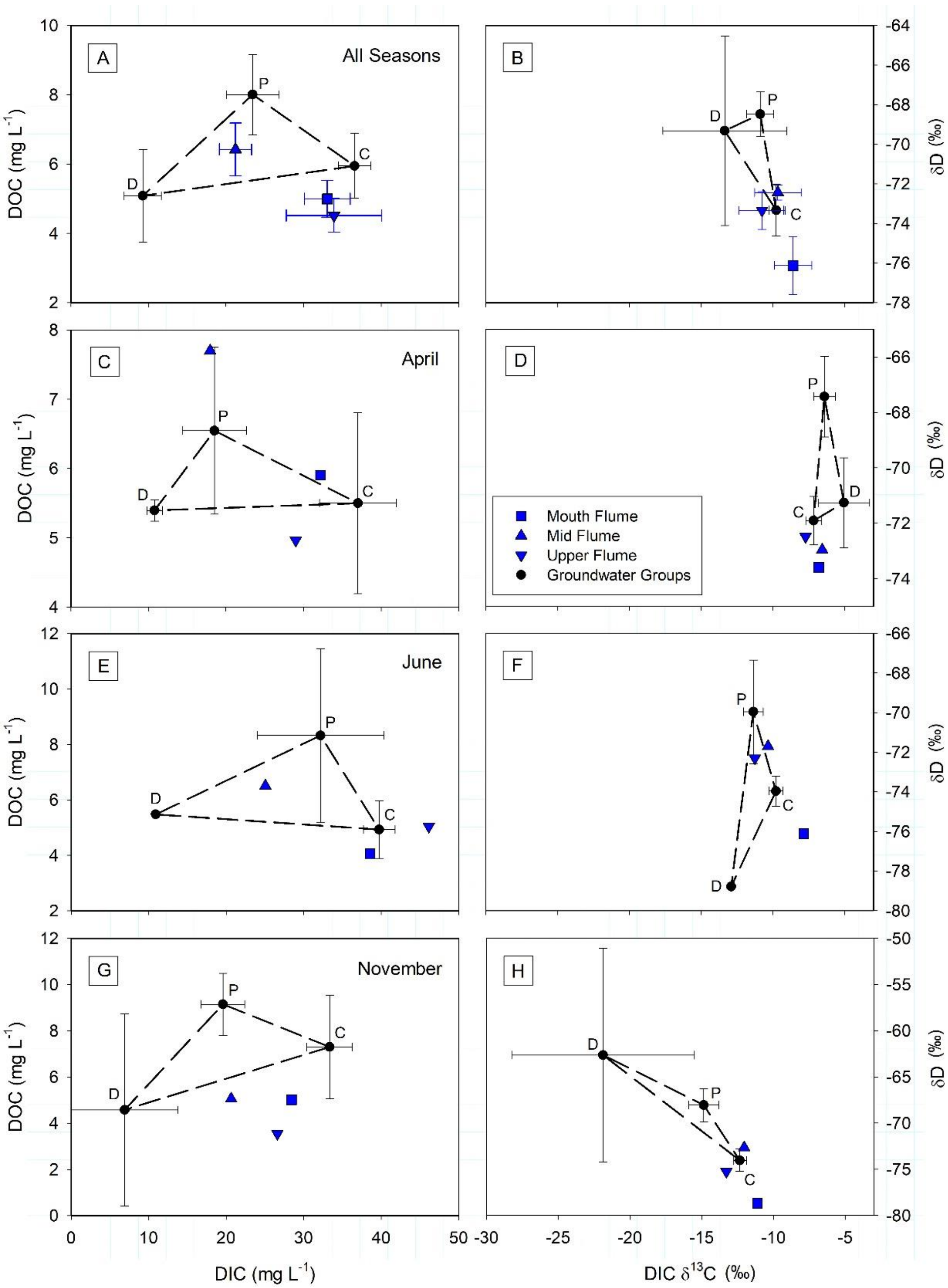


Figure 3.12: Mixing diagrams of shallow groundwater sources and surface waters based on DIC and DOC concentrations (panels A, C, E, G) and DIC $\delta^{13}C$ and $\delta D$ isotopic signatures (panels B, D, F, H). Error bars indicate standard error. Hydrologic groups (D=disconnected, P=periodically connected, C=continuously connected) provide potential surface water sources of dissolved C and water. Dashed lines indicate the area within which surface water would be completely fed by shallow groundwater.

Utilizing water table measurements from all the wells in the watershed, water table levels were significantly closer to the surface in the in the consistently connected and periodically connected groups than the disconnected group at each of the chemistry sampling times (Table 3.4). All wells had shallow groundwater at the April and early June sampling times, however the majority of wells in the disconnected group (80%) went dry during the summer and autumn. These wells were dry for a median duration of 87 days, and some wells remained dry in November even after several large storms. Approximately half of the wells (57%) in the periodic group also went dry, although these wells were dry for a much shorter period of time, with a median dry period of 5 days. In the consistently connected group, wells very rarely went dry, with only one well (5%) losing water during the 2017 sampling period (Table 3.4).

Table 3.4: Summary of water table position from the surface [cm; median ($25^{th}$, $75^{th}$ percentile)] by hydrologic group for each sampling time. Significant differences between hydrologic group water table positions are denoted with different letters. The percentage of wells that dried up for any period of time during April–Nov 2017 is also noted along with the duration of the dry period [median ($25^{th}$, $75^{th}$ percentile)].

| Hydrologic Group | April | June | November | # wells across watershed | Percentage of dry wells | Dry Period Duration (Days) |
|---|---|---|---|---|---|---|
| Disconnected | -88 (-123, -68)*a* | -119 (-170, -101)*a* | -127 (-201, -111)*a* | 5 | 80% | 86.5 (21, 89)*a* |
| Periodically Connected | -7.5 (-20, -1)*b* | -27.3 (-38,-17)*b* | -19.8 (-50.3, -7.8)*b* | 14 | 57% | 5 (0, 26)*a* |
| Consistently Connected | -6.9 (-21, -4)*b* | -15 (-30, -8)*b* | -10 (-20, -2)*b* | 21 | 5% | 0 (0,0)*b* |

***Discussion***

*Sources of Water to Honeysuckle Creek*

Throughout the April to November sampling period, approximately 80% of the water measured in Honeysuckle Creek was from a consistent source. Baseflow provides a stable supply of water derived from catchment storage, generally some form of groundwater inputs (Buttle, 2018; Neff et al., 2005). Across northern Michigan, many streams also have high baseflow contributions with BFI values of 0.8-1.0 (Neff et al., 2005). In this watershed, shallow groundwater inputs were a dominant source of water to Honeysuckle, but the origin of the water measured in shallow groundwater wells, and ultimately reaching the stream, shifted seasonally (Figure 3.6). In April, shallow groundwater likely originated from snowmelt more than recent spring rains. Linear regressions of shallow groundwater in April had shallower slopes than spring precipitation regressions as well as a mean D-excess value of 8.47‰ (± 3.8‰), indicating that the water sampled from the wells had undergone evaporative enrichment (Dansgaard, 1964; Ala-aho et al., 2018). This signal of evaporative enrichment is likely due to sublimating snow during the winter prior to the melt period (Earman et al., 2006). Stream water D-excess (12.36 ± 1.1‰) was between the shallow groundwater and precipitation (16.44 ± 2.9‰) D-excess values, suggesting that during the spring, surface water was mixture of snowmelt fed groundwater and recent precipitation. However, in summer and autumn, the similarity between shallow groundwater, surface water, and precipitation increased in both water isotope linear regressions and D-excess values, indicating that recent precipitation appears to become the increasingly dominant source of both shallow groundwater and stream water in these seasons (Figure 3.7).

Despite their different conceptual approaches and independent data inputs, mixing analyses and water balance calculations both indicate a contribution of groundwater from a deeper source to the stream mouth. Precipitation alone is not a sufficient input of water to balance the losses to evapotranspiration and stream discharge at the mouth. It is possible that some of the failure to close the water balance for the entire watershed could be due to uncertainty in the eddy flux tower measurements of evapotranspiration (*e.g.*, Hollinger and Richardson, 2005) or that Fatichi and Ivanov (2014) model estimates of evapotranspiration, which are based on the UMBS AmeriFlux tower measurements, overestimate evapotranspiration because they do not account for the lower transpiring wetland vegetation (Ewers et al., 2002) in the outwash-lake plain swamp. However, even accounting for these potential sources of uncertainty in evapotranspiration estimates, some source of water in addition to precipitation is required to close the water balance at the mouth. Additionally, the mixing diagrams indicate that a water source with a geologic DIC $\delta^{13}C$ signature and depleted $\delta D$ is contributing to surface water at the mouth, likely a groundwater source deeper than the shallow groundwater measured for this analysis. Deep groundwater interacting with the carbonate minerals in limestone and dolomite bedrock would have DIC $\delta^{13}C$ signatures around 0‰ (Jin et al., 2009). In the mixing diagrams, surface water at the mouth has a more geologic DIC $\delta^{13}C$ signature than the other surface waters and is often more enriched than the consistently connected wells to which the stream mouth is most proximal. This is especially obvious in the summer and autumn. The surface water at the mouth is also more depleted in $\delta D$ than the other surface waters or any of the shallow groundwater, except the disconnected group in June. While we do not have samples of deeper groundwater from within the watershed, water samples from a deep drinking water well (160 m) at the UMBS laboratory have $\delta^{18}O$ (-12.26‰) and $\delta D$ (-84.38‰) which are far more depleted values than any measured in our stream or shallow groundwater sampling. More depleted values of $\delta D$ have been associated with deeper groundwater sources (Lessels et al., 2016; Orlowski et al., 2016; Jasechko et al., 2017). A deep groundwater source such as this is likely a source of water to the stream mouth, given the δD value -76.13‰ (± 2.55‰) and geologic DIC $\delta^{13}C$ signatures (-8.59 ± 2.25‰) measured. In addition, 66% of the watershed area draining to the mouth has deep, sandy soils which promote fast vertical infiltration and could be recharging deeper groundwater sources which contribute to baseflow at the mouth (Figure 3.13; Hinton et al., 1993). While the three chemistry sampling events provide only snapshots of water height and chemistry across the watershed, they can give insights into the process happening across the watershed (Braken et al., 2013). We use our longer term and more continuous measurements of water table level and streamflow to expand our understanding of the spatial and temporal hydrologic connectivity occurring within the watershed.

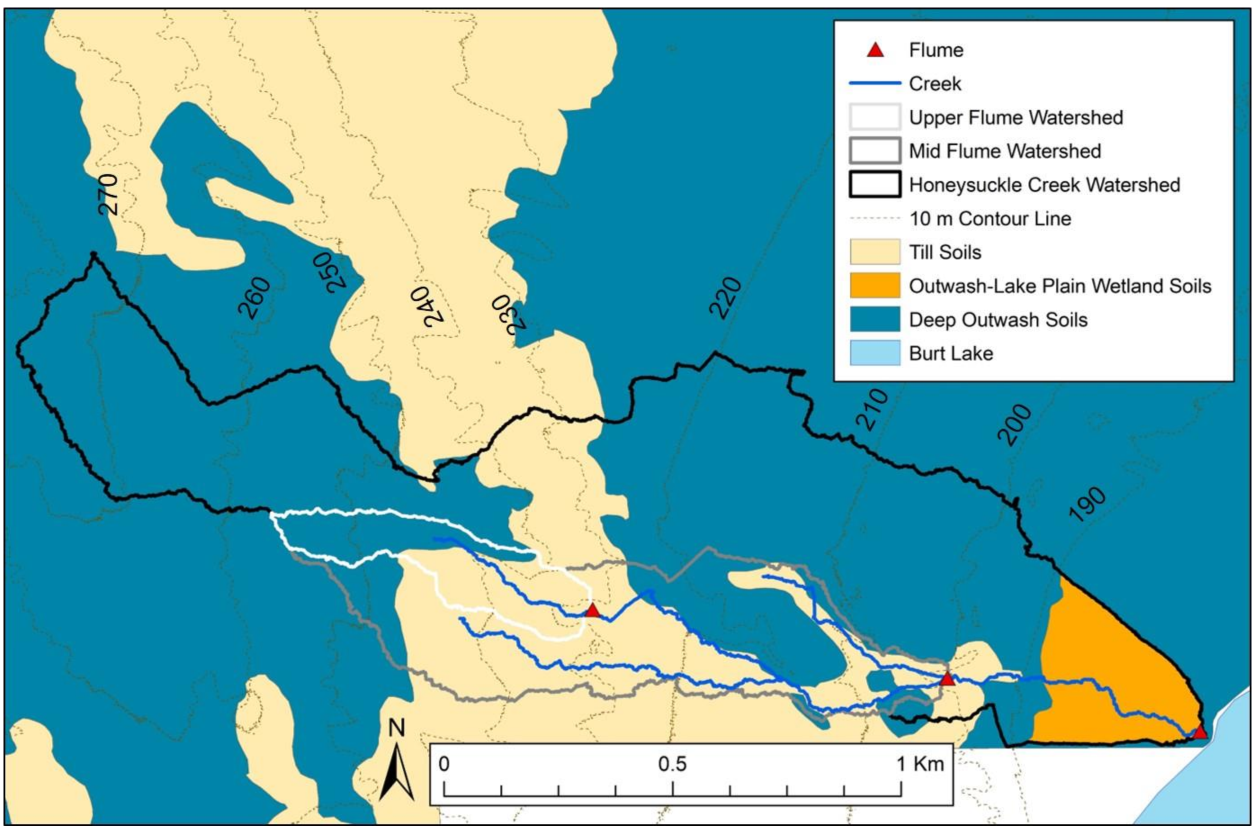


Figure 3.13: Distribution of soils across the upper, mid, and mouth watersheds. The mouth watershed has a greater percentage of deep, sandy, outwash soils (66%) than the mid (38%) or upper (45%) watersheds. These outwash soils promote fast vertical infiltration of precipitation to recharge deeper groundwater, compared to the till soils which promote lateral flow of shallow groundwater.

*Watershed Connectivity*

Across the watershed, hydrologic connectivity decreased from April to November. Vertical connectivity decreased as water levels dropped seasonally and the direct connection between surficial soil water and shallow groundwater was reduced (Figure 3.3). Water table levels were closest to the surface in all wells in the spring and fell through the summer and autumn seasons. When water table levels were close to the surface, in the spring during snowmelt and after large storms, shallow groundwater was likely interacting with soil horizons containing less degraded, more modern C (Hofmeister et al., In Prep) and higher concentrations of cycling inorganic elements (*e.g.*, Sebestyen et al., 2008; Herndon et al., 2015). Spatial connectivity between hillslopes and the stream was greatest during the spring, decreasing as water table levels dropped during the summer in all wells. Beginning in the middle of August, the majority (80%) of disconnected wells went dry and remained dry until November or even longer (Table 3.4). Approximately half of the periodically connected wells (57%) also dried up for some time in the late summer or autumn. However, most of these wells began to dry up only after a stretch with little rain and were dry for much shorter durations than the disconnected wells. In all but one of the periodically connected wells, shallow groundwater returned after large rain events. Only the wells in the upland riparian area close to the stream or in the outwash-lake plain wetland had shallow groundwater consistently throughout the growing season, with only one well drying up after 12 days of no rain. In addition, the total length of continuous surface water in the stream was greatest in April during snowmelt and decreased as the year went on, resulting in less direct connection of surface water longitudinally along the stream.

As shallow groundwater dried up in the disconnected wells and some of the periodic wells, there was a loss of spatial connectivity between these areas of the watershed and the stream. In this watershed and in others, hydrologic connectivity between the hillslopes, riparian areas, and the stream is spatially variable with transient connections during snowmelt or large storm events (Jencso et al., 2009; Detty and McGuire, 2010; Tetzlaff et al., 2014; Zimmer and McGlynn, 2018). Snowmelt and rain events can cause the lateral and vertical expansion of variable source areas across the watershed and into organic matter and nutrient rich near-surface soil horizons that are only occasionally connected to the stream (Boyer et al., 1997; Lambert et al., 2014; Herndon et al., 2015). As groundwater becomes disconnected both vertically and spatially, transport areas shrink, with the areas remaining connected to surface water via shallow groundwater acting as important conduits (Covino, 2017). In our watershed, the consistently connected wells in the riparian areas and outwash-lake plain wetland are likely important sources of water and analytes to the stream throughout the year due to the persistent soil water-groundwater connections and their close proximity to surface water. Riparian areas have been highlighted as important sources of water and elements, especially in headwater systems, and can act as key areas where near surface soil water and hillslope groundwater sources mix (McGlynn and McDonnell, 2003; Lambert et al., 2014; Tetzlaff et al., 2014). Increasing antecedent wetness due to snowmelt or storm events can increase hydrologic connectivity across the landscape and expand the areas actively contributing to the transport of water and solutes between landscape units and to streams (McGlynn and McDonnell, 2003; Ambroise, 2004; Gannon et al., 2015).

*Linkages Between Landscape Hydrologic Units*

Land units-- such as those described by our hydrologic groups-- are integrative, with physical properties that cannot be uncoupled. They are fundamental units that have internally consistent, but outwardly unique syndrome properties (Tansley, 1935; Rowe and Sheard, 1981). Physiographic factors including topography (*e.g.*, landscape position, slope) and soil characteristics (*e.g.*, soil texture, parent material mineralogic composition) are often used to distinguish land units (*e.g.*, Barnes et al., 1982; Pearsall et al., 1995) and these same factors are also often noted as bottom up controls on water storage and movement (Lin et al., 2006; Soulsby et al., 2006; Vidon and Smith, 2007; Detty and McGuire, 2010). Here, in the Honeysuckle Creek watershed, we identify four dominant landscape hydrologic units (consistently connected, periodically connected, disconnected, and never connected) to describe the vertical connectivity of soil water and shallow groundwater and hydrologic connectivity to the stream.

In landscape units with excessively well drained sandy soils, glacial till restrictive material around 2 m (115-220 cm) from the surface, and generally steep slopes (8-12%), water table levels were furthest from the surface. In these disconnected hydrologic units, the direct connections between shallow groundwater and surface waters are likely limited to the springtime when snowmelt and spring rains create saturated conditions and elevated water tables connect much of the landscape. Shallow groundwater from these areas has low concentrations of DIC, $Ca^{2+}$, $Mg^{2+}$ and low conductivity due to the soils through which the groundwater travels. Soils formed in sandy outwash have lower $Ca^{2+}$ and $Mg^{2+}$ availability (0.7-1.6 mg $g^{-1}$ $Ca^{2+}$, 0.1-0.8 mg $g^{-1}$ $Mg^{2+}$) than soils formed in mixed outwash and till because sandy soils have relatively more quartz and lower percentages of minerals whose weathering yields base cations (Adams and Boyle, 1979; 1982). Additionally, there are portions of the watershed (the "never connected" landscape hydrologic unit) where neither shallow groundwater, nor evidence of groundwater, is ever observed (Hofmeister et al., In Revision). Soils in these areas are formed in sandy outwash, with tens of meters of sand above any form of restrictive material and precipitation falling there likely is a very small direct source of water to the stream, although these areas may be important for recharging deeper groundwater sources (Naylor et al., 2016), which may contribute in part to baseflow at the mouth of Honeysuckle Creek (Figure 3.13).

The periodically connected group is the most diverse and variable landscape hydrologic unit, with a range of soil textures (sand, loamy sand, sandy loam), depth to glacial till restrictive material (50-150 cm), slopes (4.3-9.4%), and distance from surface water. Water table levels were generally around 50 cm below the surface ($-44 \pm 29$ cm), although seasonal variability was high with some wells having water levels at or above the surface in the spring and then drying up for a period in August and September. Cation concentrations were also variable, with wells on the edge of the moraine at the boundary between shallow till soils and very deep outwash soils (*e.g.*, wells at the north end of the 230 m contour line; n=2) having lower $Ca^{2+}$ ($6.7 \pm 3.7$ mg $L^{-1}$) and $Mg^{2+}$ ($3.1 \pm 1.8$ mg $L^{-1}$) concentrations than wells more centrally located within the area underlain with till (*e.g.*, the southern portion of the 220 m contour line; n=4; $Ca^{2+}$=30.0 ± 9.9 mg $L^{-1}$, $Mg^{2+}$=12.1 ± 3.8 mg $L^{-1}$). Finer-textured soils with glacial till restrictive material close to the surface have more abundant cation-bearing minerals (*e.g.*, feldspar), and therefore more cations, than the sandy outwash soils. Indeed, wells in loamy sand soils had lower $Ca^{2+}$, $Mg^{2+}$, and DIC concentrations than wells in the finer textured sandy loam soils (Figure 3.9).

Lastly, the consistently connected hydrologic unit is defined by its low-lying topographic position, whether at the hillslope or the landscape level, and soils with thick surface accumulation of organic materials. In these areas the water table is consistently near the surface in the upland riparian areas and in the low-lying outwash-lake plain wetland adjacent to Burt Lake. The outwash-lake plain wetland is fed with minerotrophic hydrologic inputs; groundwater samples have high DIC and cation concentrations (Figure 3.8) indicating that the wetland water has had considerable contact with mineral soils formed in till (Zogg and Barnes, 1995). Being in the lowest topographic position of the watershed, the outwash-lake plain wetland receives water inputs throughout the year, allowing for perennial stream flow through the wetland to the Burt Lake. The upland riparian areas also have shallow groundwater throughout the year and the combination of topography and low-permeability till near the surface funnels water along the restrictive layer into the stream channel.

This landscape-level distribution of spatial units can allow for the movement of material (*e.g.*, organic C) from disconnected upland units to periodically connected landscape units, especially in the spring when groundwater tables are most continuous across the watershed. For example, upland forests on the surrounding landscape have been intensively studied as part of long-term C research at UMBS, and while they are consistent C sinks (Curtis et al., 2005; Gough et al., 2008; Gough et al., 2016), no investigations have addressed the role of hydrologic C exports in their whole-ecosystem C balance. Significant groundwater-mediated transfers of C from these forests directly to surface waters are unlikely because they are on well-drained outwash soils with water tables >20 m below the surface (well drilling records), but portions of this intensively studied area are on landscape units that are at least seasonally wet (Nave et al., 2017b). These areas are likely connected via groundwater to lower-lying, periodically connected landscape units that extend into the Honeysuckle Creek or other headwater watersheds that ultimately empty into Burt Lake.

Setting aside this larger landscape to focus specifically on the Honeysuckle Creek watershed, the riparian areas and the outwash-lake plain wetland likely have a much stronger influence on stream chemistry and discharge than the upland disconnected or periodically connected groups, due to the perennial connections between shallow groundwater from the consistently connected areas and surface water. Riparian areas and wetlands are often identified as relatively small landscape units with a disproportionately large influence on stream chemistry

(Bishop et al., 2008; Tetzlaff et al., 2014; Lessels et al., 2016), especially with respect to C (Fiebig et al., 1990; Elder et al., 2000; Grabs et al., 2012). Stream DOC concentrations can increase during storm events or snowmelt when rising water tables and a spatial expansion of soil saturation allows for flushing of soil DOC from more surficial soil horizons in the riparian area and from upland areas that are disconnected at lower flows (Lottig et al., 2013; Ali et al., 2010; Gannon et al., 2015; Herndon et al., 2015). While upland areas do contribute C to riparian areas, the amount is small compared to the large C pools present in wetlands (Elder et al., 2000; Lottig et al., 2013; Lambert et al., 2014; Tetzlaff et al., 2014).

Mixing diagrams show that DOC concentrations at the mouth of the stream are most similar to shallow groundwater concentrations from consistently connected areas; however, at higher flow times (April, November), DOC concentrations shift, appearing to be a mixture of C from the consistently and periodically connected hydrologic units (Figure 3.12). Hofmeister et al. (In Prep) observed that when Honeysuckle Creek discharge increased, DOC concentrations also increased, and the DOC quality shifted from a more degraded organic matter source (more enriched DOC $\delta^{13}C$) to a less degraded source (more depleted DOC $\delta^{13}C$) source found in the surficial soil horizons of the upland areas. At low flows when hydrologic connections between the stream and the landscape are restricted, DOC in the stream is primarily coming from deeper soil horizons in the outwash-lake plain wetland. Together, these results suggest when stream discharge increases during snowmelt or large storm events, hydrologic connectivity increases throughout the watershed, connecting fresher organic matter from upland areas with shallow groundwater, the stream, and ultimately the lake. Transfers of C and other elements from the periodically connected hydrologic unit to the wetland likely occur during snowmelt and storms that intermittently reconnect these areas, but C inputs from the upland areas are probably small compared to what is accumulating *in situ* in the wetland (Nave et al., 2017a). While upland water and C are important for the forest ecosystem, the significant transport fluxes on this landscape are likely predominantly from the outwash-lake plain wetland to the lake.

### *Conclusions*

In this glacial landscape, riparian zones and wetlands are important terrestrial-aquatic interfaces where water and material from upland areas are transferred to surface waters. Topography and soil characteristics strongly influence water and chemical movement throughout the landscape. Shallow groundwater is the primary source of water to the headwater stream throughout the year; originating from snowmelt in the spring and shifting to recent precipitation in summer and autumn seasons. Changes to precipitation patterns under future climate conditions could impact the magnitude of stream flow and the extent of connections between the stream and surrounding landscape, particularly at the upper reaches of headwater streams. Hydrologic connectivity across the watershed is greatest during snowmelt or large storm events when shallow groundwater connections extend from the stream through riparian areas and up hillslopes. Landscape units that are disconnected from surface waters for most of the year, except during snowmelt, are likely not significant contributors of water or C reaching inland lakes, but intermittent connections could be important for transfers of material within the ecosystems comprising the wider landscape. In contrast, landscape units that are periodically or consistently connected to surface waters are likely the most important sites for biogeochemical export from the terrestrial ecosystems to streams and lakes.

REFERENCES

Adams, P.W., Boyle, J.R., 1979. Cation release from Michigan spodosols leached with aspen leaf extracts. Soil Science Society of America Journal 43, 593-596.

Adams, P.W., Boyle, J.R., 1982. The quantity and quality of nutrient cations in some Michigan spodosols. Soil Science 133, 383-398.

Ala-aho, P., Soulsby, C., Pokrovsky, O.S., Kirpotin, S.N., Karlsson, J., Serikova, S., Vorobyev, S.N., Manasypov, R.M., Loiko, S., Tetzlaff, D., 2018. Using stable isotopes to assess surface water source dynamics and hydrological connectivity in a high-latitude wetland and permafrost influenced landscape. Journal of Hydrology 556, 279-293.

Alexander, R.B., Boyer, E.W., Smith, R.A., Schwarz, G.E., Moore, R.B., 2007. The role of headwater streams in downstream water quality. Journal of the American Water Resources Association 43, 41-59.

Ali, G.A., L'Heureux, C., Roy, A.G., Turmel, M., Courchesne, F., 2011. Linking spatial patterns of perched groundwater storage and stormflow generation processes in a headwater forested catchment. Hydrological Processes 25, 3843-3857.

Ali, G.A., Roy, A.G., Turmel, M., Courchesne, F. 2010., Source-to-stream connectivity assessment through end-member mixing analysis. Journal of Hydrology 392, 119-135.

Ambroise, B., 2004. Variable 'active' versus 'contributing' areas or periods: A necessary distinction. Hydrological Processes 18, 1149-1155.

Bachmair, S., Weiler, M., 2014. Interactions and connectivity between runoff generation processes of different spatial scales. Hydrological Processes 28, 1916-1930.

Ballinger, A., Lake, P.S., 2006. Energy and nutrient fluxes from rivers and streams into terrestrial food webs. Marine and Freshwater Research 57, 15-28.

Barnes, B.V., Pregitzer, K.S., Spies, T.A., Spooner, V.H., 1982. Ecological forest site classification. Journal of Forestry 64, 179-181.

Baxter, C.V., Fausch, K.D., Saunders, W.C., 2005. Tangled webs: Reciprocal flows of invertebrate prey link streams and riparian zones. Freshwater Biology 50, 201-220.

Bishop, K., Buffam, I. Erlandsson, M., Folster, J., Laudon, H., Seibert, J., Temnerud, J., 2008. Aqua Incognita: the unknown headwaters. Hydrological Processes 22, 1239-1242.

Blewett, W.L., Winters, H.A., 1995. The importance of glaciofluvial features within Michigan's Port Huron moraine. Annals of the Association of American Geographers 85, 306-319.

Bowen, G.J., Kennedy, C.D., Henne, P.D., Zhang, T., 2012. Footprint of recycled water subsidies downwind of Lake Michigan. Ecosphere 3, 1-16.

Boyer, E.W., Hornberger, G.M., Bencala, K.E., McKnight, D.M., 1997. Response characteristics of DOC flushing in an alpine catchment. Hydrological Processes 11, 1635-1647.

Bracken, L.J., Wainwright, J., Ali, G.A., Tetzlaff, D., Smith, M.W., Reaney, S.M., Roy, A.G., 2013. Concepts of hydrological connectivity: Research approaches, pathways and future agendas. Earth-Science Reviews 119, 17-34.

Buttle, J.M., 2018. Mediating stream baseflow response to climate change: The role of basin storage 32, 363-378.

Covino, T., 2017. Hydrologic connectivity as a framework for understanding biogeochemical flux through watersheds and along fluvial networks. Geomorphology 277, 133-144.

Craig, H., 1961. Standard for reporting concentrations of deuterium and oxygen-18 in natural waters. Science 133, 1833-1834.

Curtis, P.S., Vogel, C.S., Gough, C.M., Schmid, H.P., Su, H.-B., Bovard, B.D., 2005. Respiratory carbon losses and the carbon-use efficiency of a northern hardwood forest, 1999-2003. New Phytologist 167, 437-456.

Dansgaard, W., 1964. Stable isotopes in precipitation. Tellus 16, 436-468.

Detty, J.M., McGuire, K.J., 2010. Topographic controls on shallow groundwater dynamics: Implications of hydrologic connectivity between hillslopes and riparian zones in a till mantled catchment. Hydrological Processes 24, 2222-2236.

Downing, J.A., Cole, J.J., Duarte, C.M., Middelburg, J.J., Melack, J.M., Prairie, Y.T., Kortelainen, P., Strigel, R.G., McDowell, W.H., Tranvik, L.J., 2012. Global abundance and size distributions of streams and rivers. Inland Waters 2, 229-236.

Earman, S., Campbell, A.R., Phillips, F.M., Newman, B.D., 2006. Isotopic exchange between snow and atmospheric water vapor: Estimation of the snowmelt component of groundwater recharge in the southwestern United States. Journal of Geophysical Research 111, D09302.

Elder, J.F., Rybicki, N.B., Carter, V., Weintraub, V., 2000. Sources and yields of dissolved carbon in northern Wisconsin stream catchments with differing amounts of peatland. Wetlands 20, 113-125.

Emanuel, R.E., Hazen, A.G., McGlynn, B.L., Jencso, K.G., 2014. Vegetation and topographic influences on the connectivity of shallow groundwater between hillslopes and streams. Ecohydrology 7, 887-895.

Ewers, B.E., Mackay, D.S., Gower, S.T., Ahl, D.E., Burrows, S.N., Samanta, S.S., 2002. Tree species effects on stand transpiration in northern Wisconsin. Water Resources Research 38, 1103.

Fasching, C., Ulseth, A.J., Schelker, J., Steniczka, G., Battin, T.J., 2016. Hydrology controls dissolved organic matter export and composition in an Alpine stream and its hyporheic zone. Limnology and Oceanography 61, 558-571.

Fatichi, S., Ivanov, V., 2014. Interannual variability of evapotranspiration and vegetation productivity. Water Resources Research 50, 3275-3294.

Fergus, C.E., Lapierre, J., Oliver, S.K., Skaff, N.K., Cheruvelil, K.S., Webster, K., Scott, C., Soranno, P., 2017. The freshwater landscape: lake, wetland, and stream abundance and connectivity at macroscales. Ecosphere 8, e01911.

Fiebig, D.M., Lock, M.A., Neal, C., 1990. Soil water in the riparian zone as a source of carbon for a headwater stream. Journal of Hydrology 116, 217-237.

Freeman, M.C., Pringle, C.M., Jackson, C.R., 2007. Hydrologic connectivity and the contribution of stream headwaters to ecological integrity at regional scales. Journal of the American Water Resources Association 43, 5-14.

Friedman, I., Smith, G.I., Gleason, J.D., Warden, A., Harris, J.M., 1992. Stable isotope composition of waters in southeastern California. Journal of Geophysical Research 97, 5795-5812.

Fritz, K.M., Schofield, K.A., Alexander, L.C., McManus, M.G., Golden, H.E., Lane, C.R., Kepner, W.G., LeDuc, S.D., DeMeester, J.E., Pollard, A.I., 2018. Physical and chemical connectivity of streams and riparian wetlands to downstream waters: A synthesis. Journal of the American Water Resources Association 54, 323-345.

Fuka, D.R., Walter, M.T., Archibald, J.A., Steenhuis, T.S., Easton, Z.M., 2014. EcoHydRology: A community modeling foundation for Eco-Hydrology. R package version 0.4.12. https://CRAN.R-project.org/package=EcoHydRology

Gannon, J.P., Bailey, S.W., McGuire, K.J., Shanley, J.B., 2015. Flushing of distal hillslopes as an alternative source of dissolved organic carbon in a headwater catchment. Water Resources Research 51, 8114-8128.

Gat, J.R., Bowser, C.J., Kendall, C., 1994. The contribution of evaporation from the Great Lakes to the continental atmosphere: Estimate based on stable isotope data. Geophysical Research Letters 21, 557-560.

Gburek, W.J., Needelman, B.A., Srinivasan, M.S., 2006. Fragipan controls on runoff generation: Hydropedological implications at landscape and watershed scales. Geoderma 131, 330-344.

Gomi, T., Sidle, R.C., Richardson, J.S., 2002. Understanding processes and downstream linkages of headwater systems. BioScience 52, 905-916.

Gough, C.M., Curtis, P.S., Hardiman, B.S., Scheuermann, C.M., Bond-Lamberty, B., 2016. Disturbance, complexity, and succession of net ecosystem production in North America's temperate deciduous forests. Ecosphere 7, 1-15.

Gough, C.M., Vogel, C.S., Harrold, K.H., George, K., Curtis, P.S., 2007. The legacy of harvest and fire on ecosystem carbon storage in a north temperate forest. Global Change Biology 13, 1935-1949.

Gough, C.M., Vogel, C.S., Schmid, H.P., Su, H.-B., Curtis, P.S., 2008. Multi-year convergence of biometric and meteorological estimates of forest carbon storage. Agricultural and Forest Meteorology 148, 158-170.

Grabs, T., Bishop, K., Laudon, H., Lyon, S.W., Seibert, J., 2012. Riparian zone hydrology and soil water total organic carbon (TOC): implications for spatial variability and upscaling of lateral TOC exports. Biogeosciences 9, 3901-3916.

Hardiman, B.S., Gough, C.M., Halprin, A., Hofmeister, K.L., Nave, L.E., Bohrer, G., Curtis, P.S., 2013. Maintaining high rates of carbon storage in old forests: A mechanism linking canopy structure to forest function. Forest Ecology and Management 298, 111-119.

He, L., Ivanov, V.Y., Bohrer, G., Mauer, K.D., Vogel, C.S., Moghaddam, M., 2014. Effects of fine-scale soil moisture and canopy heterogeneity on energy and water fluxes in a northern temperate mixed forest. Agricultural and Forest Meteorology 184, 243-256.

Herndon, E.M., Dere, A.L., Sullivan, P.L., Norris, D., Reynolds, B., Brantley, S.L., 2015. Landscape heterogeneity drives contrasting concentration-discharge relationships in shale headwater catchments. Hydrology and Earth System Science 19, 3333-3347.

Hinton, M.J., Schiff, S.L., English, M.C., 1993. Physical properties governing groundwater flow in a glacial till catchment. Journal of Hydrology 142, 229-249.

Hofmeister, K.L., Nave, L.E., Drevnick, P., Veverica, T., Knudstrup, R., Riha, S.J., Walter, M.T., In Preparation. Seasonal dynamics and exports of elements from a first-order stream to a large inland lake in Michigan. Hydrological Processes

Hofmeister, K.L., Nave, L.E., Riha, S.J., Schneider, R.L., Walter, M.T., In Revision. Soils and topography control seasonal and spatial patterns of forest soil moisture and water table position. Vadose Zone Journal

Hooper, R.P., 2003. Diagnostic tools for mixing models of stream water chemistry. Water Resources Research 39, 1055.

Inamdar, S., Dhillon, G., Singh, S., Dutta, S., Levia, D., Scott, D., Mitchell, M., Van Stan, J., McHale, P., 2013. Temporal variation in end-member chemistry and its influence on runoff mixing patterns in a forested, Piedmont catchment. Water resources Research 49, 1828-1844.

Inamdar, S.P., Mitchell, M.J., 2006. Hydrologic and topographic controls on storm-event exports of dissolved organic carbon (DOC) and nitrate across catchment scales. Water Resources Research 42, W03421.

James, A.L., Roulet, N.T., 2006. Investigating the applicability of end-member mixing analysis (EMMA) across scale: A study of eight small, nested catchments in a temperate forested watershed. Water Resources Research 42, W08434.

James, A.L., Roulet, N.T., 2009. Antecedent moisture condition and catchment morphology as controls on spatial patterns of runoff generation in small forest catchments. Journal of Hydrology

377, 351-366.

Jasechko, S., Wassenaar, L.I., Mayer, B., 2017. Isotopic evidence for widespread cold-season-biased groundwater recharge and young streamflow across central Canada. Hydrological Processes 31, 2196-2209.

Jin, L., Ogrinc, N., Hamilton, S.K., Szramek, K., Kanduc, T., Walter, L.M., 2009. Inorganic carbon isotope systematics in soil profiles undergoing silicate and carbonate weathering (Southern Michigan, USA). Chemical Geology 264, 139-153.

Jencso, K.G., McGlynn, B.L., 2011. Hierarchical controls on runoff generation: Topographically driven hydrologic connectivity, geology, and vegetation. Water Resources Research 47, W11527.

Jencso, K.G., McGlynn, B.L., Gooseff, M.N., Wondzell, S.M., Bencala, K.E., Marshall, L.A., 2009. Hydrologic connectivity between landscapes and streams: Transferring reach- and plot-scale understanding to the catchment scale. Water Resources Research 45, W04428.

Kilpatrick, F.A., Schneider, V.R., 1983. Use of flumes in measuring discharge: U.S. Geological Survey Techniques of Water-Resources Investigations, Book 3, Chapter A14, 46 p.

Kirchner, J.W., Tetzlaff, D., Soulsby, C., 2010. Comparing chloride and water isotopes as hydrological tracers in two Scottish catchments. Hydrological Processes 24, 1631-1645.

Klaus, J., McDonnell, J.J., 2013. Hydrograph separation using stable isotopes: Review and evaluation. Journal of Hydrology 505, 47-64.

Klaus, J., McDonnell, J.J., Jackson, C.R., Du, E., Griffiths, N.A., 2015. Where does streamwater come from in low-relief forested watersheds? A dual-isotope approach. Hydrology and Earth System Sciences 19, 125-135.

Lambert, T., Pierson-Wickmann, A.-C., Gruau, G., Jaffrezic, A., Petitjean, P., Thibault, J.N., Jeanneau, L., 2014. DOC sources and DOC transport pathways in a small headwater catchment as revealed by carbon isotope fluctuation during storm events.  Biogeosciences 11, 3043-3056.

Lapin, M., Barnes, B.V., 1995. Using the landscape ecosystem approach to assess species and ecosystem diversity. Conservation Biology 9, 1148-1158.

Leibowitz, S.G., Wigington, P.J., Schofield, K.A., Alexander, L.C., Vanderhoof, M.K., Golden, H.E., 2018. Connectivity of streams and wetlands to downstream waters: An integrated systems framework. Journal of the American Water Resources Association 54, 298-322.

Lessels, J.S., Tetzlaff, D., Birkel, C., Dick, J., Soulsby, C., 2016. Water sources and mixing in riparian wetlands revelated by tracers and geospatial analysis. Water Resources Research 52, 456-470.

Lidman, F., Boily, A., Laudon, H., Kohler, S.J., 2017. From soil water to surface water – how the riparian zone controls element transport from a boreal forest to a stream. Biogeosciences 14, 3001-3014.

Lin, H.S., Kogelmann, W., Walker, C., Bruns, M.A., 2006. Soil moisture patterns in a forested catchment: A hydropedological perspective. Geoderma 131, 345-368.

Liu, F., Bales, R.C., Conklin, M.H., Conrad, M.E., 2008. Streamflow generation from snowmelt in semi-arid, seasonally snow-covered, forested catchments, Valles Caldera, New Mexico. Water Resources Research 44, W12443.

Lottig, N.R., Buffman, I., Stanley, E.H., 2013. Comparison of wetland and drainage lake influences on stream dissolved carbon concentrations and yields in a north temperate lake-rich region. Aquatic Sciences 75, 619-630.

MacDonald, L.H., Coe, D., 2007. Influence of headwater streams on downstream reaches in forested areas. Forest Science 53, 148-168.

Matheny, A.M., Fiorella, R.P., Bohrer, G., Poulson, C.J., Morin, T.H., Wunderlich, A., Vogel, C.S., Curtis, P.S., 2017. Contrasting strategies of hydraulic control in two codominant temperate tree species. Ecohydrology 10, 1-16.

McClain, M.E., Boyer, E.W., Dent, C.L., Gergel, S.E., Grimm, N.B., Groffman, P.M., Hart, S.C., Harvey, J.W., Johnston, C.A., Mayorga, E., McDowell, W.H., Pinay, G., 2003. Biogeochemical hot spots and hot moments at the interface of terrestrial and aquatic ecosystems. Ecosystems 6, 301-312.

McGlynn, B.L., McDonnell, J.J., 2003. Role of discrete landscape units in controlling catchment dissolved organic carbon dynamics. Water Resources Research 39, 1090.

McGuire, K.J., McDonnell, J.J., Weiler, M., Kendall, C., McGlynn, B.L., Welker, J.M., Seibert, J., 2005. The role of topography on catchment-scale water residence time. Water Resources Research 41, W05002.

Nathan, R.J., McMahon, T.A., 1990. Evaluation of Automated Techniques for Base Flow and Recession Analyses. Water Resources Research, 26, 1486-1473.

National Atmospheric Deposition Program (NRSP-3), 2018. NADP Program Office, Wisconsin State Laboratory of Hygiene, 465 Henry Mall, Madison, WI 53706.

Nave, L.E., Drevnick, P.E., Heckman, K.A., Hofmeister, K.L., Veverica, T.J., Swanston, C.W., 2017a. Soil hydrology, physical and chemical properties and the carbon and mercury in a postglacial lake-plain wetland. Geoderma 305, 40-52.

Nave, L.E., Gough, C.M., Perry, C.H., Hofmeister, K.L., Le Moine, J.M., Domke, G.M., Swanston, C.W., Nadelhoffer, K.J., 2017b. Physiographic factors underlie rates of biomass production during succession in Great Lakes forest landscapes. Forest Ecology and Management 397, 157-173.

Nave, L.E., Sparks, J.P., Le Moine, J., Hardiman, B.S., Nadelhoffer, K.J., Tallant, J.M., Vogel, C.S., Strahm, B.D., Curtis, P.S., 2014. Changes in soil nitrogen cycling in a northern temperate forest ecosystem during succession. Biogeochemistry 121, 471-488.

Naylor, S., Letsinger, S.L., Ficklin, D.L., Ellett, K.M., Olyphant, G.A., 2016. A hydropedological approach to quantifying groundwater recharge in various glacial settings of the mid-continental USA. Hydrological Processes 30, 1594-1608.

Neff, B.P., Day, S.M., Piggott, A.R., Fuller, L.M., 2005. Base flow in the Great Lakes Basin: U.S. Geological Survey Investigations Report 2005-5217, 23 p.

Orlowski, N., Kraft, P., Pferdmenges, J., Breuer, L., 2016. Exploring water cycle dynamics by sampling multiple stable isotope pools in a developed landscape in Germany. Hydrology and Earth System Science 20, 3873-3894.

Pearsall, D.R., Barnes, B.V., Zogg, G.R., Lapin, M., Ring, R.R., 1995. Landscape ecosystems of the University of Michigan Biological Station. School of Natural Resources & Environment. University of Michigan, Ann Arbor, MI. 66 p.

Peng, T., Chen, K., Zhan, W., Lu, W., John Tong, L., 2015. Use of stable water isotopes to identify hydrological processes of meteoric water in montane catchments. Hydrological Processes 29, 4957-4967.

Penna, D., Mantese, N., Hopp, L., Dalla Fontana, G., Borga, M., 2015. Spatio-temporal variability of piezometric response on two steep alpine hillslopes. Hydrological Processes 29, 198-211.

R Core Team, 2017. R: A language and environment for statistical computing. R Foundation for Statistical Computing, Vienna, Austria. URL https://www.R-project.org/.

Rowe, J.S., Sheard, J.W., 1981. Ecological land classification: A survey approach. Environmental Management 5, 451-464.

Scholl, M.A., Ingebritsen, S.E., Janik, C.J., Kauahikau, J.P., 1996. Use of precipitation and groundwater isotopes to interpret regional hydrology on a tropical volcanic island: Kilauea volcano area, Hawaii. Water Resources Research 32, 3525-3537.

Sebestyen, S.D., Boyer, E.W., Shanley, J.B., Kendall, C., Doctor, D.H., Aiken, G.R., Ohte, N., 2008. Sources, transformations, and hydrological processes that control stream nitrate and dissolved organic matter concentrations during snowmelt in an upland forest. Water Resources Research 44, W12410.

Seibert, J., Grabs, T., Kohler, S., Laudon, H., Winterdahl, M., Bishop, K., 2009. Linking soil- and stream-water chemistry based on a Riparian Flow-Concentration Integration Model. Hydrology and Earth System Science 13, 2287-2297.

Shanley, J.B., Sebestyen, S.D., McDonnell., J.J., McGlynn, B.L., Dunne, T., 2015. Water's Way at Sleepers River watershed – revisiting flow generation in a post-glacial landscape, Vermont USA. Hydrological Processes 29, 3447-3459.

Singh, S., Inamdar, S., Mitchell, M., 2015. Changes in dissolved organic matter (DOM) amount and composition along nested headwater stream locations during baseflow and stormflow. Hydrological Processes 29, 1505-1520.

Soininen, J., Bartels, P., Heino, J., Luoto, M., Hillebrand, H., 2015. Toward more integrated ecosystem research in aquatic and terrestrial environments. BioScience 65, 174-182.

Soulsby, C., Tetzlaff, D., Rodgers, P., Dunn, S., Waldron, S., 2006. Runoff processes, stream water residence times and controlling landscape characteristics in a mesoscale catchment: An initial evaluation. Journal of Hydrology 325, 197-221.

Spur, S.H., Zumberge, J.H., 1956. Late Pleistocene features of Cheboygan and Emmet counties, Michigan. American Journal of Science 254, 96-109.

Tansley, A.G., 1935. The use and abuse of vegational concepts and terms. Ecology 16, 284-307.

Tetzlaff, D., Birkel, C., Dick, J., Geris, J., Soulsby, C., 2014. Storage dynamics in hydropedological units control hillslope connectivity, runoff generation, and the evolution of catchment transit time distributions. Water Resources Research 50, 969-985.

Tromp-Van Meerveld, H.J., McDonnell, J.J., 2006. On the interrelations between topography, soil depth, soil moisture, transpiration rates and species distribution at the hillslope scale. Advances in Water Resources 29, 293-310.

Vidon, P., Smith, A.P., 2007. Upland controls on the hydrological functioning of riparian zones in glacial till valleys of the Midwest. Journal of the American Water Resources Association 43, 1524-1539.

Western, A.W., Bloschl, G., Grayson, R.B., 2001. Toward capturing hydrologically significant connectivity in spatial patterns. Water Resources Research 37, 83-97.

Zimmer, M.A., McGlynn, B.L., 2018. Lateral, vertical, and longitudinal source area connectivity drive runoff and carbon export across watershed scales. Water Resources Research 54, 1576-1598.

Zogg, G.P., Barnes, B.V., 1995. Ecological classification and analysis of wetland ecosystems, northern Lower Michigan, U.S.A. Canadian Journal of Forest Resources 25, 1865-1875.